

**Mitochondrial reactive oxygen species
license pro-inflammatory signaling
in infected macrophages
via disulfide linkage of NEMO**

I n a u g u r a l – D i s s e r t a t i o n

zur

Erlangung des Doktorgrades

der Mathematisch-Naturwissenschaftlichen Fakultät

der Universität zu Köln

vorgelegt von

Marc Herb

aus Köln

Köln 2019

Erster Berichterstatter (Gutachter):

Prof. Dr. Björn Schumacher

Zweiter Berichterstatter (Gutachter):

Prof. Dr. Martin Krönke

Tag der mündlichen Prüfung:

18.01.2019

"Sat celeriter fieri quidquid fiat satis bene." ("Was gut genug getan wurde, ist auch schnell genug getan.")

– Gaius Octavius Augustus, römischer Kaiser, *gemäß Sueton: Divus Augustus 25,4*

Table of contents

1. Introduction	1
1.1. Reactive oxygen species – a double-edged sword	1
1.1.1. Cellular ROS levels – the quantity makes the poison	1
1.1.2. Cellular ROS sources – professional or accidental ROS production?	3
1.1.2.1 The Nox family – ROS professionals	3
1.1.2.2 Mitochondria – ROS only as by-product?	4
1.1.3. ROS as signaling molecules – not always brute force	5
1.2. Macrophages – all-rounders at the front line of battle	7
1.2.1. Infection with <i>Listeria monocytogenes</i> – a complicated enemy	8
1.2.2 Pro-inflammatory signaling in macrophages – a complicated response	9
1.2.3 ROS production in macrophages – with the license to kill	12
1.3 ROS in pro-inflammatory signaling – a nearly blank paper	14
1.4. Aims of this study	15
2. Materials & Methods	16
2.1. Animals, bacteria, materials	16
2.1.1 Mice	16
2.1.2 Bacteria	17
2.1.3 Chemicals and additives	17
2.1.4 Buffers, solutions and media	19
2.1.5 Antibodies	21
2.1.6 Molecularbiological materials, constructs and primers	21
2.1.7 PCR programs	22
2.1.8 Consumable materials	22
2.1.9 Technical equipment and devices	23
2.1.10 Kits	24
2.1.11 Software	24
2.2. Methods	24
2.2.1 Molecularbiological methods	24
2.2.1.1 Transformation and replication of DNA	25
2.2.1.2 Linearisation of Plasmids	25
2.2.1.3 T7-Promotor PCR	25
2.2.1.4 mRNA-Synthesis	25
2.2.2 Cultivation of bacteria	27
2.2.3 Isolation of peritoneal cells	27

2.2.4 Immunomagnetic enrichment peritoneal macrophages	27
2.2.5 Flow cytometric analysis of peritoneal macrophages	28
2.2.6 Transfection of peritoneal macrophages	28
2.2.7 Quantification of ROS	28
2.2.7.1 Measurement of extracellular ROS production	29
2.2.7.2 Measurement of cytosolic ROS production	29
2.2.7.3 Measurement of ROS production in the mitochondrial matrix	29
2.2.8 Cytokine quantification	30
2.2.8.1 Preparation of supernatants	30
2.2.8.2 ELISA (Enzyme-linked immunosorbent assay)	30
2.2.9 Measurement of mitochondrial membrane potential	30
2.2.10 Measurement of cellular ATP levels	31
2.2.11 Cell viability/cytotoxicity assays	31
2.2.11.1 Determination of cell death	31
2.2.11.2 Determination of cell viability	31
2.2.12 Cell fixation for microscopy	31
2.2.13 Immunofluorescence staining	32
2.2.13.1 Staining for translocation analysis of NF- κ B	32
2.2.13.2 Staining of mitochondria	32
2.2.13.3 Staining of FLAG-tagged NEMO and IKK β constructs	33
2.2.14 Western blotting for protein analysis	33
2.2.14.1 Preparation of cell lysates (Standard SDS-PAGE, reducing)	33
2.2.14.2 Preparation of cell lysates (SDS-PAGE, non-reducing)	33
2.2.14.3 BCA Protein Assay	33
2.2.14.4 Standard SDS-PAGE (reducing)	34
2.2.14.5 SDS-PAGE (non-reducing)	34
2.2.14.6 Western Blot	34
2.2.14.7 Antibody staining	34
2.2.14.8 Protein visualisation	34
2.2.15 Electrophoretic mobility shift assay (EMSA)	35
2.2.16 Statistical methods	35

3. Results **36**

3.1. ROS production by infected macrophages	36
3.1.1. Macrophages produce extracellular and cytosolic ROS upon bacterial infection	36
3.1.2. ROS are required for pro-inflammatory cytokine secretion during bacterial infection	38
3.1.3. Nox2 is the exclusive source of extracellular ROS	40

3.1.4. Nox/Duox enzymes do not contribute to cytosolic ROS production	40
3.1.5. Nox/Duox enzymes are dispensable for pro-inflammatory cytokine secretion	42
3.1.6. Cytosolic ROS production is crucial for pro-inflammatory cytokine secretion	42
3.1.7. Cytosolic ROS do not originate from the mitochondrial matrix	44
3.1.8. Cytosolic ROS are produced by complex III of the mitochondrial ETC	46
3.1.9. Cytosolic H ₂ O ₂ regulates pro-inflammatory signaling	48
3.2. Induction mtROS production in infected macrophages	50
3.2.1. mtROS production is not caused by mitochondrial perturbation	50
3.2.2. TRL2/MyD88/TRAF6 signaling induces mtROS production	52
3.4. Modulation of pro-inflammatory signaling pathways by mtROS	54
3.4.1. mtROS are crucial for activation of the ERK1/2 pathway	54
3.4.2. mtROS are necessary for full activation of NF-κB signaling	56
3.5. Mechanisms of mtROS-dependent pro-inflammatory signaling	58
3.5.1. mtROS do not regulate cytokine secretion by oxidative phosphatase inactivation	58
3.5.2. mtROS are crucial for IKK complex activation	59
3.5.3. mtROS induce covalent linkage of NEMO via disulfide bonds	59
3.5.4. mtROS induce NEMO complex formation by covalent linkage via Cys ⁵⁴ and Cys ³⁴⁷	61
3.5.5. mtROS-mediated covalent linkage of NEMO via Cys ⁵⁴ and Cys ³⁴⁷ is crucial for pro-inflammatory signaling	63
3.5.6. mtROS do not regulate processes up- or downstream of NEMO	64
3.5.7. Mechanism for mtROS-mediated pro-inflammatory signaling in infected macrophages	66
4. Discussion	68
4.1. Mechanisms of ROS production in infected macrophages	68
4.1.1 ROS production by Nox enzymes	68
4.1.2 ROS production by mitochondria	69
4.2 Induction of mtROS production	70
4.2.1 Stress-induced mtROS production	70
4.2.2 Receptor-induced mtROS production	71
4.3. Role of ROS for pro-inflammatory cytokine secretion	71
4.3.1 Role of Nox/Duox enzymes for pro-inflammatory cytokine secretion	71
4.3.2 Role of mtROS for pro-inflammatory cytokine secretion	72
4.4 mtROS-dependent pro-inflammatory signaling pathways	73
4.4.1 MAPK-pathways	73
4.4.2 The NF-κB pathway	74
4.5 The molecular target of mtROS-dependent pro-inflammatory signaling	74
4.5.1 Activation of the IKK complex	74

4.5.2 Modulation of NEMO	75
4.5.3 Up- and downstream processes of NEMO	76
4.6 Conclusion	76
5. References	77
6. Summary	89
7. Zusammenfassung	90
8. Danksagung	91
9. List of publications	92
10. List of Figures	93
11. List of Tables	95
12. Erklärung	96
12. Curriculum vitae	97

List of abbreviations

°C	<u>D</u> egree <u>C</u> elsius
A	<u>A</u> mpere
ABIN2	<u>A</u> 20- <u>b</u> inding <u>i</u> nhibitor of <u>NF</u> -κB activation <u>2</u>
APS	<u>A</u> mmonium <u>p</u> er <u>s</u> ulfate
ASK1	<u>A</u> ctivation of Apoptosis <u>S</u> ignal-Regulating <u>k</u> inase <u>1</u>
ATP	<u>A</u> denosin <u>t</u> ri <u>p</u> hosphate
AUC	<u>A</u> rea <u>u</u> nder the <u>c</u> urve
B.sub	<u>B</u> acillus <u>s</u> ubtilis
BCA	<u>B</u> icin <u>ch</u> oninic <u>a</u> cid
BHI	<u>B</u> rain <u>h</u> eart <u>i</u> nfusion
BMDM	<u>B</u> one <u>m</u> arrow- <u>d</u> erived <u>m</u> acrophages
BS3	<u>B</u> issulfosuccinimidyl <u>s</u> uberate
BSA	<u>B</u> ovine <u>s</u> erum <u>a</u> lbumin
caIKKβ	<u>c</u> onstitutively <u>a</u> ctive <u>IKKβ</u>
CCCP	<u>C</u> arbonyl <u>c</u> yanid-m- <u>c</u> hloro <u>p</u> henylhydrazon
CFU	<u>C</u> olony <u>f</u> orming <u>u</u> nit
CoQ	<u>C</u> oenzyme <u>Q</u> ₁₀
Cys	<u>C</u> ystein residue
Cyt c	<u>C</u> ytochrome <u>c</u>
DAPI	4',6- <u>D</u> iamidin-2- <u>p</u> henyl <u>i</u> ndol
DCF	5,6-dicarboxy-2',7'- <u>d</u> ic <u>h</u> lorodihydro <u>f</u> luorescein diacetate, di(acetoxymethyl ester)
DMEM	<u>D</u> ulbecco's <u>m</u> odified <u>e</u> agle's <u>m</u> edium
DMSO	<u>D</u> imethyl <u>s</u> ulf <u>o</u> xide
DNA	<u>D</u> esoxyribon <u>u</u> cleic <u>a</u> cid
DSMZ	<u>D</u> eutsche <u>S</u> ammlung von <u>M</u> ikroorganismen und <u>Z</u> ellkulturen GmbH
Duox	<u>D</u> ual <u>o</u> xidase
E.coli	<u>E</u> scherischia <u>c</u> oli

ECL	E nhanced c hemi l uminescence
ECSIT	E volutionarily c onserved s ignalling i ntermediate in T oll pathways
EDTA	E thylene d iamine t etraacetic a cid
EGTA	E thylene g lycol-bis(β -aminoethyl ether)-N,N,N',N'- t etraacetic a cid
EMSA	E lectrophoretic m obility s hift a ssay
ELISA	E nzyme- l inked i mmuno s orbent a ssay
ER	E ndoplasmatic r eticulum
ERK1/2	E xtracellular signal- r egulated k inase isoforms 1 and 2
ETC	E lectron t ransport c hain
FACS	F luorescence a ctivated c ell s orting
FADH₂	F lavin a denine d inucleotide (protonated)
FCS	F etal c alf s erum
Fig.	F igure
g	acceleration of g ravty
gp91^{phox}	91 -kDa g lycoprotein component of the p hagocyte NADPH o xidase
GPX	G lutathion p ero x idase
GSH	G lutathion (with a reduced S H group)
GTPase	G uanosine t ri p hosphate kinase
h	h ours
HBSS	H ank's b alanced s alt s olution
HeLa cell line	H enrietta L acks-derived cell line
HEPES	4-(2- h ydroxy e thyl)-1- p iperazine e thane s ulfonic acid
HK L.m.	H eat- k illed L.m.
HRP	H orse r adish p ero x idase
IFM	I mmuno f luorescence m icroscopy
IgG	I mmuno g lobulin G
IKK	I κ B k inase
IL	I nter l eukin

IMS	<u>I</u>nter<u>m</u>embrane <u>s</u>pace (of mitochondria)
IRAK1/2/4	<u>I</u>nterleukin 1 <u>r</u>eceptor-<u>a</u>ssociated <u>k</u>inase isoforms <u>1,2 and 4</u>
IκB	<u>I</u>nhibitor of NF-<u>κ</u>B
JNK1/2	c-<u>J</u>un <u>N</u>-terminal <u>k</u>inase isoforms <u>1 and 2</u>
kDa	<u>k</u>ilo <u>D</u>alton
KI	<u>k</u>nock<u>i</u>n
KO	<u>k</u>nock<u>o</u>ut
L.m.	<u>L</u>isteria <u>m</u>onocytogenes
LLO	<u>L</u>isteriolysin <u>O</u>
LPS	<u>L</u>ipopolysaccharide
LTA	<u>L</u>ipoteichoic <u>a</u>cid
MACS	<u>M</u>agnetic <u>a</u>ctivated <u>c</u>ell <u>s</u>orting
MAPK	<u>M</u>itogen-<u>a</u>ctivated <u>p</u>rotein <u>k</u>inases
M-CSF	<u>M</u>acrophage <u>c</u>olony-<u>s</u>timulating <u>f</u>actor
MEF	<u>M</u>ouse <u>e</u>mbryonic <u>f</u>ibroblasts
MEK1/2	<u>M</u>APK of <u>E</u>RK1/2
MHC	<u>M</u>ajor <u>H</u>istocompatibility <u>C</u>omplex
min	<u>m</u>inutes
MKK	<u>M</u>APK <u>k</u>inase
MOI	<u>M</u>ultiplicity <u>o</u>f <u>i</u>nfection
MOM	<u>M</u>itochondrial <u>o</u>uter <u>m</u>embrane
MOPS	3-(N-<u>m</u>orpho<u>l</u>ino)<u>p</u>ropane<u>s</u>ulfonic acid
mRNA	<u>m</u>essenger <u>R</u>NA
mtROS	<u>m</u>itochondrial <u>R</u>OS
MW	<u>m</u>olecular <u>w</u>eight
MyD88	<u>M</u>yeloid <u>d</u>ifferentiation primary response gene <u>88</u>
n.d.	<u>n</u>ot <u>d</u>etectable
n.i.	<u>n</u>ot <u>i</u>nfected
n.s.	<u>n</u>ot <u>s</u>ignificant
n.t.	<u>n</u>ot <u>t</u>reated

NAC	<u>N</u>-<u>a</u>cetyl-<u>l</u>-<u>c</u>ysteine
NADPH	<u>N</u>icotinamide <u>a</u>denine <u>d</u>inucleotide <u>p</u>hosphate (protonated)
NEM	<u>N</u>-<u>E</u>thyl<u>m</u>aleimide
NEMO	<u>NF</u>-<u>κ</u>B <u>e</u>ssential <u>m</u>odulator
NEMO^{Cys54/374A}	<u>C</u>ystein residues at positions 54 and 374 in the NEMO protein mutated to <u>a</u>lanine (redox-insensitive)
NEMO^{wt}	<u>w</u>ild <u>t</u>ype NEMO
NF-κB	<u>N</u>uclear <u>f</u>actor '<u>κ</u>appa light chain enhancer' of activated <u>B</u>-cells
nM/μM/mM	<u>n</u>ano<u>m</u>olar, <u>m</u>ikro<u>m</u>olar, <u>m</u>illimolar
NMS	<u>N</u>ormal <u>m</u>ouse <u>s</u>erum
NOD2	<u>N</u>ucleotide-binding <u>o</u>ligomerization <u>d</u>omain-containing protein 2
Nox	<u>N</u>ADPH <u>o</u>xidase
O/N	<u>O</u>ver <u>n</u>ight
OD₆₀₀	<u>O</u>ptical <u>d</u>ensity at 600 nm
OXPHOS	<u>O</u>xidative <u>p</u>hosphorylation
p.i.	<u>p</u>ost <u>i</u>nfection
p22^{phox}	22-kDa <u>p</u>rotein component of the <u>p</u>hagocyte NADPH <u>o</u>xidase
p40^{phox}	40-kDa <u>p</u>rotein component of the <u>p</u>hagocyte NADPH <u>o</u>xidase
p47^{phox}	47-kDa protein component of the <u>p</u>hagocyte NADPH <u>o</u>xidase
p67^{phox}	67-kDa <u>p</u>rotein component of the <u>p</u>hagocyte NADPH <u>o</u>xidase
PAMP	<u>P</u>athogen-<u>a</u>ssociated <u>m</u>olecular <u>p</u>attern
PBS	<u>P</u>hosphate <u>b</u>uffered <u>s</u>aline
PCR	<u>P</u>olymerase <u>c</u>hain <u>r</u>eaction
PE	<u>P</u>hyco<u>e</u>rythrin
PFA	<u>P</u>ara<u>f</u>orma<u>a</u>ldehyde
pH	<u>p</u>otenia <u>H</u>ydrogenii, negative decadic logarithm of the H₃O⁺ concentration
PM	<u>P</u>eritoneal <u>m</u>acrophages
PMA	<u>P</u>horbol-12-<u>m</u>yristat-13-<u>a</u>cetate
PRR	<u>P</u>attern <u>r</u>ecognition <u>r</u>eceptor

RIG-I	<u>R</u>etonic acid-<u>i</u>nducible <u>g</u>ene <u>I</u>
RIPA	<u>R</u>adio <u>i</u>mmunop<u>r</u>ecipitation <u>a</u>ssay
RLU	<u>R</u>elative <u>l</u>ight <u>u</u>nit
RNA	<u>R</u>ibon<u>n</u>ucleic <u>a</u>cid
RNS	<u>R</u>eactive <u>n</u>itrogen <u>s</u>pecies
ROS	<u>R</u>eactive <u>o</u>xygen <u>s</u>pecies
rpm	<u>r</u>evolutions <u>p</u>er <u>m</u>inute
RT	<u>R</u>oom <u>t</u>emperature
s	<u>s</u>econds
SDS	<u>S</u>odium <u>d</u>odecyl <u>s</u>ulfate
SDS-PAGE	SDS-<u>p</u>oly<u>a</u>crylamide <u>g</u>el <u>e</u>lectrophoresis
SEM	<u>S</u>tandard <u>e</u>rror of the <u>m</u>ean
SOD	<u>S</u>uper<u>o</u>xide <u>d</u>ismutase
TAB	<u>T</u>AK1-<u>b</u>inding protein
TAE	<u>T</u>ris-<u>a</u>ctetate-<u>E</u>DTA buffer
TAK1	<u>T</u>ransforming Growth Factor β-<u>a</u>ctivated <u>k</u>inase <u>1</u>
TBE	<u>T</u>ris-<u>b</u>orate-<u>E</u>DTA buffer
TBS	<u>T</u>ris-<u>b</u>uffered <u>s</u>aline
TBS-T	<u>TBS</u>-<u>T</u>ween 20
TEMED	<u>T</u>etram<u>e</u>thylethylend<u>i</u>amine
TGS	<u>T</u>ris/<u>G</u>lycine/<u>S</u>DS
TPL2	<u>T</u>umor <u>p</u>rogression <u>l</u>ocus <u>2</u>
TLR	<u>T</u>oll-<u>l</u>ike <u>r</u>eceptor
TMRE	<u>T</u>etram<u>e</u>thylrhodamine, <u>E</u>thylester
TNF	<u>T</u>umor <u>n</u>ecrosis <u>f</u>actor
TRAF6	<u>T</u>NF <u>r</u>eceptor-<u>a</u>ssociated <u>f</u>actor <u>6</u>
U/ml	<u>U</u>nits per <u>m</u>l
UBC13	E2 <u>u</u>biquitin-<u>c</u>onjugating enzyme <u>13</u>
V	<u>V</u>olt
VDAC	<u>V</u>oltage-<u>d</u>ependent <u>a</u>nion <u>c</u>hannel

w/o	<u>w</u>ith<u>o</u>ut
WT	<u>w</u>ild <u>t</u>ype
wtIKKβ	<u>w</u>ild <u>t</u>ype IKKβ
Δhly L.m.	<u>L.m.</u> deficient for the <u>h</u>aemol<u>ys</u>in LLO
Δprf L.m.	<u>L.m.</u> deficient for the virulence master regulator <u>prf</u>A

1. Introduction

1.1. Reactive oxygen species – a double-edged sword

The term reactive oxygen species (ROS) defines a group of chemical molecules with at least one oxygen atom and with higher reactivity than molecular oxygen. This group consists of highly reactive free radicals like the superoxide anion (O_2^-), the hydroxyl radical ($\text{OH}\cdot$) and peroxy radicals ($\text{OOR}\cdot$) and nonradical species such as singlet oxygen ($^1\text{O}_2$), ozone (O_3), hypochlorite anion (OCl^-) and the relatively stable hydrogen peroxide (H_2O_2). ROS are generated under harsh inorganic conditions (e.g. $\text{OOR}\cdot$, O_3 and OCl^- in the atmosphere), but are also produced by nearly all organisms and cells (Chavez et al., 2009; Niethammer et al., 2009; Pendyala et al., 2009; Ha et al., 2005; Levine et al., 1994). All cellular ROS sources produce O_2^- by single electron transfer to molecular oxygen. O_2^- then acts as precursor of all other cellular ROS species (Lambeth et al., 2014; Cheeseman et al., 1993) (Fig. 1).

Figure 1

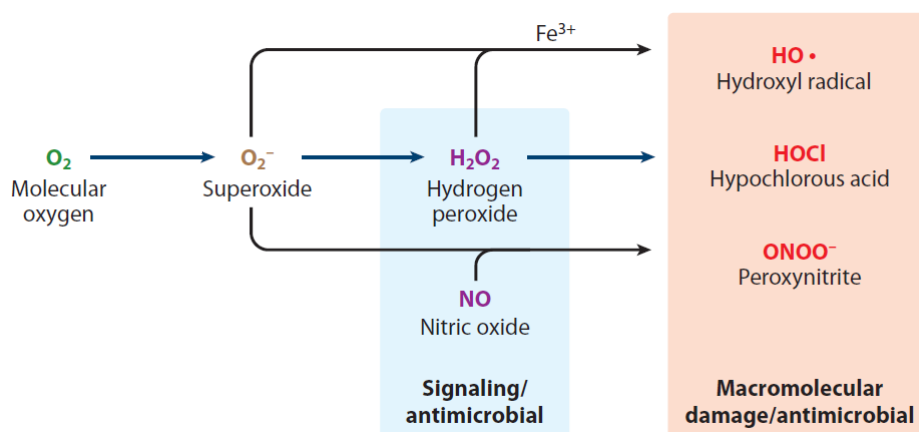


Figure 1: Major ROS subspecies in organisms (modified from Lambeth et al., 2014)

All cellular ROS sources produce O_2^- by single electron transfer to molecular oxygen. O_2^- then acts as precursor of all other ROS species. Nitric oxide (NO) and peroxynitrite (ONOO^-) are not ROS but reactive nitrogen species (RNS). The oxidation of O_2^- by ferric iron (Fe^{3+}) is called Fenton reaction and rarely happens in cells.

1.1.1. Cellular ROS levels – the quantity makes the poison

Cellular ROS levels are in a dynamic but stable equilibrium that consists of the sum of all producing and eliminating factors in the cell. ROS can be produced as byproducts of oxidative metabolic processes (Kelley et al., 2010; Nohl et al., 2003), as a cellular response to foreign stimuli such as pathogenic infections (Gluschko and Herb et al., 2018; Schramm et al., 2014; Hoeven et al., 2011; West et al., 2011b; Babior, 2002) or intrinsic stimuli such as cytokines (Bulua et al., 2011a; Kim et al., 2010).

The antioxidant defense system, which counterbalances excessive ROS production includes three superoxide dismutases (SOD1, 2, 3) (decomposition of $\cdot\text{O}_2^-$ to H_2O_2) and catalase (dismutation of H_2O_2 to H_2O and O_2), as the most important components (Poljsak et al., 2013; Ha et al., 2005; Fridovich, 1997). SOD1 is localized in the cytosol and the intermembrane space of mitochondria (IMS), SOD2 is found exclusively in the mitochondrial matrix and SOD3 is an extracellular enzyme (Lambeth et al., 2014; Melov et al., 1999). Catalase is mainly localized in organelles called peroxisomes, but is also present in the cytosol and in mitochondria (Kirkman et al., 2007). In addition, a pool of soluble (e.g. glutathione in combination with glutathione peroxidase) and membranous molecules (e.g. α -tocopherol, coenzyme Q) contribute to ROS scavenging (Jones et al., 2016; Poljsak et al., 2013; Schafer et al., 2010).

Excessive ROS production is often referred to as oxidative stress and associated with damage of lipids, proteins and DNA (Lambeth et al., 2014; Diaz et al., 2012; Schumacher et al., 2008; Fiers et al., 1999). This ROS-dependent direct damage of cellular molecules can cause a number of pathologies (Thimmulappa et al., 2006; Rangasamy et al., 2005; Cross et al., 1987) but can be useful when molecular structures of pathogens are targeted and damaged (Winterbourn et al., 2013). However, growing evidence suggests that a slight elevation of ROS production has important signaling functions during immunological, physiological and biological processes (Nathan et al., 2013a; Finkel, 2011; Tai et al., 2009; Reczek et al.). Therefore, maintaining the balance between dampening of harmful ROS levels and a sufficient production of ROS levels for beneficial processes (e.g. cell signaling and redox regulation) is the major function of the antioxidant system (Nathan et al., 2013a) (Fig.2).

Figure 2

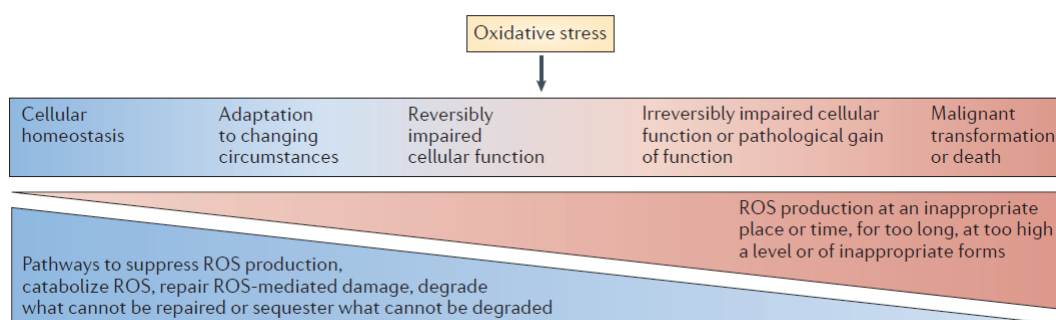


Figure 2: Balance of cellular ROS (from Nathan et al., 2013)

Balancing between dampening of harmful ROS levels and a sufficient production of ROS levels for beneficial processes (e.g. cell signaling and redox regulation) is the major function of the antioxidant system.

1.1.2. Cellular ROS sources – professional or accidental ROS production?

$\cdot\text{O}_2^-$, as the precursor of all other ROS, and H_2O_2 , which rapidly dismutates from $\cdot\text{O}_2^-$ spontaneously or enzymatically by catalase, are both generated by various cellular sources. The enzyme family of NADPH oxidases (Nox) (Lambeth et al., 2014; Bedard et al., 2007) and the respiratory electron transport chain (ETC) of mitochondria (West et al., 2011b; Brand, 2010; Murphy, 2009) are the major ROS generating systems in many eukaryotic cell types.

1.1.2.1 The Nox family – ROS professionals

The regulated production of ROS is the sole function of the members of the Nox enzyme family. The family consists of the NADPH oxidases Nox1, Nox2, Nox3, Nox4, Nox5 and the dual oxidases Duox1 and Duox2. All isoforms are membrane-bound and transfer electrons from NADPH to molecular oxygen generating $\cdot\text{O}_2^-$ and subsequently H_2O_2 . Nox1, Nox2, Nox3 and Nox4 require the membrane-bound subunit $\text{p}22^{\text{phox}}$ (Nakano et al., 2008; Kawahara et al., 2005), while Nox5, Duox1 and Duox2 do not, but are activated through calcium binding to their EF-hand calcium-binding domain (Lambeth et al., 2007) (Fig. 3).

Figure 3

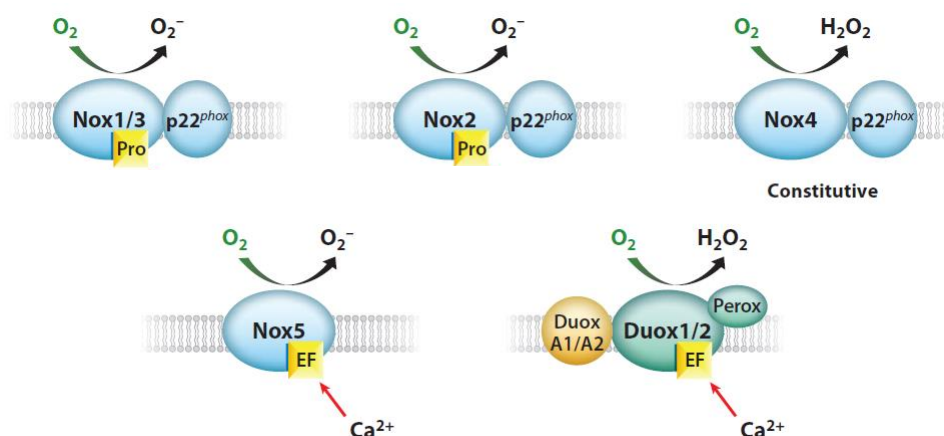


Figure 3: The Nox family enzymes (modified from Lambeth et al., 2014)

The family consists of the NADPH oxidases Nox1, Nox2, Nox3, Nox4, Nox5 and the dual oxidases Duox1 and Duox2. Different stimuli can trigger ROS production by Nox1, 2 and 3, while Nox4 is constitutively active. Nox5, Duox1 and Duox2 are activated by calcium binding through the cytoplasmic EF-hand calcium binding domain.

The Nox isoforms have multiple functions in a wide range of organisms, organs, tissues and cell types, including vasoregulation, hormone synthesis, regulation of gene expression, cell proliferation and cell differentiation (Lambeth et al., 2014; Aguirre et al., 2010; Bedard et al., 2007). In contrast to Nox2, as the predominant source of ROS in phagocytes, which produces large quantities of ROS to inactivate invading pathogens (Pollock et al., 1995), the other Nox isoforms produce smaller amounts of ROS for modulation of signaling pathways or during

anabolic processes (Carnesecci et al., 2011; Dikalova et al., 2010; Donko et al., 2010; Gavazzi et al., 2006; Banfi et al., 2004).

1.1.2.2 Mitochondria – ROS only as by-product?

Mitochondria, as energy generating organelles, produce ROS as a byproduct of respiratory activity (Lambeth et al., 2014; Nohl et al., 2003). By shuttling electrons from NADH and FADH₂ through the four complexes I-IV of the ETC, a proton gradient is generated that drives ATP production by complex V (Fig. 4). The initial ROS subspecies produced by the mitochondrial respiratory chain mainly by complexes I and III is $\cdot\text{O}_2^-$. Complex I produces $\cdot\text{O}_2^-$ into the mitochondrial matrix, where it is quickly dismutated by SOD2. Complex III also produces $\cdot\text{O}_2^-$ into the matrix but, moreover, can produce ROS into the IMS of the mitochondrion (Lanciano et al., 2013; West et al., 2011b; Murphy, 2009; Fridovich, 1997). Besides their well-known roles as ROS- and ATP-generating organelles, mitochondria have important functions as regulators of cellular homeostasis (Nomura et al., 2016; Liemburg-Apers et al., 2015; Minton, 2013; Raturi et al., 2013) and as signaling platforms (Banoth et al., 2018; Denora et al., 2017; Chandel, 2014; Lartigue et al., 2013; Zhou et al., 2011; Seth et al., 2005).

Figure 4

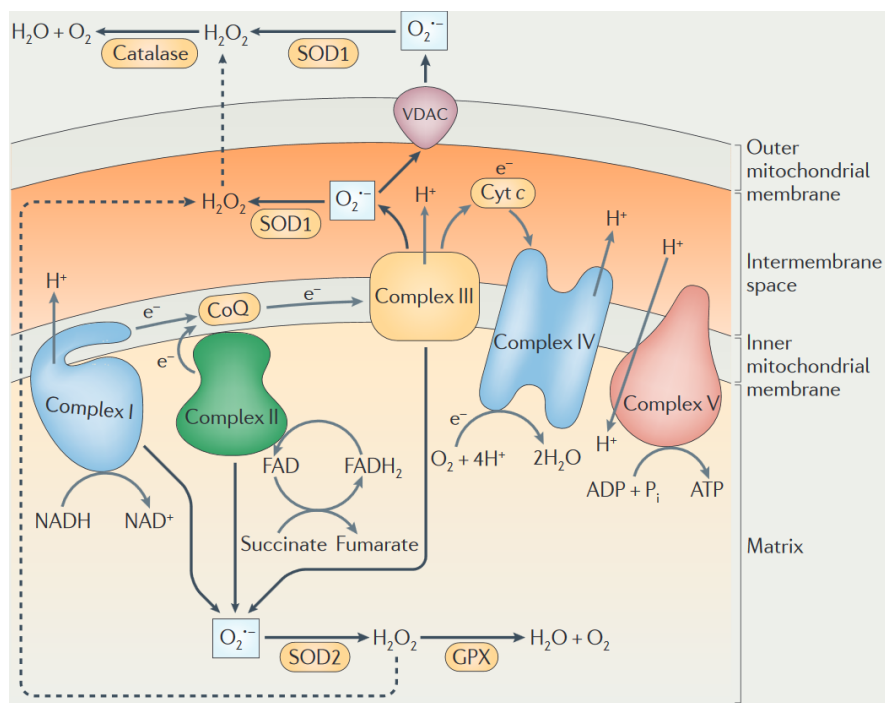


Figure 4: ROS production of the ETC (West et al., 2011)

By shuttling electrons from NADH and FADH₂ through the four complexes I-IV of the ETC and the electron carriers coenzyme Q (CoQ) and cytochrome c (Cyt c), a proton gradient is generated that drives (continued on next page)

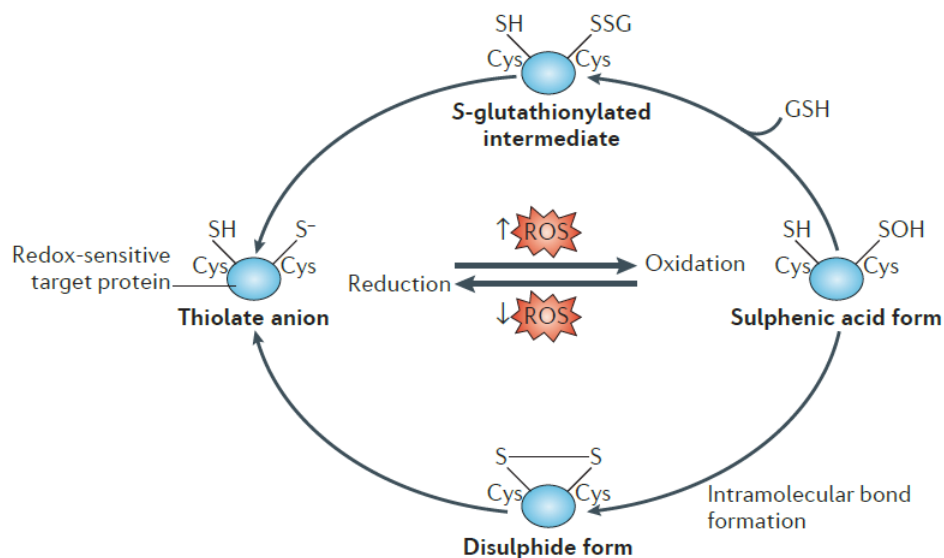
Figure 4 (continued): ROS production of the ETC (West et al., 2011)

ATP production by complex V. Mitochondria generate ROS mainly by complexes I and III of the ETC. SOD2 and glutathione peroxidase (GPX) detoxify ROS in the mitochondrial matrix, while SOD1 and catalase decompose ROS in the cytosol. H_2O_2 can reach the cytosol from the IMS easily by diffusion. O_2^- can cross the outer mitochondrial membrane only by voltage-dependent anion channels (VDACs).

1.1.3. ROS as signaling molecules – not always brute force

The role of ROS as exclusive damaging and toxic molecules, especially for H_2O_2 , is outdated and accumulating evidence is growing that ROS act as important signaling molecules in cells (Holmström et al., 2014; Lambeth et al., 2014; Nathan et al., 2013a). O_2^- is more reactive than H_2O_2 , has a shorter half time and cannot cross membranes without support of channels (e.g. VDAC) (Shoshan-Barmatz et al., 2010). Therefore, an increase of O_2^- is often associated with oxidative stress and damage. However, some proteins are regulated by irreversible O_2^- -dependent inactivation (Chen et al., 2009).

H_2O_2 as a diffusible and, compared to other ROS subspecies, relatively stable molecule is more suitable as signaling molecule in cells (Zhang et al., 2016; Marinho et al., 2013). A well understood mechanism of H_2O_2 -mediated signaling is the oxidation of cysteine residues (Jones et al., 2016; Short et al., 2016; Rhee, 2006; Chiarugi et al., 2001). At physiological pH, the thiol groups of cysteines exposed to the cytosol exist in a deprotonated state (Cys-S⁻) and are susceptible to oxidation (Finkel, 2011). H_2O_2 -dependent signaling occurs in a nanomolar concentration range (~100 nM), leading to the reversible oxidation of the thiolate group (Cys-S⁻) to a sulfenic group (Cys-SOH) (Fig. 5).

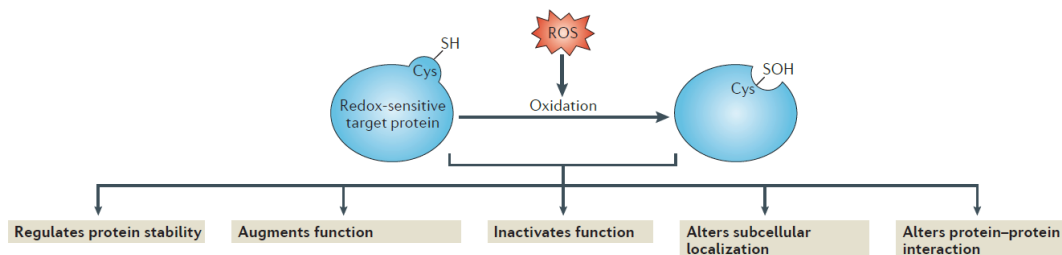
Figure 5

(Legend on next Page)

Figure 5: Oxidation and reduction of cysteine residues by ROS (modified from Holmström et al., 2014)

At physiological pH, the thiol groups of cysteines exist in a deprotonated state (Cys-S⁻) and are susceptible to oxidation. These oxidation steps are reversible by antioxidant enzyme systems and molecules such as glutathion (GSH).

Proteins oxidized by H₂O₂ often undergo allosterical changes. These changes can result in different binding capabilities of substrates, directly inactivate or activate enzymatic functions (Kamata et al., 2005; Tonks, 2005; Meng et al., 2002; Lee et al., 1998), or lead to covalent linkage with other redox-dependent molecules by disulfide bonds (Cys-S-S-Cys) (Zhou et al., 2014b; Cote et al., 2013b; Herscovitch et al., 2008a; Tegethoff et al., 2003). Since these oxidation steps are reversible by antioxidant enzyme systems, these redox-sensitive molecules function as important redox switches during various cellular responses (Holmström et al., 2014; Barford, 2004) (Fig. 6). By contrast, excessive H₂O₂ production leads to further oxidation of the sulfenic group to sulfinic (Cys-SO₂H) and sulfonic groups (Cys-SO₃H), which are irreversible and result in protein damage (Winterbourn et al., 2008).

Figure 6**Figure 6: Protein modifications induced by ROS (modified from Holmström et al., 2014)**

Redox-sensitive molecules function as important redox switches during various cellular responses.

In addition to the different ROS-inducing stimuli, ROS sources, ROS subspecies and their specificity and selectivity for their targets, the compartmentalization of ROS production is an important factor to determine if damage or redox signaling will occur (Kaludercic et al., 2014; Ushio-Fukai, 2009).

Nox2-dependent ROS production by macrophages, for example, takes place at the plasma membrane, damaging invading pathogens, while mitochondria-dependent ROS production is dynamically translocated by the organelle to the place where ROS are needed (Al-Mehdi et al., 2012; West et al., 2011b). ·O₂⁻ production into the mitochondrial matrix has other consequences than production in the cytosol regarding cellular damage (Fig. 7). Accordingly, SOD2-KO mice

show a more severe pathological phenotype than SOD1-KO mice (Lambeth et al., 2014; Melov et al., 1999). Thus, all of these factors that influence ROS production have to be considered when new mechanistic insights of ROS-dependent signaling are to be investigated.

Figure 7

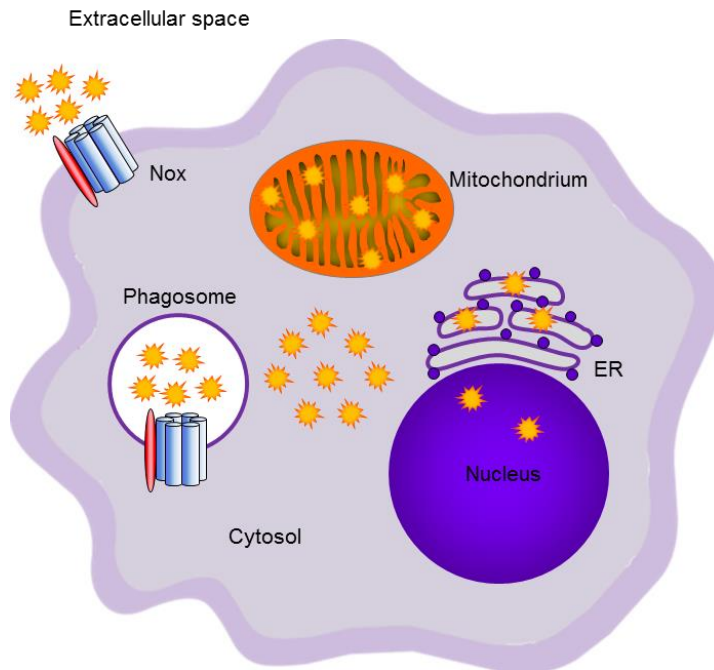


Figure 7: ROS production in different subcellular compartments.

The compartmentalization of ROS production is an important factor to determine, if mechanistic insights of ROS-dependent functions are investigated.

1.2. Macrophages – all-rounders at the front line of battle

Macrophages are cells of the innate immune system and the first line of defense against invading pathogens (Epelman et al., 2014; Davies et al., 2013). They engulf bacteria by phagocytosis and subsequently kill them by degradation in phagolysosomes (Haas, 2007; Djaldetti et al., 2002). To inactivate phagocytosed bacteria, macrophages employ an array of directly antimicrobial responses, e.g. the generation of ROS and RNS into the phagosome and the delivery of cathepsins and other hydrolases during phagosomal maturation (Mitchell et al., 2016; Weiss et al., 2015; Schramm et al., 2014; del Cerro-Vadillo et al., 2006; Aktan, 2004; Utermohlen et al., 2003; Alvarez-Dominguez et al., 2000). Via indirect antimicrobial mechanisms like the secretion of cytokines and chemokines, macrophages help to orchestrate the subsequent innate and adaptive immune responses (Arango Duque et al., 2014).

1.2.1. Infection with *Listeria monocytogenes* – a complicated enemy

Listeria monocytogenes (L.m.) is a gram-positive, rod-shaped bacterium, which causes severe food-borne infections (Radoshevich et al., 2018; Farber et al., 1991). For immunocompromised individuals, newborns and pregnant women, L.m. infection is often lethal (Ray et al., 2009; McLauchlin et al., 2004; McLauchlin, 1990). After ingestion, L.m. is able to cross the intestinal barrier by invading the cells of intestinal epithelial layers. As facultative intracellular bacterium (Freitag et al., 2009), L.m. can partly escape phagosomal degradation in resident macrophages and utilize the cell as a host for replication and as transport vehicle (Pillich et al., 2012). Therefore, it is of critical importance that other cells of the innate and adaptive immune system are activated and recruited to the sites of infection (Regan et al., 2014; Iwasaki et al., 2010). For this purpose, macrophages produce and secrete cytokines and chemokines in response to L.m. infection (Arango Duque et al., 2014; Cavaillon, 1994).

Pro-inflammatory cytokines like IL-6, TNF and IL-1 β are necessary for activation of other immune cells like neutrophils or, in combination with other signals, for self-activation of macrophages enhancing their killing capabilities (Schramm et al., 2014; Yazdanpanah et al., 2009; Mosser et al., 2008; Harrington-Fowler et al., 1981). After secretion chemokines generate a chemotactic gradient, which leads to recruitment of immune cells from the surrounding tissues and the blood stream to the site of infection (Arango Duque et al., 2014).

L.m. is a pathogen that has already been used to unravel numerous immunological processes (Mitchell et al., 2016; Pamer, 2004; Goldberg, 2001). L.m. specializes in escaping phagolysosomal degradation in macrophages by lysing the phagosomal membrane with its pore-forming toxin Listeriolysin O (LLO) (Seveau, 2014; Hamon et al., 2012; Meyer-Morse et al., 2010; Beauregard et al., 1997). Therefore, recognition of L.m. infection not only involves surface pattern recognition receptors (PRR) such as Toll-like receptors (TLRs) (Ley et al., 2016; Regan et al., 2014; West et al., 2006), scavenger receptors and C-type lectin receptors (Taylor et al., 2005) but also intracellular PRR such as NOD-like receptors and RIG-I-like receptors (Motta et al., 2015; Hagmann et al., 2013). Moreover, L.m. can also be recognized by a number of phagocytic receptors such as opsonic receptors and integrins (Gluschko and Herb et al., 2018; Lischke et al., 2013; Ehlers, 2000). One of the consequences of the simultaneous activation of these receptors is a robust induction of pro-inflammatory cytokine secretion making L.m. an ideal model to study the pro-inflammatory response of macrophages to infection with a bacterial pathogen (Fig 8).

Figure 8

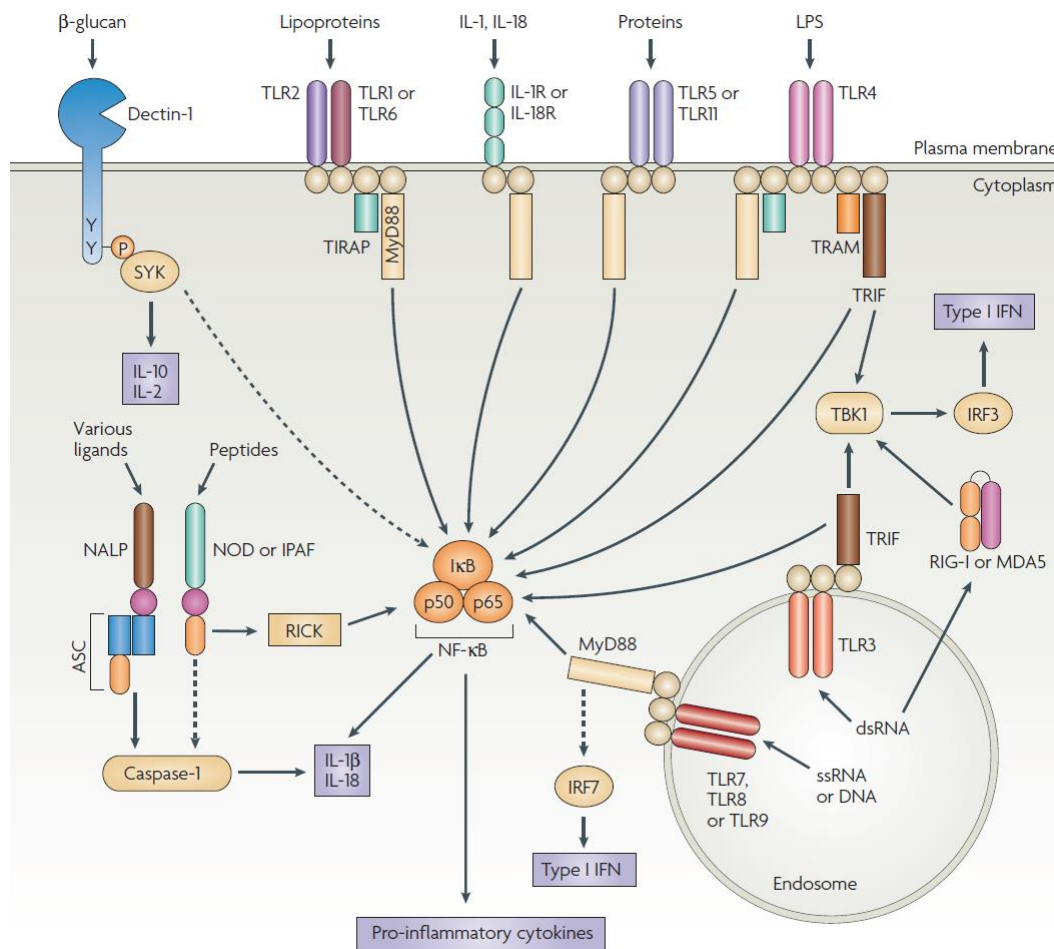


Figure 8: Receptor repertoire of macrophages (modified from Trinchieri et al., 2007)

Recognition of L.m. not only involves surface PRR such as TLR but also intracellular PRR such as NOD-like receptors and RIG-I-like receptors. Besides receptors that recognize bacterial structures, macrophages also can detect fungal cell wall components by the Dectin-1 receptor and viral nucleic acids by RIG-I or MDA5.

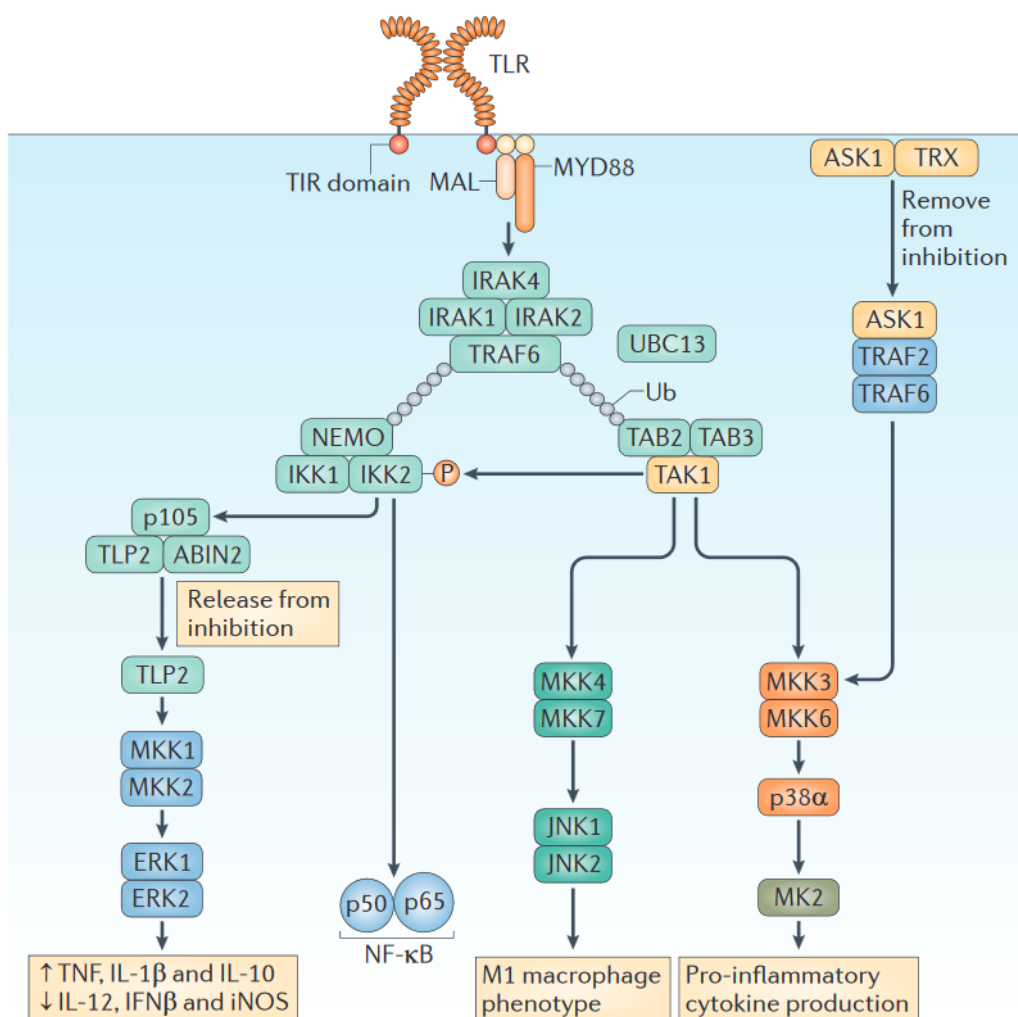
1.2.2 Pro-inflammatory signaling in macrophages – a complicated response

As described in 1.2., one of the major functions of macrophages during infection is the secretion of pro-inflammatory cytokines. The pro-inflammatory response leading to cytokine secretion is initiated by complex signaling cascades that culminate in activation of the NF- κ B pathway and the mitogen-activated protein kinase (MAPK) pathways. The three major MAPK pathways initiated upon infection finally result in the activation of the MAPKs p38, JNK1/2 and ERK1/2 (Arthur et al., 2013; Newton et al., 2012; Kawai et al., 2011).

Upon infection with a gram-positive pathogen like L.m., this signaling cascade is mostly initiated by receptor heterodimers of TLR2-1 and TLR2-6 that recognize cell wall components of gram-positive bacteria (O'Neill et al., 2013; Newton et al., 2012). TLR2 directly engages the adaptor

protein MyD88 (Lee et al., 2015; Adachi et al., 1998), which mediates interactions with the serine/threonine kinases IRAK4 and IRAK1/2 (Lin et al., 2014). The MyD88-IRAK4/1/2 complex then recruits the E3 ubiquitin ligase TRAF6, which catalyzes formation of K36 polyubiquitin chains on both TRAF6 itself and IRAK1/2 (Tenekeci et al., 2016; Zhang et al., 2010; Skaug et al., 2009). Recruitment of the kinase TAK1 along with its adaptor proteins TAB2/3 (Kanayama et al., 2004; Ishitani et al., 2003) to K36 polyubiquitinated TRAF6 triggers TAK1-mediated activation of the p38 and JNK1/2 MAPK pathways (Israel, 2010; Sato et al., 2005; Shim et al., 2005). TAK1 is not an obligatory general kinase of this complex but more a regulatory modulator that is activated in a cell-type and stimulus-specific manner (Hinz et al., 2014; Ajibade et al., 2012; Liu et al., 2012). In macrophages, the ERK1/2 pathway and the NF- κ B pathways are activated TAK1-independently by the IKK complex (Ajibade et al., 2012; Gantke et al., 2012; Mercurio et al., 1997). The IKK complex consists of the kinase subunits IKK α (IKK1) and IKK β (IKK2) and the regulatory subunit IKK γ (NEMO) (referred to as NEMO in this thesis) (Israel, 2010) (Fig.9).

Figure 9



(Legend on next page)

Figure 9: The activation of NF- κ B and the MAPK pathways (modified from Arthur et al., 2013)

The pro-inflammatory response leading to cytokine secretion is initiated by complex signaling cascade that culminates in activation of the NF- κ B pathway and the MAPK pathways. TRAF6 can also be induced independently from the IRAK1/2/4 complex by binding to TRAF2 and ASK1.

NEMO is of particular importance for IKK complex activation as it regulates both, activity and substrate interactions of IKK α and IKK β (Maubach et al., 2017; Hinz et al., 2014; Clark et al., 2011). Several studies described different possible oligomeric structures of NEMO such as dimers, trimers or tetramers (Herscovitch et al., 2008a; Marienfeld et al., 2006; Agou et al., 2004; Tegethoff et al., 2003). The primary functional unit of the IKK complex is a constitutive, non-covalently linked dimer of NEMO associated with a homo- or heterodimer of IKK α/β (Zhou et al., 2014a; Cote et al., 2013a). In resting cells, these minimal functional units are organized via direct interactions and binding of NEMO to ubiquitin chains into higher-order lattice-like structures (Scholefield et al., 2016). In response to pro-inflammatory stimuli, NEMO reorganizes from these lattice-like structures into condensed supramolecular complexes (Scholefield et al., 2016). The NEMO complexes undergo further polyubiquitination and bind to polyubiquitin chains on the pre-formed TLR/MyD88/TRAF6 complex (Tarantino et al., 2014; Arthur et al., 2013; Tokunaga et al., 2012; Laplantine et al., 2009; Rahighi et al., 2009; Windheim et al., 2008; Wu et al., 2006a; Tang et al., 2003; Deng et al., 2000).

In addition to ubiquitination and supramolecular rearrangements, NEMO can be modulated by various other post-translational modifications such as phosphorylation (Palkowitsch et al., 2008; Wu et al., 2006b; Carter et al., 2003; Prajapati et al., 2002) or SUMOylation (Lee et al., 2011; Mabb et al., 2006; Huang et al., 2003). However, despite the strict dependency of NEMO for several downstream signaling pathways, the exact roles of NEMO in the signaling complex are not fully understood (Liu et al., 2012; Israel, 2010; Shifera, 2010). So far, a function as scaffolding protein that mediates binding and organization of up- and downstream signaling components is well established (Schrofelbauer et al., 2012; Clark et al., 2011; Chariot et al., 2002; Harhaj et al., 1999; Rothwarf et al., 1998). All of the studies that investigated NEMO function and structure used either ligands that activate only one specific signaling pathway (e.g. TNF, IL-1 β , LPS) (Scholefield et al., 2016; Xu et al., 2009; Herscovitch et al., 2008a; Windheim et al., 2008; Marienfeld et al., 2006; Tang et al., 2003; Chen et al., 2002; Cooke et al., 2001) or investigated the response of non-immune cells (e.g. HeLa cells, porcine kidney cells, HEK 293T cells) to infection (Brady et al., 2017; de Jong et al., 2016; Wang et al., 2012; Soundararajan et al., 2011; Ashida et al., 2010). Therefore, the structural and post-translational modifications as

well as the role of NEMO during bacterial infection in immune cells in general or in macrophages in particular remain elusive.

Initiation and assembly of a functional TLR/MyD88/TRAF6/NEMO complex leads to activation of IKK α/β by phosphorylation (Polley et al., 2013). Phosphorylated IKK β then directly induces ubiquitin-mediated degradation of the inhibitory subunits p105 (ERK1/2 pathway) and I κ B α (NF- κ B pathway) (Kanarek et al., 2012; Li et al., 1999; Brown et al., 1995; Traenckner et al., 1995). p105, together with ABIN2, releases the kinase TPL2 that initiates a phosphorylation cascade resulting in activation of ERK1/2 (Gantke et al., 2012; Beinke et al., 2004; Waterfield et al., 2004) (Fig. 9). I κ B α sequesters NF- κ B in the cytosol and its degradation releases NF- κ B. Activation of the ERK1/2 and NF- κ B pathways lead to nuclear translocation and/or activation of transcription factors that are crucial for the pro-inflammatory response (Newton et al., 2012). Regulation of this response to individual PAMPs such as LPS (gram-negative) or lipoteichoic acid (gram-positive) that stimulate individual TLR signaling pathways has been extensively studied (Kawai et al., 2011; Hambleton et al., 1996). However, again, much less is known about the response to complex stimuli such as pathogenic bacteria that simultaneously activate multiple signaling pathways.

1.2.3 ROS production in macrophages – with the license to kill

Recognition of pathogens by macrophages leads to a substantial and fast increase of ROS production into the extracellular space and into the phagosome (Gluschko and Herb et al., 2018; Craig et al., 2009). This rapid increase of ROS accompanied by elevated oxygen consumption is known as the respiratory burst. It is catalyzed by Nox2, the predominant and well-characterized ROS source in phagocytes including macrophages (Babior, 2002).

Nox2 consists of two membrane bound subunits, gp91^{phox} and p22^{phox} that form the catalytic unit, named flavocytochrome b₅₅₈, three cytosolic subunits (p40^{phox}, p47^{phox}, p67^{phox}) and the small GTPase Rac1 (Fig 10) (Kawahara et al., 2005; Ago et al., 2003; Ito et al., 1995). Different chemical and biological stimuli (e.g. pathogenic infection) result in translocation of p67^{phox} to the flavocytochrome b₅₅₈ guided by p40^{phox} and/or p47^{phox}. p67^{phox} and Rac1 then mediate electron transfer from NADPH to the prosthetic groups of gp91^{phox} (FADH₂ and two hemes). gp91^{phox} finally transfers the electrons to molecular oxygen forming $\cdot\text{O}_2^-$ (Haslund-Vinding et al., 2017; Bedard et al., 2007). Several studies have shown that a functional and active Nox2 and the subsequently produced ROS are crucial players in anti-microbial immunity (Gluschko and Herb et al., 2018; Herb et al., 2018; Singel et al., 2016; Schramm et al., 2014; Leto et al., 2009).

Figure 10

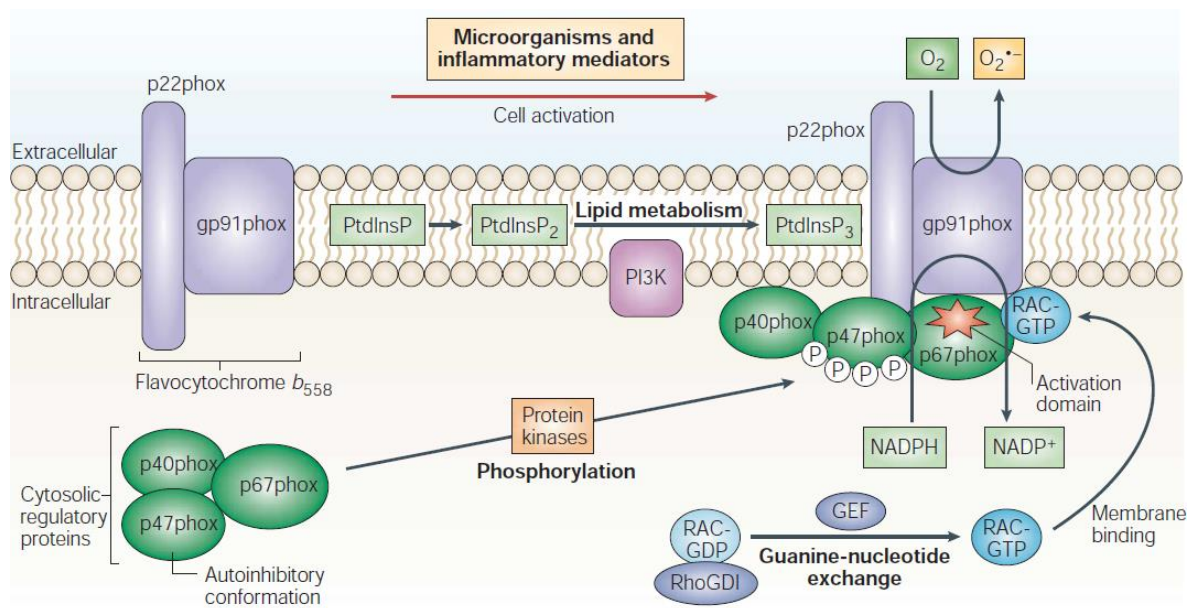


Figure 10: Activation and ROS production by Nox2 (adapted from Lambeth et al., 2004)

Different chemical and biological stimuli, including pathogenic infections result in the activation of Nox2, which requires recruitment of the cytosolic subunits p40^{phox}, p47^{phox}, p67^{phox} and activation of the small GTPase Rac1 (RAC-GTP). Rac1 is released from its inhibitor Rho GDP dissociation inhibitor (RhoGDI) after exchange of GDP with GTP by different guanine exchange factors (GEF). Nox2 activation also needs membrane lipid remodelling. Phosphatidylinositol 3 kinase (PI3K) adds a phosphate group to phosphatidylinositol diphosphate (PtdInsP₂), which is necessary for re-organization of the Nox2 subunits p22^{phox} and gp91^{phox}. Finally, fully active Nox2 produces ROS into the extracellular space.

For a long time, it was generally accepted that mitochondria, as energy generating organelles, produce ROS only as an “accidental” by-product of respiratory activity and increased mitochondrial ROS production was only seen in a harmful context (Yang et al., 2016; Li et al., 2013; Yuan et al., 2013; Dillin et al., 2002). However, several studies have shown that mitochondrial ROS production can be actively triggered and increased by macrophages upon recognition of bacteria or bacterial PAMPs (Zorov et al., 2014). Furthermore, this increased mitochondrial ROS production is necessary for direct antimicrobial host defense (Garaude (Garaude et al., 2016; West et al., 2011b) (Fig. 11).

Figure 11

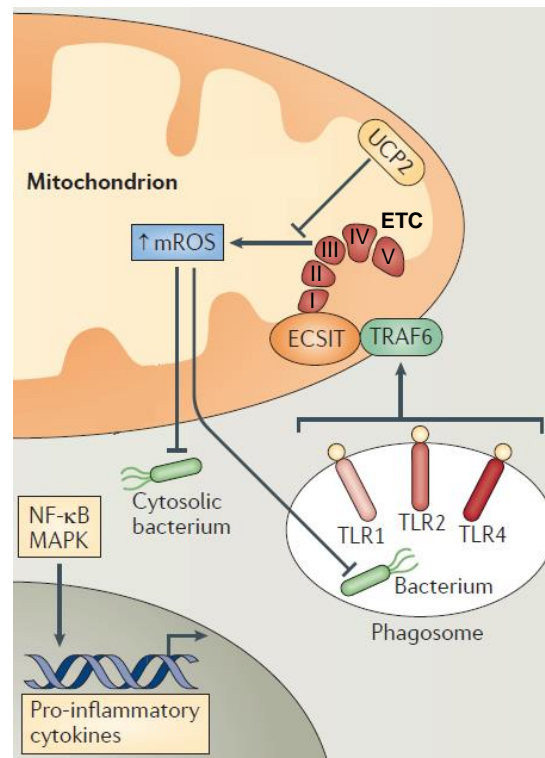


Figure 11: Mitochondrial ROS production is necessary for direct antimicrobial host defense (adapted from West et al., 2011).

Mitochondrial ROS production into the phagosome is actively triggered via relocation of ECSIT/TRAFA6 to complex I of the ETC after recognition of gram-negative bacteria. The mitochondrial ROS production has been shown to be necessary for bacterial clearance.

1.3 ROS in pro-inflammatory signaling – a nearly blank paper

The direct anti-bacterial role of Nox2-derived as well as mitochondrial ROS against invading bacteria was shown in several studies (Gluschko and Herb et al., 2018; Garaude et al., 2016; Schramm et al., 2014; Roca et al., 2013; West et al., 2011b; Arsenijevic et al., 2000). However, the role of ROS in the pro-inflammatory response of macrophages to pathogenic bacteria in general or infection with *L.m.* in particular is incompletely understood (Brune et al., 2013; Forman et al., 2002).

Deficiency for Nox2 and Nox2-derived ROS not only leads to severe immunodeficiency but also influences MHC-dependent antigen presentation and leads to a hyper-inflammatory response accompanied by elevated cytokine levels (Allan et al., 2014; Rieber et al., 2012). The lack of ROS-mediated inactivation of cathepsins has been suggested as a possible mechanism during both processes (Allan et al., 2014; Deffert et al., 2012).

If and how mitochondrial ROS contribute to pro-inflammatory signaling in macrophages remains an open question as several studies have come to different, sometimes contrasting conclusions (Kelly et al., 2015; Bulua et al., 2011a; Zhou et al., 2011; Chandel et al., 2000). Inactivation of redox-sensitive phosphatases has been suggested as ROS-dependent regulatory step (Bulua et al., 2011a; Meinhard et al., 2001). Nearly nothing is known about the role of mitochondrial ROS during pro-inflammatory signaling in infected macrophages, since all of the studies that investigated this topic used either PAMP such as LPS or intrinsic molecules such as TNF that activate only one distinct signaling pathway. In particular, the underlying molecular mechanisms by which mitochondrial ROS may regulate pro-inflammatory signaling and cytokine secretion upon bacterial infection have remained completely elusive.

1.4. Aims of this study

The aim of this thesis is to investigate if and how Nox-derived and/or mitochondrial ROS regulate the pro-inflammatory response during bacterial infection and to identify the ROS-dependent molecular mechanisms involved in this process.

2. Materials & Methods

2.1. Animals, bacteria, materials

2.1.1 Mice

Mice were heterozygously backcrossed to the C57BL/6 strain at least to the 10th generation. Animals were bred under specific pathogen-free conditions at the animal facilities of the Medical Centre of the University of Cologne (Cologne, Germany). Homozygous transgenic knock-out mice and corresponding wild-type littermates, six to ten weeks old, were used for experiments. All experiments were performed in accordance with the Animal Protection Law of Germany in compliance with the Ethics Committee at the University of Cologne.

Nox1^{-/-} mice

Breeding pairs of mice deficient for Nox1 (Gavazzi et al., 2006) were kindly provided by K.-H. Krause (Department of Pathology and Immunity, Université de Genève, Geneva).

Nox2^{-/-} mice

Breeding pairs of mice deficient for the Nox2 subunit gp91^{phox} (Pollock et al., 1995) were kindly provided by R. Brandes (Institute for Cardiovascular Physiology, University Hospital Frankfurt, Frankfurt).

Nox4^{-/-} mice

Breeding pairs of mice deficient for Nox4 (Carneseccchi et al., 2011) were kindly provided by R. Brandes (Institute for Cardiovascular Physiology, University Hospital Frankfurt, Frankfurt).

p22^{phox}^{-/-} mice

Breeding pairs of mice deficient for the catalytic subunit of Nox1-Nox4 p22^{phox} (Nakano et al., 2008) were kindly provided by J. Woo (Dept of Cardiothoracic Surgery, Stanford University Medical Center, Stanford).

Duox1^{-/-} mice

Breeding pairs of mice deficient for Duox1 (Donko et al., 2010) were kindly provided by M. Geiszt (Institute for Physiology, Semmelweis University, Budapest).

Duox2^{-/-} mice

Breeding pairs of mice deficient for Duox2 (Johnson et al., 2007) were purchased from the Jackson Laboratory (USA).

TLR2^{-/-} mice

Breeding pairs of mice deficient for TLR2 (Wooten et al., 2002) were purchased from the Jackson Laboratory (USA).

MyD88^{-/-} mice

Breeding pairs of mice deficient for MyD88 (Adachi et al., 1998) were kindly provided by M. Pasparakis (University of Cologne, Cologne).

TRAF6^{MYEL-KO} mice

Breeding pairs of TRAF6^{fl/fl}/LysMCre^{+/-} (Imai et al., 2008) mice were kindly provided by M. Pasparakis (University of Cologne, Cologne).

Mitochondrial Catalase knockin (mCAT-KI) mice

Breeding pairs of mice with a mitochondrial catalase knock-in (Schriner et al., 2005) were purchased from the Jackson Laboratory (USA).

TNF^{-/-} mice

Breeding pairs of mice deficient for TNF (Adachi et al., 1998) were kindly provided by S. Nedoskasov (German Rheumatism Research Center, Berlin).

2.1.2 Bacteria

Wild-type *L. monocytogenes*, strain EGD, serotype 1/2a was kindly provided by C. Knocks (Harvard Medical School, Boston, USA). The isogenic Δhly - and $\Delta prfA$ -deletion mutants of *L. monocytogenes* (Peters et al., 2003) were kindly provided by E. Domann (University of Giessen, Germany). The wild-type *B. subtilis subsp. spizizenii* strain and *E. coli* K12 DH5-alpha strain were purchased from the DSMZ (DSM 6405). Single colonies of strains were expanded in BHI medium at 37 °C and 220 rpm until log-phase growing. Aliquots of cultures were stored in DMSO at -80 °C for long term storage.

2.1.3 Chemicals and additives

Chemicals were of research grade and stored at 2-8 °C as not stated otherwise. All stock solutions were prepared in H₂O (*aqua ad iniectabilia*) or H₂O_{bidest} from an EASYpure UV/UF

H₂O purification unit (Werner Reinstwassersysteme, Leverkusen) and sterilized by filtration by using a 0.2 µm filter as not further indicated.

Table 1: List of Chemicals and additives (continued on next page)

Name	Stock solution/Manufacturer
[γ-P32]ATP	Hartmann Analytic
2-Propanol	Carl-Roth GmbH & Co. KG, stored at RT
5,6-Dicarboxy-2',7'-dichlorodihydrofluorescein diacetate, di(acetoxymethyl ester)	20 mM Stock in DMSO, Thermo Scientific, stored at -20 °C
Acrylamide 4K-Solution Mix (40 %)	AppliChem
Agarose	Biobudget Technologies GmbH, stored at RT
Antimycin A	30 mM Stock in DMSO, Sigma-Aldrich, stored at -20 °C
APS	Sigma-Aldrich
Benzonase® Nuclease	Merck Millipore, stored at -20 °C
Bromphenol blue	Sigma-Aldrich, stored at RT
BSA Fraction V	Sigma-Aldrich
Calyculin A	Merck Millipore, stored at -20 °C
CCCP	100 mM, Sigma-Aldrich, stored at -20 °C
CD11b Micro beads (human, mouse)	Miltenyi Biotec
DAPI	Sigma-Aldrich, stored at -20 °C
Deoxycholic acid	Sigma-Aldrich
DEPC	Sigma-Aldrich
Dithiothreitol	Sigma-Aldrich
DMSO	Merck Millipore, stored at RT
EDTA	Carl Roth GmbH & Co. KG, stored at RT
EGTA	Carl Roth GmbH & Co. KG, stored at RT
FCS	Biowest AG
Glycerol	AppliChem, stored at RT
HCl	Carl-Roth GmbH & Co. KG, stored at RT
HiMark™ Pre-stained Protein Standard	Thermo Scientific, stored at -20 °C
Horseradish Peroxidase	400 U/ml in HBSS, Merck Millipore, stored at -20 °C
Innovative Grade US Origin CD-1 Mouse Complement	Dunn Lab, stored at -20 °C
Isoluminol	50 mM Stock, Sigma-Aldrich, stored at RT
LCS-1	Calbiochem, stored at -20 °C
LumiGLO Reserve Chemiluminescent substrate	KPL Inc
Malonate	100 mM Stock, Sigma-Aldrich, stored at -20 °C
Milk powder	Carl Roth GmbH & Co. KG
Mito-TEMPO	50 mM Stock in DMSO, Sigma-Aldrich, stored at -20 °C
MOPS	Sigma-Aldrich
Na-Acetate	Merck-Millipore
N-Acetylcysteine	500 mM Stock in PBS pH 7.4, Sigma-Aldrich
NaCl	AppliChem
Na-orthovanadate	Merck Millipore, stored at -20 °C
Na-Pyruvate (100 mM)	Biochrom AG
Nonidet P40 (NP40)	Sigma-Aldrich

Okadaic acid	Merck Millipore, stored at -20 °C
PageRuler Prestained Protein Ladder	Thermo Scientific, stored at -20 °C
Paraformaldehyde	Merck Millipore
PD98059	Merck Millipore, stored at -20 °C
Phosphatase Inhibitor Cocktail Tablets (PhosSTOP)	Roche Lifescience, stored at -20 °C
PMA	6 µg/ml Stock in DMSO , Sigma-Aldrich, stored at -20 °C
Poly(dI:dC)	Roche
Polynucleotide kinase	Roche, stored at -20 °C
ProLong Gold antifade reagent	Invitrogen, stored at -20 °C
Protease Inhibitor Cocktail Tablets (cOmplete)	Roche Lifescience, stored at -20 °C
PTP-Inhibitor I	Merck Millipore, stored at -20 °C
Rotenone	50 mM Stock in DMSO, Sigma-Aldrich, stored at -20 °C
Sanguinarine	Sigma-Aldrich, stored at -20 °C
Saponin from quillaja bark	Sigma-Aldrich, stored at RT
SDS	AppliChem
Tautomycin	Merck Millipore, stored at -20 °C
TEMED	AppliChem
TMRE	50 mM in DMSO, Invitrogen, stored at -20 °C
Tris	Th. Geyer GmbH & Co. KG, stored at RT
Triton X-100	Sigma-Aldrich, stored at RT
Tween-20	AppliChem, stored at RT
Ultrapure LPS from <i>E. coli</i> O111:B4	5 mg/ml Stock, Invivogen, stored at -20 °C
β-mercaptoethanol (98 %)	Merck Millipore, stored at RT

2.1.4 Buffers, solutions and media

All buffers and solutions were prepared with deionized water (H₂O_{bidest}) and sterilized by either autoclavation or sterile filtration using 0.2 µm filters. All liquids were stored at 2-8 °C as not indicated otherwise.

Table 2: List of Buffers, solutions and media (continued on next pages)

Name	Chemical composition/Manufacturer
<i>Aqua ad iniectabilia</i>	Delta-Pharma, Inc.
AT-Lysis buffer	20 mM HEPES, 150 mM NaCl, 1 % Triton X-100, 20 % Glycerol, 1 mM EDTA, 1mM EGTA, 20 mM NEM, pH 7.4, stored at RT
BHI medium	Beckton Dickinson GmbH
Blocking buffer (Microscopy)	3 % BSA in PBS
Blocking buffer (Western Blot)	5 % BSA in TBS-T, stored at -20 °C
Dulbeccos MEM (1X)	Biochrom AG
EDTA solution	0.2 M EDTA in PBS, stored at RT
EGTA solution	0.2 M EGTA in PBS, stored at RT
EMSA binding buffer	5 mM HEPES (pH 7.8), 5 mM MgCl ₂ , 50 mM KCl, 5 mM DTT, 10 % glycerol

EMSA buffer A	10 mM HEPES, 10 mM KCl, 0.1 mM EDTA, 0.1 mM EGTA, for usage add 1 mM DTT and 1 mM PMSF
EMSA buffer C	20 mM HEPES, 0.4 mM NaCl, 1 mM EDTA, 1 mM EGTA
FACS Fix solution	2.5 % formaldehyde, 1 % FCS in PBS, stored at RT
Formaldehyde buffer (10X)	200 mM MOPS, 50 mM Na-Acetate, 10 mM EDTA in DECP-treated RNase-free H ₂ O _{bidest} , pH 7.0
Formaldehyde solution (37 %)	Carl Roth GmbH & Co. KG, stored at RT
H ₂ O ₂ -Solution (30 %)	Sigma-Aldrich
HBSS (1X, with Ca ²⁺ , with Mg ²⁺ , no phenol red)	Life Technologies
HEPES buffer (1 M)	Biochrom AG
Laemmli buffer (5X) (Non-reducing Western Blot)	30 mM Tris/HCL, 12.5 % Glycerol, 1 % SDS, 0.01 % bromphenol blue, stored at -20 °C
Laemmli buffer (5X) (Standard Western Blot)	60 mM Tris-HCl, 25 % Glycerol, 10 % β-mercaptoethanol, 2 % SDS, 0.2 % bromphenol blue, stored at -20 °C
MACS buffer	0.5 % BSA, 200 mM EDTA in PBS
NaCl lysis buffer (0.2 %)	0.2 % NaCl in H ₂ O
NaCl lysis buffer (1.6 %)	1.6 % NaCl in H ₂ O
NEM	20 mM in 99.8 % Ethanol ROTIPURAN®, stored at -20 °C
NP40 solution	10 % NP40 in PBS
Paraformaldehyde solution	3 % PFA in PBS pH 7.4, stored at -20 °C
PBS Dulbecco (1X, pH 7.4)	Biochrom AG
RIPA buffer	150 mM NaCl, 50 mM TrisHCl, 1 % SDS, 0.5 % NP40, 0.1 % deoxicolic acid, stored at RT
RNA loading buffer (5X)	16 µL saturated bromphenol blue solution, 4 mM EDTA, 720 µL formaldehyde solution (37 %), 20 % glycerol, 3.084 ml formamide solution, 4 mL formaldehyde buffer (10X) in 10 mL DECP-treated RNase-free H ₂ O _{bidest}
Roti-Blot A anode buffer (10X)	Carl Roth GmbH & Co. KG, stored at RT
Roti-Blot K cathode buffer (10X)	Carl Roth GmbH & Co. KG, stored at RT
Running buffer (RNA gel)	50 ml formaldehyde buffer (10X), 10 ml formaldehyde solution (37 %) in 440 ml DECP-treated RNase-free H ₂ O _{bidest}
Saponin blocking buffer	0.1 % Saponin, 3 % BSA in PBS
Saponin washing buffer	0.1% Saponin in PBS
TAE buffer (50X)	2 M Tris-acetate, 50 mM EDTA, pH 8.5
TBE buffer (10X)	0.89 mM boric acid, 20 mM EDTA, pH 8.5
TBS (10X)	150 mM NaCl, 10 mM Tris-HCl, pH 7.4, stored at RT
TBS-T	0.1 % Tween 20 in 1X TBS, stored at RT
TGS buffer (10X) (running buffer)	Bio-Rad Laboratories, Inc, stored at RT
Tris-HCl buffer (0.5 M and 1.5 M)	Bio-Rad Laboratories, Inc, stored at RT
Trypan blue solution (1X)	Sigma-Aldrich, stored at RT

2.1.5 Antibodies

Table 3: List of antibodies

Antigen	Specification	Manufacturer
β -actin IgG	Monoclonal mouse-anti- β -actin antibody	Sigma-Aldrich
CD11b IgG	Rat-anti-mouse CD11b antibody, APC-conjugated	BD Biosciences
CD16/CD32 IgG	Rat-anti-mouse CD16/32 (mouse Fc receptor block)	BD Biosciences
F4/80 IgG	Anti-mouse F4/80 antibody, PE-conjugated	eBioscience
<i>L. monocytogenes</i>	Polyclonal rabbit anti- <i>L. monocytogenes</i> antibody	US Biologicals
Mouse IgG	Goat-anti-mouse antibody, HRP-conjugated	Sigma-Aldrich
Rabbit IgG	Goat-anti-rabbit antibody, AlexaFluor 405-conjugated	Molecular Probes
Rabbit IgG	Goat-anti-rabbit antibody, AlexaFluor 488-conjugated	Molecular Probes
Rabbit IgG	Goat-anti-rabbit antibody, AlexaFluor 568-conjugated	Molecular Probes
Rabbit IgG	Goat-anti-rabbit antibody, HRP-conjugated	Sigma-Aldrich
NF- κ B p65 (F-6) (Microscopy)	Monoclonal mouse-anti-NF κ B p65 antibody	Santa Cruz Biotechnology, Inc.
FLAG (Microscopy)	Monoclonal mouse-anti-FLAG antibody	Sigma-Aldrich
FLAG (Western Blot)	Monoclonal mouse-anti-FLAG antibody	Cell Signaling Technology
NEMO/IKK γ	Monoclonal mouse-anti-IKK γ antibody	Invitrogen
IRAK1	Monoclonal rabbit-anti-IRAK1 antibody	Cell Signaling Technology
Phospho-IKK α/β (Ser176/180)	Monoclonal rabbit-anti-phospho-IKK α/β antibody	Cell Signaling Technology
I κ B α IgG	Polyclonal rabbit-anti-I κ B- α antibody	Santa Cruz Biotechnology, Inc.
Phospho-NF- κ B p65 (Ser536) IgG	Monoclonal rabbit-anti-phospho-NF- κ B p65 antibody	Cell Signaling Technology
Phospho-SAPK/JNK (Thr183/Tyr 185)	Polyclonal rabbit-anti-phospho-IKK α/β antibody	Cell Signaling Technology
Phospho-MEK1/2 (Ser217/221)	Polyclonal rabbit-anti-phospho-IKK α/β antibody	Cell Signaling Technology
Phospho-ERK1/2	Polyclonal rabbit-anti-phospho-ERK1/2 antibody	Cell Signaling Technology
Phospho-p38 (Thr180/Tyr182) IgG	Monoclonal rabbit-anti-phospho-p38 antibody	Cell Signaling Technology

2.1.6 Molecularbiological materials, constructs and primers

Table 4: Molecularbiological materials, constructs and primers (continued on next page)

Material/Construct/Primer	Sequence	Manufacturer
5mCTP		Jena Bioscience, stored at -20 °C
Antarctic phosphatase		New England BioLabs, stored at -20 °C
FastDigest XbaI		Thermo Scientific

GelRed™		Biotium
Mutant IKKβ IKK-2 ^{S177/181E} construct	Cat#: 11104	Addgene, stored at -20 °C
Mutant NEMO ^{C54/347A} construct	Cat#: 27268	Addgene, stored at -20 °C
O'GeneRuler™ 1 kb DNA Ladder		Thermo Scientific
Orange DNA Loading Dye (6X)		ThermoScientific
Pseudo-UTP		Jena Bioscience, stored at -20 °C
Q5® High-Fidelity DNA-Polymerase		New England Biolabs Inc
ssRNA ladder		NewEngland Biolabs
T7-Promotor forward primer	5- GAAATTAATACGACTCACTATAGGGTT GATCTACCATGGACTA-CAAAGACG-3	XXX, stored at -20 °C
T7-Promotor reverse primer	5-GAGGAAGCGAGAGCTCCATCTG-3	XXX,stored at -20 °C
Wild type control IKKβ IKK-1 construct	Cat#: 11103	Addgene, stored at -20 °C
Wild type control NEMO construct		Addgene, stored at -20 °C

2.1.7 PCR programs

Table 5: PCR programs

Program/reaction step	Temperature (°C)	Time (s)
T7-Promotor PCR		
Initial denaturation	98	30
Denaturation	98	10
30 Cycles		
Annealing	56	20
Elongation	72	120
Final elongation	72	180
Standby	4	∞

2.1.8 Consumable materials

Table 6: Consumable materials (continued on next page)

Name	Manufacturer
96F Non-treated Microwell SI (white, black)	Thermo Scientific, Nunc
Amersham ECL hyperfilm	GE Healthcare
BD Microlance 3 Needles (Nr.1, 14, 20)	Beckton Dickinson GmbH
Blood agar plates (sheep)	Oxoid Deutschland GmbH
Cover glass (Ø 13 mm)	VWR International
Criterion Empty Cassettes	Bio-Rad Laboratories, Inc.
FACS tubes (5 ml)	BD Biosciences
Falcon tubes (15, 50 ml)	Greiner Bio-One
Microscope slides	Engelbrecht
MS MACS Separation Columns (LS)	Miltenyi Biotec
Omnifix Syringes (5, 10 ml)	B. Braun
Parafilm	American National Can

Pipette tips (5, 10, 25 ml)	Sarstedt
Prot/Elec Tips (gel loading)	Bio-Rad Laboratories, Inc.
Tissue Culture Test plates (6-, 12-, 24-, 96F-, 96U-Well)	TPP
Whatman 3MM filter paper	GE Healthcare
Whatman Nitrocellulose membrane	GE Healthcare

2.1.9 Technical equipment and devices

Table 7: Technical equipment and devices (continued on next page)

Device	Specification	Manufacturer/Distributor
Balance	Sartorius L2200P	Gemini B. V.
Cell counting chamber	Neubauer Improved	LO Laboroptik
Centrifuges	Heraeus Multifuge 4KR	Thermo Scientific
	Eppendorf 5417R	Thermo Scientific
ChemiDoc	ChemiDoc™ Imaging System	Bio-Rad Laboratories, Inc.
Developer	Curix	AGFA
Diaphragm vacuum pump	Vacuubrand	Bachofer Labor Geräte
EasyCool™ Beer Cooling Device	EasyCool 1.0	Gluscho Bioreserch, Inc.
Electrophoresis cell	Criterion cell	Bio-Rad Laboratories, Inc.
Flow cytometer	FACSCalibur	BD Biosciences
Fluorescence microscope (confocal)	IX81	Olympus
Gel electrophoresis chamber		Bio-Rad Laboratories, Inc.
H ₂ O purification unit	EASYpure UV/UF	Werner Reinstwassersysteme
Incubator (bacteria)	Kelvitron T	Heraeus Instruments GmbH
Incubator (cells)	Hera Cell 240	Heraeus Instruments GmbH
Incubator shaker	Innova 4200	New Prunswick Scientific
Laminar flow hood	HERAsafe	Thermo Scientific
	HERAsafe KS	Thermo Scientific
Magnetic mixer	RCT basic	Kika Labortechnik
Magnetic Seperator	QuadroMACS	Miltenyi Biotec
Microcentrifuge	GalaxyMiniStar	VWR International
Microscope	CKX41	Olympus
Microtiterplate-reader	Tecan infinite M1000	Tecan Group Ltd.
	TriStar2 LB 942	Berthold Technologies
Nanodrop	Nanodrop 2000	Thermo Scientific
PCR Thermocycler	T3000	Biometra
Photometer	Eppendorf Bio	Thermo Scientific
Power Supply	Power Pac 3000	Bio-Rad Laboratories, Inc.
Protein blotting system	Trans-Blot Turbo	Bio-Rad Laboratories, Inc.
Shaker	Titramax 101	Heidolph
Thermomixer	Eppendorf comfort	Thermo Scientific
Tumbling table	Biometra WT 12	Biometra GmbH
Vacuum gas pump	VP 86	VWR International
Vortexing device	Omnilab REAX 2000	Heidolph

2.1.10 Kits

Table 8: Kits

Name	Manufacturer
Amersham ECL Detection reagents	GE Healthcare
BCA Protein Assay Kit	Thermo Scientific
BD OptEIA™ TMB Substrate Kit for ELISA	BD Biosciences
CellTiter-Glo® Luminescent Cell Viability Assay	Promega
CyQuant®Direct Cell Proliferation Assay Kit	Molecular Probes
CytoTox-Glo™ Cytotoxicity Assay	Promega
DuoSet ELISA 15 Plate (mouse IL-1 beta/IL-1F2, IL-6, TNF-α)	R&D Systems, Inc.
HiScribe T7 ARCA mRNA kit (with polyA tailing)	New England BioLabs
jetMESSENGER®	Polyplus transfection
MEGAclean transcription clean-up kit	Qiagen
ProcartaPlex™ Multiplex Immunoassay	eBioscience
QIAquick PCR purification	Qiagen

2.1.11 Software

Table 9: Software

Programm	Provider
CellQuest Pro	BD Bioscience
Fluoview FV10 ASW 1.7b	Olympus Corporation
GraphPad Prism 5.04	GraphPad Software, Inc.
ImageJ 1.46h	Wayne Rasband
Micro Win 2000	Berthold Technologies
Nanodrop 2000 software	Thermo Scientific
Office Professional Plus 2010	Microsoft
Photoshop CS3	Adobe
Tecan i-control 1.7	Systat Software, Inc

2.2. Methods

All cells were plated and incubated overnight at 37 °C with 5 % CO²-enriched and water vapour saturated atmosphere without antibiotics one day prior to experiments were performed. All cells were centrifuged at 650 x g, at 4 °C for 5 min unless otherwise specified.

2.2.1 Molecularbiological methods

All PCR reactions were performed in a PCR Thermocycler T3000 (Biometra) and nucleic acids concentrations were determined with a Nanodrop (Thermo Scientific) as not further indicated. Wild type and NEMO^{C54/347A} constructs (originally aquired from Addgene) were kindly provided by T. Gilmore (Boston University, Massachusetts, USA).

2.2.1.1 Transformation and replication of DNA

Transformation and replication of wild type NEMO, mutant NEMO^{C54/374A}, IKK1 and IKK2 plasmids was kindly achieved by Daniela Grumme from AG Krönke with the QIAGEN Plasmid Miniprep Kit in accordance with the manufacturer's instructions. Plasmids were purified with the QIAquick PCR Purification Kit in accordance with the manufacturer's instructions.

2.2.1.2 Linearisation of Plasmids

Linearisation of the wild type NEMO and mutant NEMO^{C54/374A} DNA plasmids was achieved with the FastDigest XbaI restriction kit. 10 µg of DNA was mixed with 80 µl RNase-free water, 10 µl 10X FastDigest buffer and 5 µl XbaI FastDigest, vortexed and briefly centrifuged. Restriction was achieved by incubation at 37 °C with 500 rpm O/N. Linearised plasmids were purified with the QIAquick PCR Purification Kit in accordance with the manufacturer's instructions.

2.2.1.3 T7-Promotor PCR

All kit components were thawed, vortexed, briefly centrifuged and kept on ice.

Linearised NEMO constructs already contain a T7-Promotor sequence. Addition of the T7-Promotor to IKK1 and IKK2 DNA templates was achieved by using the Q5® High-Fidelity Polymerase. 10 ng of linearized DNA template was mixed with 0.1 µl T7-Promotor forward primer and 0.1 µl T7-Promotor reverse primer. The reaction mix was filled up to 25 µl total with RNase-free water, vortexed and briefly centrifuged. The program „T7-Promotor PCR” (Table 5) was used for this PCR. Linearised T7-Promotor-plasmids were purified with the QIAquick PCR Purification Kit in accordance with the manufacturer's instructions.

Quality control was assessed by electrophoresis on a 1 % agarose gel. Gels were prepared by heating 1 gram agarose in TAE buffer (1X) until dissolved. 10 µl GelRed® was added. After 30 min of polymerization, gels were assembled in a tank filled with TAE (1X). 1 µl per DNA sample was mixed with 2 µl Orange DNA loading dye (1X) and 7 µl of H₂O_{bidest.}, vortexed, briefly centrifuged and immediately loaded into the gel. For DNA length determination 6 µl of O'GeneRuler™ was loaded into the gel. Electrophoresis was performed at 100 V constant current. Gels were analyzed with a ChemiDoc™ (Bio-Rad Laboratories, Inc.).

2.2.1.4 mRNA-Synthesis

All kit components were thawed, vortexed, briefly centrifuged and kept on ice. All incubation steps were performed at 400 rpm and 37 °C with a Thermomixer (Thermo Scientific) as not further indicated.

T7-mRNA synthesis was achieved by using the HiScribe™ ARCA mRNA Kit (with Tailing) (NEB) in accordance with the manufacturer's instructions. 1 µg of T7-Promotor DNA template was mixed with 10 µl of 2X ARCA/NTP Mix and 2 µl T7 RNA Polymerase Mix. In addition, 0.5 µl of Pseudo-UTP and 0.5 µl 5mCTP were added for immunogenic reduction. The reaction mix was filled up to 20 µl total with RNase-free water, vortexed, briefly centrifuged and incubated for 30 min to generate a T7-Promotor guided mRNA construct.

2 µl of DNase was added to the 20 µl reaction mix. The mix was vortexed, briefly centrifuged and incubated for 15 min to remove T7-DNA templates.

22 µl of mRNA was mixed with 5 µl of 10X Poly(A) Reaction Polymerase Reaction buffer and 5 µl Poly(A) Polymerase. The reaction mix was filled up to 50 µl total with 18 µl of RNase-free water, vortexed, briefly centrifuged and incubated for 30 min to add a Poly(A)-Tail to the construct. This step enhances durability in the cytosol of transfected cells.

50 µl of Poly(A)-tailed mRNA was mixed with 6 µl of 10X Antarctic phosphatase Reaction buffer and 3 µl Antarctic phosphatase. The reaction mix was filled up to 60 µl total with 1 µl of RNase-free water, vortexed, briefly centrifuged and incubated for 30 min to remove phosphate residues from mRNA 5'- and 3'-ends. Samples were heated at 80 °C for 2 min to inactivate the phosphatase. This step prevents religation of mRNA constructs.

To remove unused NTPs, enzymes and buffer components, synthesized and modified mRNA constructs were purified with the MEGAclean™ Transcription Clean-up Kit in accordance with the manufacturer's instructions.

Quality control of mRNA synthesis and purification was assessed by electrophoresis on a denaturing formaldehyde agarose gel. Gels were prepared by heating 0.6 g agarose in 1X Running buffer until dissolved, then cooled to 65 °C. 900 µl formaldehyde (37 %) and 0.5 µl ethidium bromide was added. After 30 minutes of polymerisation gels were assembled in a tank filled with Running buffer (1X) and incubated for another 30 minutes for equilibration. 10 µl per RNA sample was mixed with 2.5 µl of RNA loading buffer (5X) vortexed, heated at 65 °C for 5 minutes and after short cooling on ice immediately loaded into the gel. For RNA length determination 32 µl of RNA ladder was mixed with 8 µl of RNA loading buffer (5X) and also loaded into the gel. Electrophoresis was performed at 7 V/cm and 60 V constant current. Gels were analyzed with a ChemiDoc™ (Bio-Rad Laboratories, Inc.).

2.2.2 Cultivation of bacteria

Log-phase cultures of wt, Δhly , and Δprf *Listeria monocytogenes* (wt L.m., Δhly L.m., Δprf L.m.), *Bacillus subtilis* (B.sub), *Escherichia coli* (E.coli), were thawed and plated out on blood agar plates and grown overnight at 37 °C. Single colonies were picked and expanded in 5 ml BHI overnight at 37 °C and 220 rpm. Before experiments, overnight cultures were diluted 1:25 in pre-warmed BHI medium and incubated at 37 °C for two hours with 220 rpm. Bacteria were harvested during midlog-growth phase with an optical density of 0.3 at 600 nm (OD_{600}). Bacterial suspensions were transferred into a 50 ml falcon tube and centrifuged at 3000 x g for 5 min and 4 °C. Supernatants were removed and pellets were washed once with 10 ml ice-cold PBS. After centrifugation, supernatants were removed and pellets were resuspended in 1 ml of ice-cold PBS. Bacterial suspensions were mixed by vortexing and diluted 1:20 in PBS for OD measurement. Density of bacteria was determined by OD_{600} measurement (OD_{600} 1 corresponds to 5×10^8 CFU/ml) and bacterial suspensions were diluted to a stock concentration of 1×10^9 CFU/ml. The stock suspension was used for adjusting the inocula for the experiments. Serial dilutions of inocula were plated on blood agar plates to quantify adjusted CFUs.

2.2.3 Isolation of peritoneal cells

Mice were sacrificed by cervical dislocation and peritoneal cells were harvested by peritoneal lavage with 8 ml ice-old PBS. Peritoneal lavages of mice with the same genotype were pooled. After centrifugation, supernatants were removed and red blood cells were lysed in 5 ml 0.2 % NaCl solution for 30 s. Lysis was stopped by adding 5 ml of 1.6 % NaCl solution.

2.2.4 Immunomagnetic enrichment peritoneal macrophages

After peritoneal lavage and red blood cell lysis, cells were centrifuged and supernatant was removed. Cell pellets were resuspendend in MACS buffer (97.5 μ l per 1 peritoneal exudate). CD11b-specific monoclonal antibodies conjugated to paramagnetic beads (CD11b MicroBeads) were added to the cell suspension (2.5 μ l per 1 peritoneal exudate) and cells were labeled on ice for 15 min with 300 rpm. After labeling, cells were washed three times and sorted in accordance with the protocol of the manufacturer (Miltanyi, Biotec). After elution from the MS columns, cells were resuspendend in DMEM supplemented with 10 % heat-inactivated FCS (DMEM + FCS), cells were diluted and counted in Trypan Blue in a Neubauer chamber for cell number determination and exclusion of dead cells.

2.2.5 Flow cytometric analysis of peritoneal macrophages

All incubation steps were performed for 15 min on ice and 300 rpm. Aliquots from counted cell suspensions were transferred in a 96-well clear V-bottom plate and 1 μ l FcBlock (BD Pharmingen) was added in order to block unspecific Fc-binding sites. After incubation, cells were incubated with 0.5 μ l PE-conjugated F4/80 antibodies (clone BM8), 0.5 μ l APC-conjugated CD11b antibodies (clone M1/70) or a combination of both. Cells were washed three times by centrifugation and resuspension with MACS buffer. Finally, cells were fixed with FACS Fix solution and transferred to FACS tubes. The percentage of F4/80^{high}/CD11b^{high} peritoneal macrophages was determined by flow cytometry with a FACS Calibur flow cytometer (BD Biosciences) and CellQuest Pro software (BD Biosciences). Peritoneal macrophages were diluted in DMEM + FCS to desired densities, plated out and shortly centrifuged for better adherence.

2.2.6 Transfection of peritoneal macrophages

For transfection of peritoneal macrophages 200 ng of indicated mRNA constructs were complexed to jetMESSENGER (Polyplus-transfection) in accordance with the manufacturer's instructions. After 6 h of infection, medium was exchanged and cells were subjected to further experiments.

2.2.7 Quantification of ROS

Peritoneal macrophages were plated out at a density of 5×10^5 cells/well as triplicates in DMEM + FCS in sterile 96F plates. White or black closed bottom plates were used for luminescence or fluorescence measurements, respectively. Pre-treatments were applied by adding 10 μ l of the given substance diluted in DMEM + FCS followed by incubation for 30 min at 37 °C. Cells were centrifuged and washed once with HBSS to remove non-adherent cells and added substances for pre-treatment. For infection or co-incubation, ice cold suspensions of wt *L.m.*, Δhly *L.m.* or Δprf *L.m.*, *B.sub.*, or *E.coli* with a multiplicity of infection (MOI) of 1 or heat-killed *L.m.* (HK *L.m.*) at an MOI-equivalent of 1 were added to wells. Cells without infection received ice-cold HBSS without bacteria. Contact of bacteria to macrophages was achieved by synchronization at 850 x g for 5 min at 4 °C. Every working step after infection was performed on ice. Non-adherent bacteria were removed by washing for three times with ice-cold HBSS. Cells were covered with ice cold HBSS and test compounds were added. As a positive control for extra- and cytosolic ROS measurements PMA, a chemical stimulator of ROS, was added with a final concentration of 1 ng/ml. For ROS measurement in the mitochondrial matrix rotenone, an inhibitor of complex I of electron transport chain, was used as a positive control with a final concentration of 100 μ M.

2.2.7.1 Measurement of extracellular ROS production

For detection of extracellular ROS, a prepared ice-cold solution of cell-impermeable isoluminol and horseradish peroxidase (HRP) in HBSS was used with final concentrations of 50 μM and 3.2 U/ml, respectively. The enzyme horseradish peroxidase uses the produced ROS to catalyze the conversion of isoluminol to the excited 3-aminophthalate. This product decays to lower energy state and emits light in the process, which can be detected as chemiluminescence. After infection and treatment with substances (2.2.7), isoluminol/HRP solution was added to the wells and chemiluminescence was recorded for 60 min with 60 s intervals at 37 °C in a Tristar² multimode plate reader LB 942 (Berthold Technologies). To calculate cell-specific luminescence, the luminescence of cell-free wells containing HBSS with or without used substances was subtracted.

2.2.7.2 Measurement of cytosolic ROS production

For detection of cytosolic ROS, the substance 5,6-carboxy-2',7'-dichlorodihydrofluorescein diacetate, di(acetoxymethyl ester) (referred to as DCF in this thesis) (Invitrogen) was used. DCF was diluted to a final concentration of 20 μM in HBSS. Cells were incubated with DCF solution at 37 °C for 15 min. DCF is a hydrophilic molecule, which readily enters cells by diffusion during incubation. After reaching the cytosol, ester groups of the DCF molecule are cleaved by cytosolic esterases, leading to the loss of hydrophilicity. Lipophilic DCF is trapped in cytosol as dihydrofluorescein. Cleaving of the ester groups also leads to the exposure of functional groups that are able to react with ROS. After reaction with ROS, dihydrofluorescein is converted to its oxidized and fluorescent derivative fluorescein. After incubation, cells were centrifuged and washed for two times with ice cold HBSS. Cells were infected as described in 2.2.7. After infection and addition of test compounds, cells were covered with ice cold HBSS. Fluorescein was excited at 495 nm and emitted fluorescence at 520 nm was recorded for 60 min with 60 s intervals at 37 °C in TriStar² multimode plate reader LB 942 (Berthold Technologies). To calculate cell-specific fluorescence, the fluorescence of cell-free wells containing HBSS with or without used substances was subtracted.

2.2.7.3 Measurement of ROS production in the mitochondrial matrix

ROS production in the mitochondrial matrix was detected by using the fluorescence probe MitoSOX Red (ThermoFisher Scientific). MitoSOX Red was diluted to a final concentration of 5 μM in HBSS. Cells were incubated with MitoSOX Red solution at 37 °C for 15 min. MitoSOX Red accumulates in the mitochondrial matrix and is oxidized exclusively by superoxide. After incubation, cells were washed for three times with ice cold HBSS. Cells were infected as described in 2.2.7. After infection and addition of test compounds, cells were covered with ice

cold HBSS. MitoSOX Red was excited at 510 nm and emitted fluorescence at 580 nm was recorded for 60 min with 60 s intervals at 37 °C in a TECAN infinite M 1000 microplate reader (Tecan Group, Ltd.). To calculate cell-specific fluorescence, the fluorescence of cell-free wells containing HBSS with or without used substances was subtracted.

2.2.8 Cytokine quantification

2.2.8.1 Preparation of supernatants

Peritoneal macrophages were plated at a density of 1.5×10^5 cells/well as duplicates in DMEM + FCS in sterile 24-well plates. Pre-treatments were applied by adding 10 µl of the given substance diluted in DMEM + FCS followed by incubation for 30 min at 37 °C. Cells were centrifuged and washed with HBSS to remove non-adherent cells and added substances for pre-treatment. For infection, ice cold suspensions of L.m, B.sub or E.coli with a MOI of 1 were added to the wells. Cells without infection received ice-cold HBSS without bacteria. Contact of bacteria to macrophages was achieved by synchronization at 850 x g for 5 min at 4° C. Non-adherent bacteria were removed by washing for three times with ice-cold HBSS. Cells were covered with pre-warmed HBSS with 5 % heat-inactivated NMS (HBSS + NMS) with or without test compounds and incubated at 37 °C. At indicated time points supernatants were transferred into a 96U-plate and centrifuged at 650 x g for 5 min at 4 °C to remove cell debris. Cleared supernatants were transferred into a 96F-plate and stored at -80 °C until cytokine determination.

2.2.8.2 ELISA (Enzyme-linked immunosorbent assay)

Cytokines in supernatants were measured by ELISA using capture- and detection antibodies (R&D Systems) in accordance with the manufacturer's instructions. Absorbance was measured with a TECAN infinite M 1000 (Tecan Group, Ltd.).

2.2.9 Measurement of mitochondrial membrane potential

Peritoneal macrophages were isolated and immunomagnetically enriched as described in 2.2.3 and 2.2.4. TMRE (Tetramethylrhodamine, ethyl ester) was diluted to a final concentration of 50 nM in HBSS. Cell pellets were resuspended in 1 ml TMRE solution and filled up to 5 ml final volume. Cells were incubated on a spinning wheel at 37 °C for 15 min. TMRE accumulates in the mitochondrial matrix due to its cationic properties and the negative charge of the matrix. The negative charge is stable as long as protons are pumped across the inner mitochondrial membrane. The charge separation across the membrane causes the mitochondrial membrane potential. Accumulated TMRE shows a red shift in its fluorescence properties and represents stable membrane potential. Loss of membrane potential results in release of TMRE from mitochondria and in a decreased fluorescence signal. After centrifugation, cells were

resuspended and washed three times with pre-warmed HBSS. Cell numbers were determined as described in **2.2.4**. Cells were plated at a density of 0.5×10^6 cells/well and incubated for two hours to allow adhesion. Infection was performed as described in **2.2.7**. Finally, cells were covered with HBSS + NMS with or without test compounds and incubated at 37 °C. The proton shuttling substance carbonyl cyanide m-chlorophenyl hydrazone (CCCP) was used as a negative control. At indicated time points TMRE was excited at 549 nm. Emitted fluorescence at 575 nm was recorded with a TECAN infinite M 1000 microplate reader (Tecan Group, Ltd.). To calculate cell-specific fluorescence, the fluorescence of cell-free wells containing HBSS with or without used substances was subtracted.

2.2.10 Measurement of cellular ATP levels

Cells were plated and infected as described in **2.2.7**. Cells were covered with pre-warmed HBSS + NMS with or without test compounds and cells were incubated at 37 °C. CCCP was used as a negative control. ATP content was determined by using the CellTiter-Glo® Luminescent Cell Viability Assay in accordance to the manufacturer's instructions (Promega). At indicated time points, chemiluminescence was recorded in a Tristar² multi mode plate reader LB 942 (Berthold Technologies). To calculate cell-specific luminescence, the luminescence of cell-free wells containing HBSS with or without used substances was subtracted.

2.2.11 Cell viability/cytotoxicity assays

Cells were plated, infected and treated as described in **2.2.7**. Cells were covered with pre-warmed HBSS + NMS with or without test compounds and cells were incubated at 37 °C.

2.2.11.1 Determination of cell death

The CytoTox-Glo™ Cytotoxicity Assay was used to determine death due to loss of membrane integrity. At indicated time points, cells were treated in accordance with the manufacturer's instructions (Promega) and fluorescence was recorded with a TECAN infinite M 1000 microplate reader (Tecan Group, Ltd.).

2.2.11.2 Determination of cell viability

The CyQUANT® Direct Cell Proliferation Assay was used to determine cell viability. At indicated time points, cells were treated in accordance with the manufacturer's instructions (Promega) and fluorescence was recorded with a TECAN infinite M 1000 microplate reader (Tecan Group, Ltd.).

2.2.12 Cell fixation for microscopy

Peritoneal macrophages were plated at a density of 3×10^5 cells/well in DMEM + FCS on sterile 13 mm Ø cover cells in sterile 24-well plates. Cells were infected, treated and incubated as

described in **2.2.8**. At indicated time points medium was removed, cells were washed once with ice cold PBS and fixed with 3 % PFA in PBS for 20 min at RT. PFA was removed, cells were covered with PBS and stored at 4 °C until immunofluorescence staining (**2.2.13**).

2.2.13 Immunofluorescence staining

All antibodies used for extracellular staining were diluted in PBS containing 3 % BSA and all antibodies used for intracellular staining were diluted in PBS containing 3 % BSA and 0.1 % saponin as not described otherwise. All incubation steps were performed for 30 min at RT as not otherwise specified.

PBS was removed and cells were covered with 1 ml 3 % BSA in PBS for 15 min to block unspecific binding sites. Extracellular L.m. were stained with primary rabbit anti-L.m. antibody. Cells were washed three times with 1 ml PBS and secondary anti-rabbit-antibody, conjugated to AlexaFlour 405 fluorescence dye, was added to cells. Cells were permeabilized before intracellular staining by incubation with 0.1 % saponin in PBS for 15 min. Unspecific binding sites were blocked using 3 % BSA and 0.1 % saponin in PBS for 15 min. Intracellular L.m. were stained with primary rabbit anti-*L. monocytogenes* antibody diluted in 3 % BSA and 0.1 % saponin in PBS. Cells were washed three times with 1 ml PBS. Intracellular L.m. were stained with secondary anti-rabbit antibody, conjugated to AlexaFluor 568 fluorescence dye. Cells were washed twice with PBS and once with H₂O_{bidest}. Additional stainings were performed dependent to the following experiments (see **2.2.13.1**, **2.2.13.2** and **2.2.13.3**). Finally, cells were mounted on microscope slides in ProLong Gold antifade reagent. Sections of preparations were analyzed with an IX81 confocal fluorescence microscope (Olympus).

2.2.13.1 Staining for translocation analysis of NF-κB

Intracellular NF-κB p65 was stained with primary mouse anti-NF-κB p65 antibodies. After washing, NF-κB p65 was stained with secondary anti-mouse antibodies, conjugated to AlexaFlour 488 fluorescence dye. Nuclei were stained with DAPI, diluted with secondary antibodies.

2.2.13.2 Staining of mitochondria

For analysis of the mitochondrial network, mitochondria were stained with the mitochondrial membrane potential-sensitive dye MitoTracker Red CMXRos (Thermo Scientific) at 100 nM for 15 min at 37 °C. After staining peritoneal macrophages were infected, treated and incubated as described in **2.2.8**. CCCP was used as positive control (50 μM).

2.2.13.3 Staining of FLAG-tagged NEMO and IKK β constructs

Transfection (2.2.6), infection (2.2.8) and fixation (2.2.12) were performed as described before. Peritoneal macrophages were permeabilized with 0.25 % Triton X-100. After blocking with 10 % BSA in PBS, FLAG-tagged proteins were stained using a monoclonal antibody against FLAG at 37 °C for 2 h. After washing, NEMO constructs or IKK β constructs were stained with secondary anti-mouse antibodies, conjugated to AlexaFlour 488 fluorescence dye. Nuclei were stained with DAPI, diluted with secondary antibodies. Samples were mounted on glass microscopic slides and stored at 4 °C until analysis.

2.2.14 Western blotting for protein analysis

All incubation steps were performed at RT on an orbital shaker with 300 rpm as not further indicated.

2.2.14.1 Preparation of cell lysates (Standard SDS-PAGE, reducing)

Peritoneal macrophages were plated at a density of 1×10^6 cells/well in DMEM + FCS in sterile 12-well plates. Cells were transfected (2.2.6), infected (2.2.8), treated and incubated (2.2.8) as described before. At indicated time points medium was removed and cells were washed once with ice cold PBS. Ice cold RIPA lysis buffer was added and cells were lysed for 10 min at RT with 1000 rpm. Cell lysates were transferred into 1.5 ml tubes and proteases were inactivated by heating for 10 min at 95 °C. Finally, lysates were incubated on ice for 1 min, briefly centrifuged at 10,000 x g and stored at -80 °C until determination of protein concentration (2.2.14.3).

2.2.14.2 Preparation of cell lysates (SDS-PAGE, non-reducing)

Peritoneal macrophages were plated at a density of 1×10^6 cells/well in DMEM + FCS in sterile 12-well plates. Cells were transfected (2.2.6), infected (2.2.8), treated and incubated (2.2.8) as described before. At indicated time points medium was removed and cells were washed once with ice cold PBS. AT-Lysis buffer was added and cells were lysed for 1 h at RT with 1000 rpm. Cell lysates were transferred into 1.5 ml tubes and proteases were inactivated by heating for 10 min at 95 °C. Finally, lysates were incubated on ice for 1 min, briefly centrifuged at 10,000 x g and directly subjected to non-reducing SDS-PAGE (2.2.14.5).

2.2.14.3 BCA Protein Assay

Protein concentration was determined by using the BCA Protein Assay Kit in accordance with the manufacturer's instructions (Pierce, Thermo Scientific). Final protein concentrations were equally adjusted for each experiment in 5X Laemmli buffer (with or without β -mercaptoethanol) and H₂O_{bidest.}.

2.2.14.4 Standard SDS-PAGE (reducing)

SDS-PAGE was performed in accordance with the protocol of the manufacturer (Bio-Rad Laboratories, Inc.) by using a Criterion Gel cassette containing a 12 % Tris/HCl gel mounted in a Criterion Cell filled with 1X TGS running buffer. Lysates were heated for protein denaturation for 10 min at 95 °C, incubated on ice for 1 min and briefly centrifuged (10,000 x g, 1 min, RT) before gel loading. SDS-PAGE was performed at a constant voltage of 70 V. Gels were incubated in 1X Roti®-Blot K cathode buffer until protein transfer.

2.2.14.5 SDS-PAGE (non-reducing)

SDS-PAGE was performed in accordance with the protocol of the manufacturer (Bio-Rad Laboratories, Inc.) by using a Criterion Gel cassette containing a 10 % Tris/HCl gel mounted in a Criterion Cell filled with 1X TGS running buffer. Lysates were heated for protein denaturation for 10 min at 95 °C without β -mercaptoethanol, incubated on ice for 1 min and briefly centrifuged (10,000 x g, 1 min, RT) before gel loading. SDS-PAGE was performed at a constant voltage of 70 V. Gels were incubated in 1X Roti®-Blot K cathode buffer until protein transfer.

2.2.14.6 Western Blot

Protein transfer from the gel onto a nitrocellulose membrane was achieved by using a Trans-Blot® Turbo™ Transfer system. Blotting was performed with the StandardSD protocol (constant 25 V, 1 A, 30 min) in accordance to the manufacturer's instructions.

2.2.14.7 Antibody staining

After protein transfer, membranes were incubated in blocking buffer for 1 h to block unspecific binding sites. Blocking buffer was removed and membranes were incubated with primary antibody diluted in blocking buffer O/N at 4 °C. Next day unbound primary antibodies were removed by triple washing in TBS-T for 5 min. Afterwards, membranes were incubated with HRP-conjugated secondary antibodies for 1 h. Unbound secondary antibodies were removed by double washing in TBS-T. Membranes were washed once in TBS to remove remaining detergent and stored in TBS at 2-8 °C until visualization.

2.2.14.8 Protein visualisation

Immune complexes were visualized by incubating membranes in Amersham ELC detection reagents (GE Healthcare) or LumiGlo Reserve Chemiluminescent substrate (KPL, Inc.) for 1 min and detected by exposure to Amersham Hyperfilms (GE Healthcare). Films were developed in a Curix Developer (AGFA) or with a ChemiDoc™ (Bio-Rad Laboratories, Inc.). PageRuler Prestained Protein Ladder (Thermo Scientific) or HiMark™ Pre-stained Protein Standard was used for protein size determination and specific bands were quantified by densitometry using the ImageJ 1.46 software (Wayne Rasband, NHI).

2.2.15 Electrophoretic mobility shift assay (EMSA)

Peritoneal macrophages were plated out at a density of 1×10^6 cells/well in DMEM + FCS in sterile 12-well plates. Cells were transfected, infected, treated and incubated as described in 2.2.6 and 2.2.8. At indicated time points medium was removed and cells were washed once with ice cold PBS. After washing 200 μ l cold EMSA buffer A was added and cells were incubated for 4 min on ice. Lysis of cells was achieved by adding 12.5 μ l of 10 % Triton and incubation for another 3 min on ice. Lysates were transferred to 1.5 ml tubes and centrifuged at 17,900 g for 5 min. The cytosolic fractions in supernatants were removed by careful. The pellet containing the nuclear fraction was resuspended in 30 μ l of EMSA buffer C and incubated at 4 °C with 1400 rpm for 20 min. Nuclear lysates were centrifuged at 17,900 g for 5 min. The nuclear lysates in supernatants were carefully transferred to 1.5 ml tubes and stored at -80 °C. The pellet containing cell debris and chromatin was discarded. Nuclear extracts were normalized for protein content with BCA (2.2.14.3). The NF- κ B-specific oligonucleotides containing two tandemly arranged NF- κ B binding sites of the HIV-1 long terminal repeat enhancer (5-ATCAGGGACTTTCCGCTGGGGACTTTCCG-3) were end-labeled with [γ -P32]ATP using a polynucleotide kinase. EMSA was performed by incubating 5 μ g of nuclear extract with 500 ng poly(dI:dC) in EMSA binding buffer in a final volume of 20 μ l for 20 min at RT. Then, end-labeled double-stranded oligonucleotide probe (2x10⁴ cpm) was added, and the reaction mixture was incubated for 7 min. The samples were fractionated by electrophoresis through a 6 % polyacrylamide gel in low-ionic-strength buffer (0.25 X TBE).

2.2.16 Statistical methods

The statistical analysis of data was performed using Student's t-test. P-values smaller than 0.05 were considered as statistically significant (n.s., not significant; * $p < 0.05$, ** $p < 0.01$ and *** $p < 0.001$). Data were shown as mean \pm standard error of the mean (SEM).

3. Results

3.1. ROS production by infected macrophages

The sources, locations, amount, subspecies and different roles of ROS vary greatly in dependency of stimuli and the cell type, tissue or organ investigated. Therefore, I first analyzed if and how peritoneal macrophages, as mature tissue macrophages, respond to bacterial infection.

3.1.1. Macrophages produce extracellular and cytosolic ROS upon bacterial infection

ROS can be produced and act in different subcellular locations such as the lumen of phagosomes and the extracellular milieu (extracellular ROS) or the cytoplasm (intracellular ROS). Extracellular ROS can be measured with cell-impermeable dyes such as isoluminol (Lundqvist et al., 1996) (Fig. 12A), whereas intracellular ROS levels can be assessed by cell-permeable dyes such as the DCF derivative 5,6-carboxy-2',7'-dichlorodihydrofluorescein diacetate, di(acetoxymethyl ester) (referred to as DCF throughout this thesis) that exclusively measures ROS that reach the cytosol (Hempel et al., 1999) (Fig. 12B).

Macrophages produced substantial quantities of both extracellular (Fig. 12C) and cytosolic ROS (Fig. 12D) after L.m. infection. In addition, co-incubation of macrophages with apathogenic bacteria such as *Bacillus subtilis* (B.sub) (Fig. 12E-F) or *Escherichia coli* (E.coli) (Fig. 12G-H) also induced extracellular and cytosolic ROS production but to a lower degree as compared to L.m. infection, indicating that ROS production is a general response of macrophages after bacterial recognition.

Figure 12

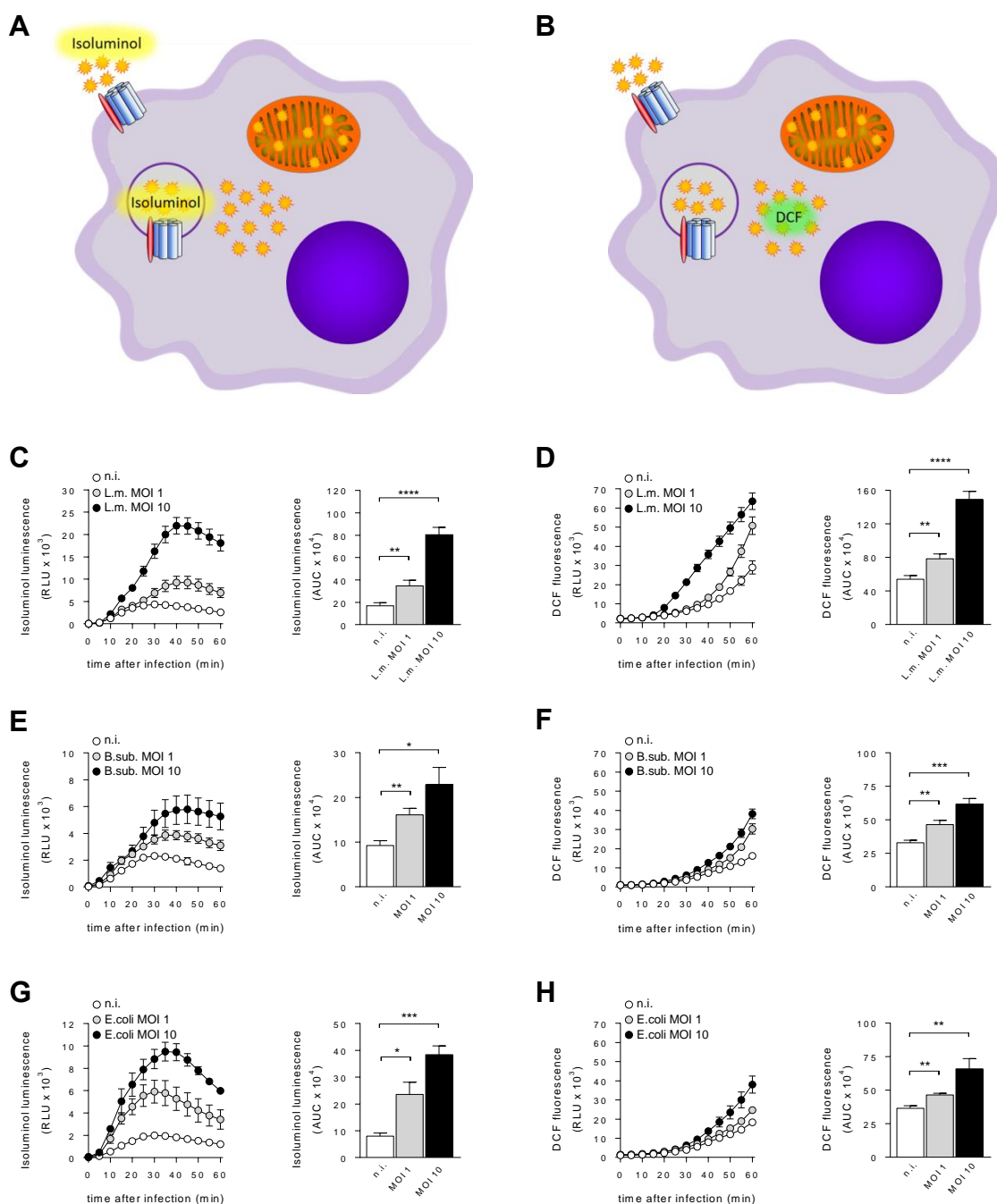


Figure 12: Macrophages produce extracellular and cytosolic ROS upon bacterial infection

Macrophages were infected with L.m. or co-incubated with B.sub or E.coli at a MOI of 1 or 10. The kinetics of ROS production and the area under the curve (AUC), as a measure for the total amount of ROS produced, are shown.

(A) Isoluminol detects extracellular ROS.

(B) DCF detects cytosolic ROS.

(C, E, G) Extracellular ROS production was quantified by measuring isoluminol chemiluminescence (n=7).

(D, F, H) Cytosolic ROS production was quantified by measuring DCF fluorescence (n=9).

3.1.2. ROS are required for pro-inflammatory cytokine secretion during bacterial infection

While the direct anti-bacterial roles of ROS in macrophages are well characterized (Gluschko and Herb et al., 2018; Herb et al., 2018; Garaude et al., 2016; Schramm et al., 2014; Fang, 2011; West et al., 2011b), so far only few studies exist that investigated possible roles of ROS in pro-inflammatory signaling (Kelly et al., 2015; Bulua et al., 2011a). These studies came to different and partly contrasting conclusions, probably because of the use of different cell types such as bone marrow-derived macrophages (BMDM) (Kelly et al., 2015) and mouse embryonic fibroblasts (MEFS) (Bulua et al., 2011a). Moreover, none of these studies investigated pro-inflammatory signaling in response to bacterial infection. I used the pathogen L.m. as a well-established infection model for macrophages that activates multiple signaling pathways (Ley et al., 2016; Mitchell et al., 2016). Therefore L.m. infection is well-suited to investigate the roles of ROS in the pro-inflammatory response of macrophages to a complex pathogenic stimulus.

Both extracellular and intracellular ROS have been reported to contribute to pro-inflammatory signaling in macrophages (Kelly et al., 2015; Deffert et al., 2012; Bulua et al., 2011a). To investigate if infection-induced ROS play a role in pro-inflammatory signaling, macrophages were treated with the global ROS scavenger N-acetyl cysteine (NAC) (Fig. 13A+B), which resulted in strong reduction of both extracellular (Fig. 13C) and cytosolic (Fig. 13D) ROS production. Macrophages responded to bacterial infection by secretion of pro-inflammatory cytokines such as IL-1 β , IL-6 and TNF. Notably, scavenging of ROS with NAC strongly reduced secretion of these cytokines in response to L.m. (Fig. 13E) and B.sub (Fig. 13F), whereas cytokine secretion in response to E.coli was also significantly reduced yet to a minor extent (Fig. 13G). These data indicate that ROS play an important role in the pro-inflammatory response to bacterial infection in macrophages.

Figure 13

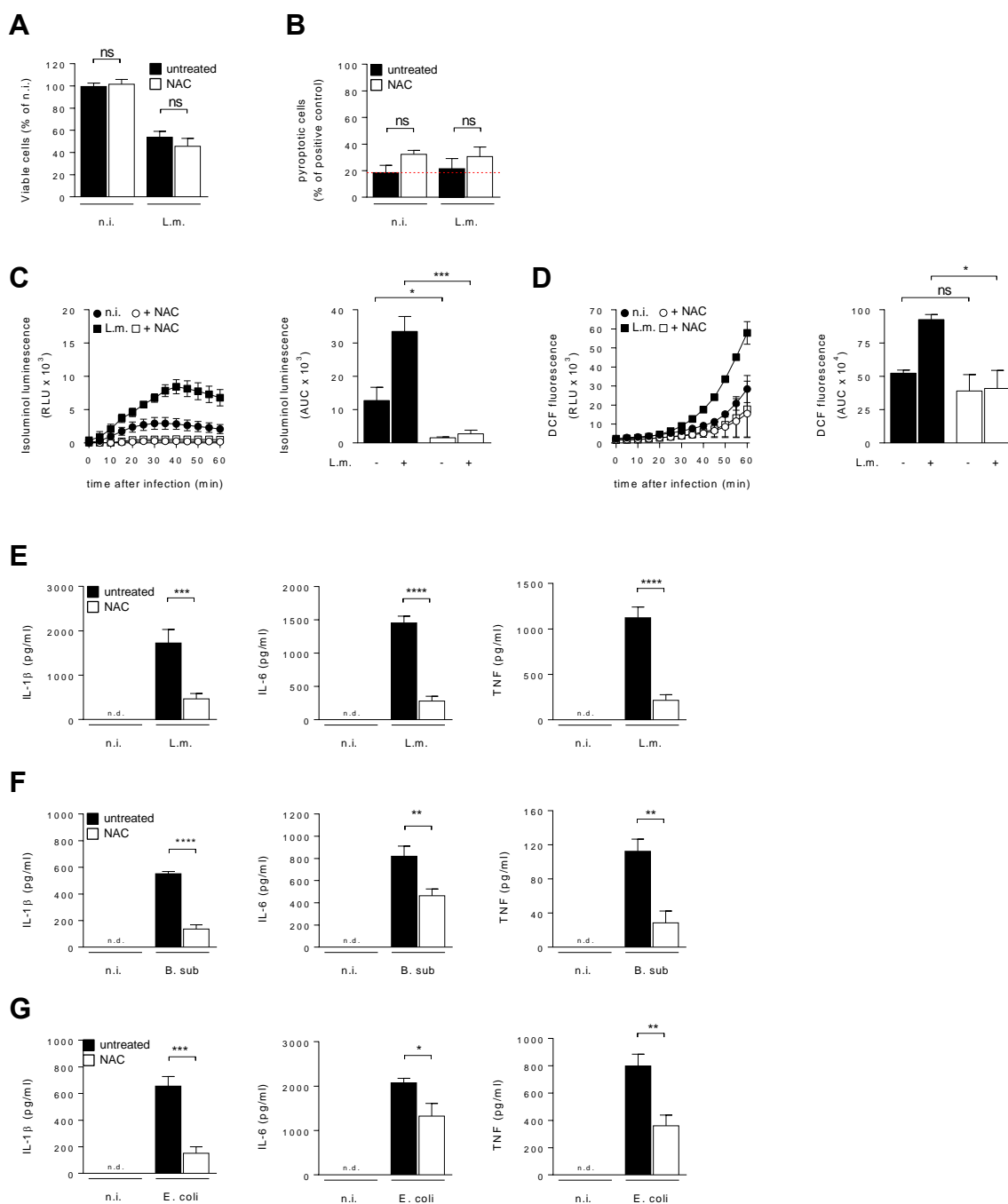


Figure 13: ROS are required for pro-inflammatory cytokine secretion during bacterial infection

(A) Viability of macrophages after infection at a MOI of 1 for 5 hours in the presence or absence of 50 mM NAC (n=4).

(B) Pyroptotic cell death of macrophages after infection at a MOI of 1 for 5 hours in the presence or absence of 50 mM NAC. Macrophages were treated with 10 μ g/ml Digitonin as a positive control (n=4).

(C-D) Macrophages were infected with L.m. at a MOI of 1. The kinetics of ROS production and the area under the curve (AUC), as a measure for the total amount of ROS produced, are shown.

(E) Extracellular ROS production was quantified by measuring isoluminol chemiluminescence (n=3) (Legend continued on next page).

Figure 13 (continued): ROS are required for pro-inflammatory cytokine secretion during bacterial infection

(D) Cytosolic ROS production was quantified by measuring DCF fluorescence (n=3).

(E-G) Macrophages were infected with *L.m.* or co-incubated with *B.sub* or *E.coli* at a MOI of 1 for 5 hours in the presence or absence of 50 mM NAC. Secretion of IL-1 β , IL-6 and TNF was quantified by ELISA (n=5).

3.1.3. Nox2 is the exclusive source of extracellular ROS

As NAC is cell-permeable and therefore scavenges both extracellular and intracellular ROS, I next investigated the subcellular sources of the ROS required for secretion of pro-inflammatory cytokines by infected macrophages. The major ROS source in phagocytes, including macrophages, is the NADPH oxidase 2 (Nox2) (Gluschko and Herb et al., 2018; Sheppard et al., 2005; Pollock et al., 1995). Macrophages deficient for Nox2 did not produce any detectable amounts of extracellular ROS after infection with *L.m.* (Fig. 14A). Even infection with an increased number of *L.m.* per macrophage did not induce ROS production in Nox2-deficient macrophages (Fig. 14A) clearly identifying Nox2 as the exclusive extracellular ROS source in *L.m.*-infected macrophages.

By contrast, the increase in cytosolic ROS levels induced by *L.m.* infection was not compromised in Nox2-deficient macrophages (Fig. 14B) showing that Nox2-derived ROS, in contrast to extracellular ROS production, do not contribute to cytosolic ROS levels.

3.1.4. Nox/Duox enzymes do not contribute to cytosolic ROS production

In addition to Nox2, the family of NADPH oxidases comprises five other isoforms that could be responsible for the increase of cytosolic ROS levels: Nox1-5 and Duox1-2 (Lambeth et al., 2014; Bedard et al., 2007). As Nox3 is only expressed in the inner ear (Banfi et al., 2004) and Nox5 is absent in mice (Banfi et al., 2001; Cheng et al., 2001), neither was addressed in this thesis. *L.m.*-infected Nox1-, Nox4-, Duox1- and Duox2-deficient macrophages produced unaltered amounts of cytosolic ROS in comparison to corresponding wild type (WT) cells (Fig. 14C-F). Moreover, simultaneous deficiency for Nox1-4 in macrophages deficient for p22^{phox}, the common catalytic subunit of Nox1-4, did not compromise production of cytosolic ROS (Fig. 14G).

Figure 14

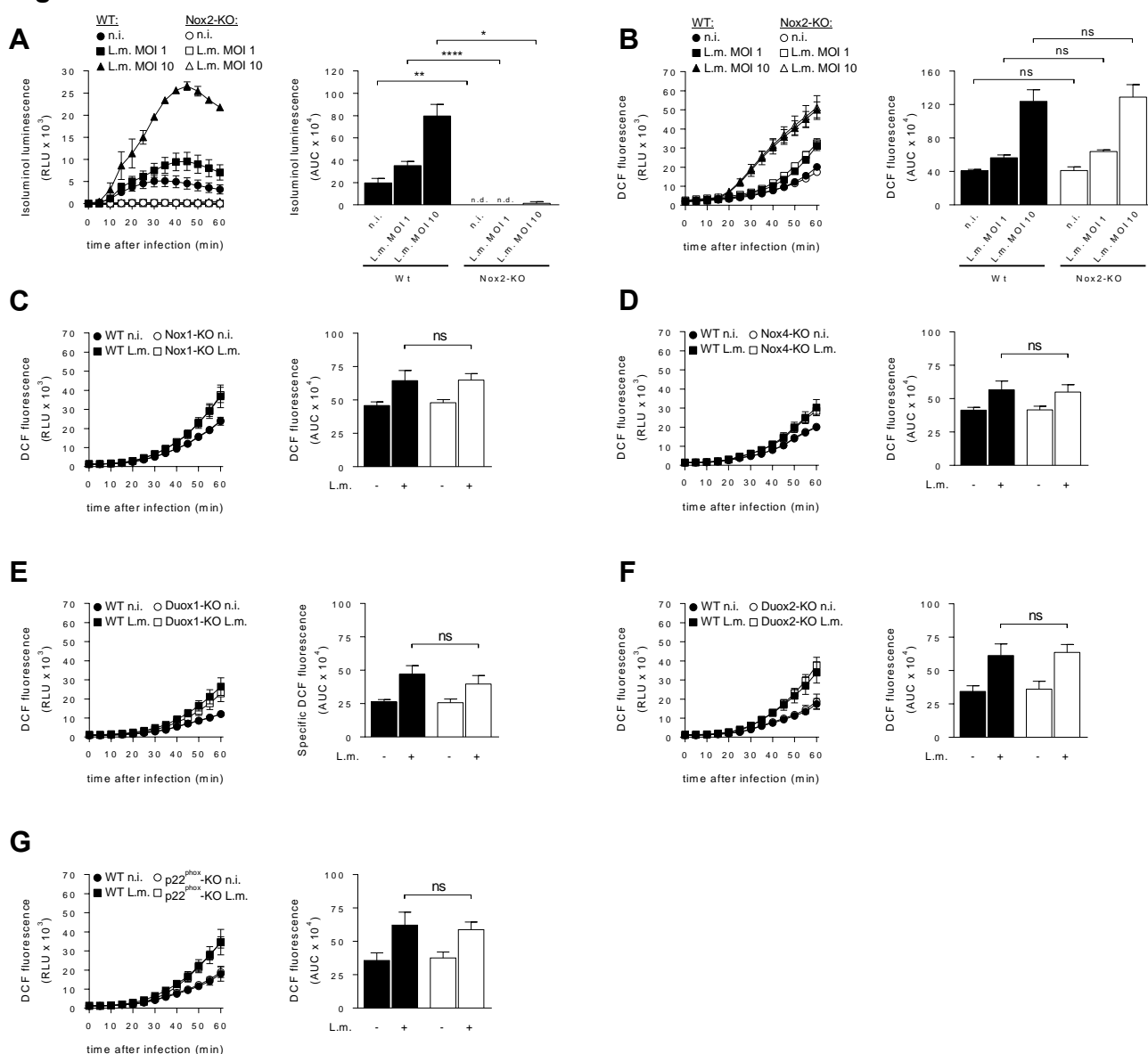


Figure 14: Nox2 is the exclusive source of extracellular ROS, whereas Nox/Duox enzymes do not contribute to cytosolic ROS production

Macrophages were infected with *L.m.* at MOI 1 or 10. The kinetics of ROS production and the area under the curve (AUC), as a measure for the total amount of ROS produced, are shown.

(A) Extracellular ROS production by WT or Nox2-KO macrophages was quantified by measuring isoluminol chemiluminescence (n=5).

(B-G) Cytosolic ROS production by WT or Nox2-KO, Nox1-KO, Nox4-KO, Duox1-KO, Duox2-KO and p22^{phox}-KO macrophages was quantified by measuring DCF fluorescence (n=5, 4, 3, 3, 4 and 4, respectively).

3.1.5. Nox/Duox enzymes are dispensable for pro-inflammatory cytokine secretion

Since a regulatory role for Nox2-derived ROS during pro-inflammatory signaling was described before (Deffert et al., 2012), I next investigated a possible role for Nox2-derived extracellular ROS in cytokine secretion by infected macrophages. Cytokine secretion by L.m.-infected Nox2-deficient macrophages was normal for IL-6 and TNF and even increased for IL-1 β (Fig. 15A), indicating that extracellular Nox2-derived ROS are dispensable for secretion of pro-inflammatory cytokines by infected macrophages. In addition to the previously described unaltered cytosolic ROS production (Fig. 14C-G), macrophages deficient for Nox1, Nox4, Duox1 and Duox2 showed also no alterations in pro-inflammatory cytokine secretion after L.m. infection (Fig. 15B-E). Macrophages deficient for the p22^{phox}-subunit showed enhanced IL-1 β secretion (Fig. 15F), phenocopying the pro-inflammatory cytokine profile of Nox2-deficient macrophages. Thus, Nox/Duox enzymes are dispensable for pro-inflammatory cytokine secretion in infected macrophages.

3.1.6. Cytosolic ROS production is crucial for pro-inflammatory cytokine secretion

Since cytosolic ROS production was unaltered in Nox2-deficient macrophages, I additionally treated these cells with NAC to eliminate Nox2-independent cytosolic ROS production. Importantly, additional ROS scavenging with NAC in Nox2-deficient macrophages reduced secretion of cytokines to a similar degree as in WT macrophages (Fig. 15A) suggesting a role for cytosolic ROS in cytokine secretion. These results clearly indicate that none of the Nox/Duox family members is involved in cytosolic ROS production or pro-inflammatory cytokine secretion by infected macrophages and show that cytosolic ROS, but not extracellular, Nox2-derived ROS, play a crucial role in pro-inflammatory cytokine secretion.

Figure 15

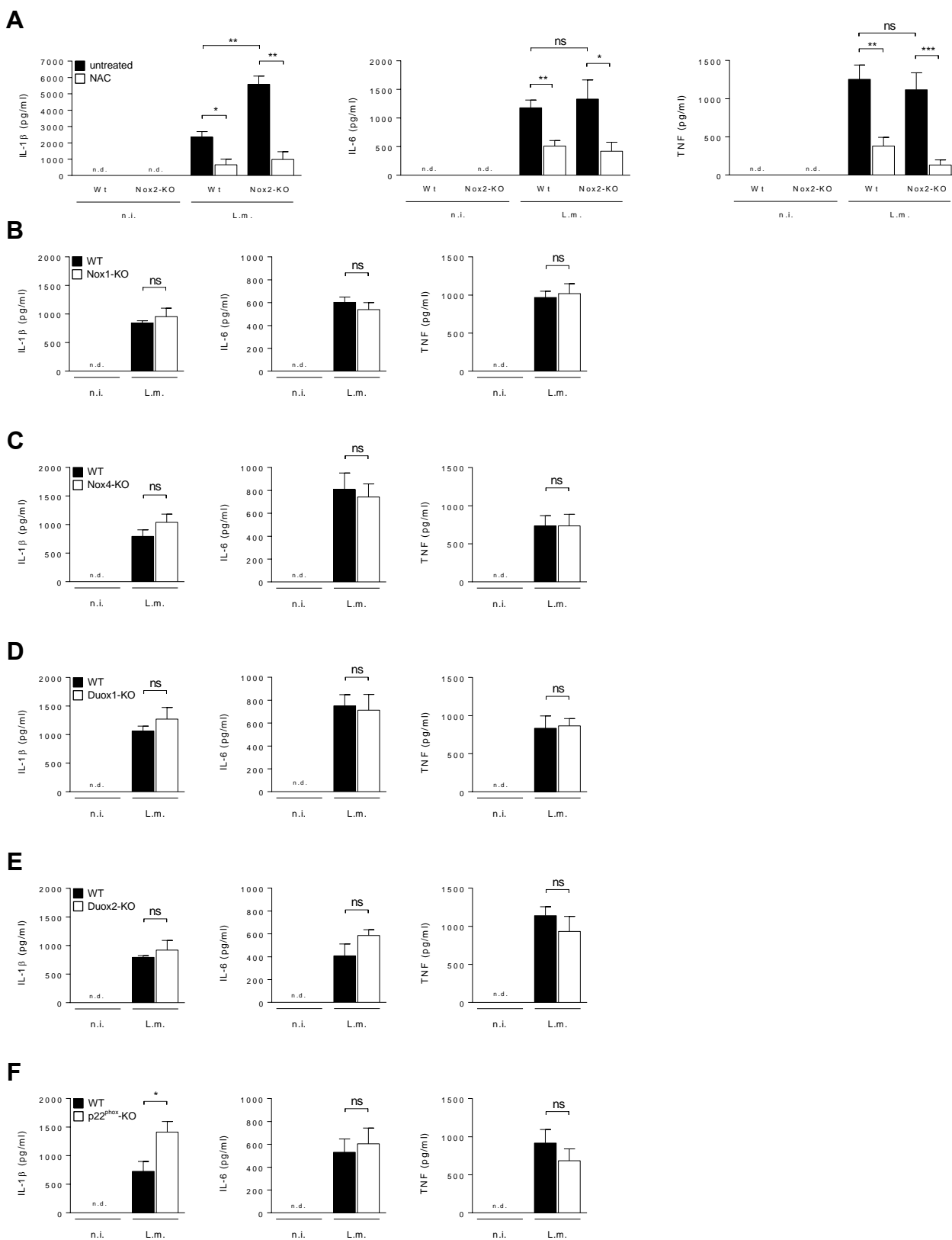


Figure 15: Cytosolic ROS production independent of Nox/Duox enzymes is necessary for pro-inflammatory cytokine secretion (Legend continued on next page).

Figure 15 (continued): Cytosolic ROS production independent of Nox/Duox enzymes is necessary for pro-inflammatory cytokine secretion

Macrophages were infected with L.m. at a MOI of 1 for 5 hours in the presence or absence of 50 mM NAC.

(A-F) Secretion of IL-1 β , IL-6 and TNF by WT or Nox2-KO, Nox1-KO, Nox4-KO, Duox1-KO, Duox2-KO and p22^{phox}-KO macrophages was quantified by ELISA (n=9, 6, 6, 6, 3 and 5, respectively).

3.1.7. Cytosolic ROS do not originate from the mitochondrial matrix

Another source of cytosolic ROS are mitochondria, which generate ROS by the respiratory electron transport chain (ETC) as byproduct of energy production (Cortassa et al., 2014). The mitochondrial ETC produces ROS either into the mitochondrial matrix (via complexes I, II and III) or into the IMS (via complex III, exclusively) (Dan Dunn et al., 2015; West et al., 2011b). From the IMS, ROS can reach the cytosol by diffusion. Several studies showed that bacterial infection can trigger ROS production into the mitochondrial matrix (Kelly et al., 2015; Bulua et al., 2011a; West et al., 2011b; Zhou et al., 2011; Chandel et al., 2000). Therefore, I first tested if L.m. infection induces ROS production into the mitochondrial matrix and if these ROS contribute to pro-inflammatory signaling. ROS production into the mitochondrial matrix can be quantified with MitoSOX Red, which is specifically targeted to the mitochondrial matrix (Mukhopadhyay et al., 2007; Robinson et al., 2006) (Fig. 16A). Rotenone-mediated blockade of electron transfer from complex I to complex III of the ETC is commonly used as a positive control for MitoSOX measurements because of reverse electron flow and subsequent ROS production into the matrix (Sazanov, 2014; Orr et al., 2013). Accordingly, rotenone treatment (Fig. 16B-C) increased ROS production into the mitochondrial matrix (Fig. 16D) showing that ROS production can be induced and quantified with this approach in macrophages. Notably, while L.m. infection of macrophages significantly increased cytosolic ROS levels (Fig. 12D) it did not increase ROS production into the mitochondrial matrix (Fig. 16D). Furthermore, scavenging of ROS specifically in the mitochondrial matrix with a mitochondrial matrix-targeted version of the $\cdot\text{O}_2^-$ scavenger TEMPO (MitoTEMPO) (Fig. 16E) or by expression of the H₂O₂-decomposing enzyme catalase in the mitochondrial matrix (mCAT-knockin macrophages) (Schriner et al., 2005) did neither reduce cytosolic ROS levels (Fig. 16F+H) nor cytokine secretion (Fig. 16G+I). These data show that ROS production into the mitochondrial matrix is not induced upon L.m. infection and does not contribute to cytosolic ROS levels or pro-inflammatory cytokine secretion.

Figure 16

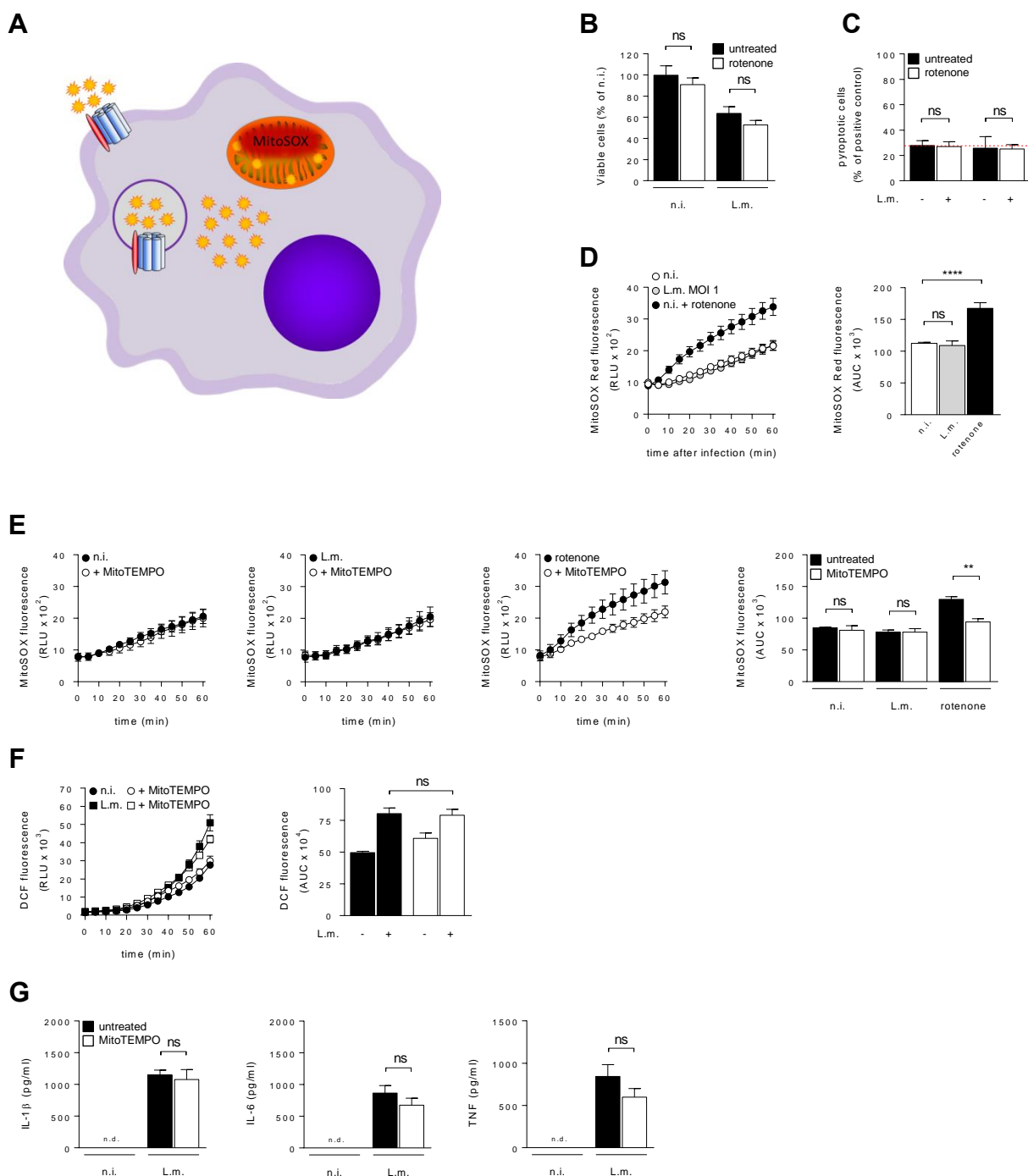


Figure 16: Cytosolic ROS do not originate from the mitochondrial matrix (Figure continued on next page)

(A) MitoSOX Red measures ROS inside of the mitochondrial matrix.

(B, C, G, I) Macrophages were infected with L.m. at a MOI of 1 for 5 hours.

(D, E, F, H) Macrophages were infected with L.m. at a MOI of 1. The kinetics of ROS production and the area under the curve (AUC), as a measure for the total amount of ROS produced, are shown.

(B) Viability of macrophages after infection in the presence or absence of 100 μ M rotenone (n=4).

(C) Pyroptotic cell death of macrophages after infection in the presence or absence of 100 μ M rotenone (n=4). Macrophages were treated with 10 μ g/ml Digitonin as a positive control (n=4) (legend continued on next page).

Figure 16 (continued)

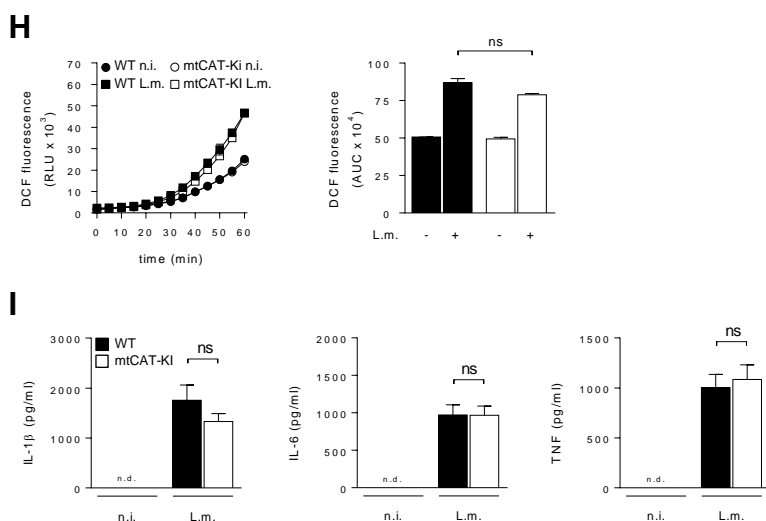


Figure 16 (continued): Cytosolic ROS do not originate from the mitochondrial matrix

(D) ROS production into the mitochondrial matrix was quantified by measuring MitoSOX Red fluorescence in the presence or absence of 100 μ M rotenone as positive control ($n=7$).

(E) ROS production into the mitochondrial matrix was quantified by measuring MitoSOX Red fluorescence after 30 minutes pre-incubation with 500 μ M MitoTEMPO. Treatment with 100 μ M rotenone was used as positive control ($n=7$).

(F) Cytosolic ROS production was quantified by measuring DCF fluorescence after 30 minutes pre-incubation with 500 μ M MitoTEMPO ($n=4$).

(G) Secretion of IL-1 β , IL-6 and TNF after pre-incubation with 500 μ M MitoTEMPO was quantified by ELISA ($n=6$).

(H) Cytosolic ROS production was quantified by measuring DCF fluorescence in WT and mitochondrial catalase-knockin (mCAT-KI) macrophages ($n=2$).

(I) Secretion of IL-1 β , IL-6 and TNF by WT or mitochondrial catalase-knockin (mCAT-KI) macrophages was quantified by ELISA ($n=8$).

3.1.8. Cytosolic ROS are produced by complex III of the mitochondrial ETC

Surprisingly, in contrast to its induction of ROS production into the mitochondrial matrix, rotenone-mediated blockade of electron transfer from complex I to complex III of the ETC almost completely abrogated cytosolic ROS production (Fig. 17A) as well as pro-inflammatory cytokine secretion in L.m.-infected macrophages (Fig. 17B). Garaude and colleagues have reported ROS production by complex II after E.coli infection (Garaude et al., 2016). Inhibition of complex II with malonate did not alter cytosolic ROS production (Fig. 17C) or cytokine secretion (Fig. 17D) induced by L.m. infection in macrophages. By contrast, blockade of electron transfer from complex III to complex IV with antimycin A (Bleier et al., 2013; Park et al., 2007) strongly increased cytosolic ROS levels in uninfected and infected macrophages (Fig. 17E). Together, these data indicate that the infection-induced cytosolic ROS, which are crucial for pro-

inflammatory cytokine secretion by macrophages, are produced by mitochondria, but do not originate from the mitochondrial matrix. Instead, they are directly produced into the IMS by complex III from where they diffuse into the cytosol.

Figure 17

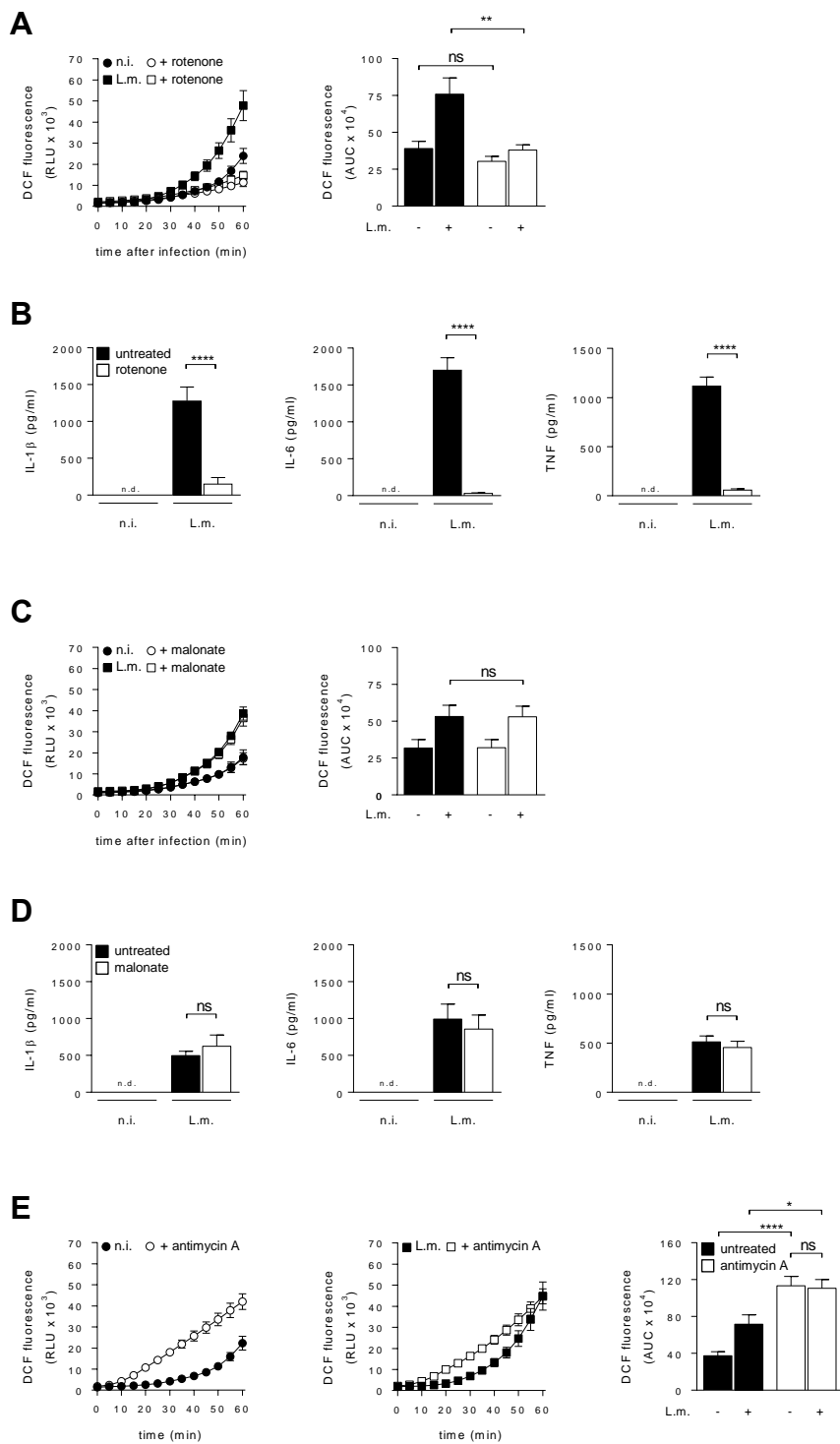


Figure 17: Cytosolic ROS are produced by complex III of the mitochondrial ETC (Legend on next page)

(A, C, E) Macrophages were infected with L.m. at a MOI of 1. The kinetics of ROS production and the area under the curve (AUC), as a measure for the total amount of ROS produced, are shown.

(B, D) Macrophages were infected with L.m. at a MOI of 1 for 5 hours.

(A) Cytosolic ROS production was quantified by measuring DCF fluorescence in the presence or absence of 100 μ M rotenone (n=9).

(B) Secretion of IL-1 β , IL-6 and TNF in the presence or absence of 100 μ M rotenone was quantified by ELISA (n=9).

(C) Cytosolic ROS production was quantified by measuring DCF fluorescence in the presence or absence of 100 μ M malonate (n=8).

(D) Secretion of IL-1 β , IL-6 and TNF in the presence or absence of 100 μ M malonate was quantified by ELISA (n=5).

(E) Cytosolic ROS production was quantified by measuring DCF fluorescence in the presence or absence of 30 μ M antimycin A (n=8).

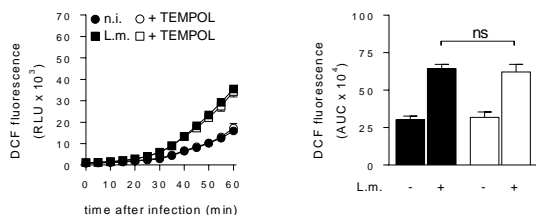
3.1.9. Cytosolic H₂O₂ regulates pro-inflammatory signaling

ROS produced into the mitochondrial IMS can access the cytosol either in the form of $\cdot\text{O}_2^-$ or H₂O₂, and both molecules can function as signaling molecules (Short et al., 2016; Chen et al., 2009). In contrast to $\cdot\text{O}_2^-$, which requires voltage-dependent anion channels (VDAC) to cross the mitochondrial outer membrane (MOM) (Shoshan-Barmatz et al., 2010; Imai et al., 2008), H₂O₂ can leave the IMS by diffusion over the MOM. To address the question which of these two ROS subspecies is necessary for pro-inflammatory signaling, I used specific ROS-scavenging chemicals. Scavenging of cytosolic $\cdot\text{O}_2^-$ in L.m.-infected macrophages with TEMPOL did neither alter cytosolic ROS levels (Fig. 18A) nor markedly reduced cytokine secretion (Fig. 18B). By contrast, specific scavenging of cytosolic H₂O₂ with ebselen, a glutathione reductase-mimetic (Nakamura et al., 2002), reduced both cytosolic ROS levels (Fig. 18C) and cytokine secretion (Fig. 18E) indicating that infection-induced mitochondrial ROS reach the cytosol from the IMS as H₂O₂. In support of this notion, inhibition of SOD1 with the SOD1-specific inhibitor LCS-1 almost completely abrogated cytokine secretion by L.m.-infected macrophages (Fig. 18F). Since SOD1 converts $\cdot\text{O}_2^-$ into H₂O₂ both in the cytosol and in the IMS, these data further indicate that H₂O₂ is the cytosolic ROS subspecies that regulates pro-inflammatory cytokine secretion.

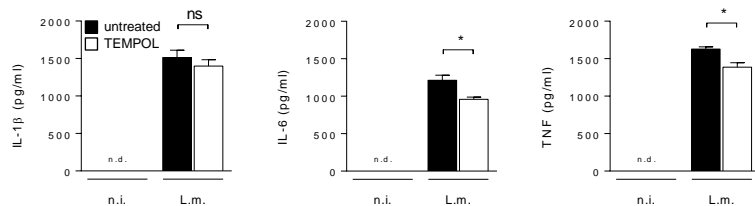
Collectively, the data presented in this section show that bacterial infection of macrophages induces both, production of Nox2-derived extracellular ROS and mitochondria-derived cytosolic ROS (mtROS). Specifically, infection triggers $\cdot\text{O}_2^-$ production into the IMS by complex III of the ETC. Here, O_2^- is converted by SOD1 into H₂O₂ that diffuses into the cytosol. Moreover, while Nox2-derived extracellular ROS are completely dispensable for pro-inflammatory cytokine secretion, mtROS are crucial for secretion of pro-inflammatory cytokines.

Figure 18

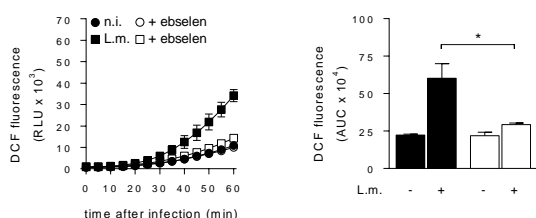
A



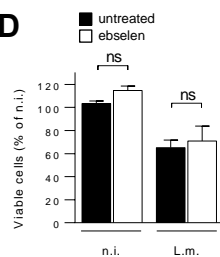
B



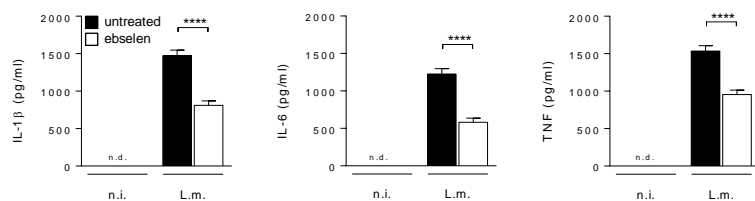
C



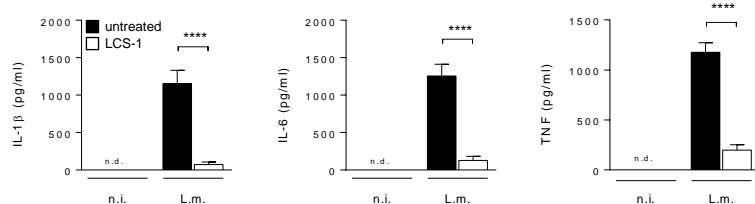
D



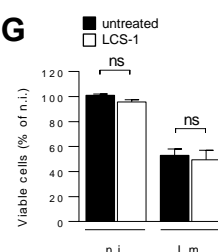
E



F



G

Figure 18: Cytosolic H₂O₂ regulates pro-inflammatory signaling

(A, C) Macrophages were infected with L.m. at a MOI of 1. The kinetics of ROS production and the area under the curve (AUC), as a measure for the total amount of ROS produced, are shown.

(B, D, E, F, G) Macrophages were infected with L.m. at a MOI of 1 for 5 hours.

(A) Cytosolic ROS production was quantified by measuring DCF fluorescence in the presence or absence of 500 μ M TEMPOL (n=2) (continued on next page).

Figure 18 (continued): Cytosolic H₂O₂ regulates pro-inflammatory signaling

(B) Secretion of IL-1 β , IL-6 and TNF in the presence or absence of 500 μ M TEMPOL was quantified by ELISA (n=4).

(C) Cytosolic ROS production was quantified by measuring DCF fluorescence after 60 minutes pre-incubation with 20 μ M ebselen (n=3).

(D) Viability of macrophages after infection after 60 minutes pre-incubation with 20 μ M ebselen (n=4).

(E) Secretion of IL-1 β , IL-6 and TNF after 60 minutes pre-incubation with 20 μ M ebselen was quantified by ELISA (n=6).

(F) Secretion of IL-1 β , IL-6 and TNF in the presence or absence of 7.5 μ M LCS-1 was quantified by ELISA (n=10).

(G) Viability of macrophages after infection in the presence or absence of 7.5 μ M LCS-1 (n=4).

3.2. Induction mtROS production in infected macrophages

3.2.1. mtROS production is not caused by mitochondrial perturbation

Perturbation of mitochondria can lead to uncontrolled production of large quantities of ROS (Zhang et al., 2016; Motori et al., 2013; Detmer et al., 2007). The pore-forming toxin LLO of *L.m.* has been shown to damage mitochondria, which results in fragmentation of the mitochondrial network, and thereby impair mitochondrial function in HeLa cells (Stavru et al., 2011). *L.m.* deficient for LLO (Δhly) or for the transcriptional master regulator of *L.m.* virulence factors, *prfA* ($\Delta prfA$), induced mtROS production to a similar level as wt *L.m.* (Fig. 17A) excluding a role for *L.m.* virulence factors in induction of mtROS in macrophages. Furthermore, while carbonyl cyanide *m*-chlorophenyl hydrazine (CCCP), a protonophore that uncouples the mitochondrial membrane potential (Fig. 17C), induced mitochondrial fragmentation (Fig. 17B), infection with *L.m.* did neither led to collapse of the membrane potential (Fig. 17C) nor to fragmentation of the mitochondrial network (Fig. 17B). Thus, mtROS production induced by *L.m.* infection in macrophages is not caused by LLO-mediated perturbation of the mitochondrial network.

The ETC produces energy, conserved as ATP, during oxidative phosphorylation (OXPHOS). mtROS are generated in every respiring cell as a byproduct of OXPHOS because of electron leakage (Lambeth et al., 2014; Nohl et al., 2003). To test if mtROS production after *L.m.* infection of macrophages is a side effect of increased ATP generation, I investigated cellular ATP levels. *L.m.*-infected macrophages showed a rapid drop of ATP levels (Fig. 17D), suggesting that response to *L.m.*-infection is an energy consuming process. Since treatment with rotenone resulted in a strong reduction of both mtROS production (Fig. 15A) and pro-inflammatory cytokine secretion (Fig. 15B) in *L.m.*-infected macrophages, I wanted to analyze if these effects are not caused by energy deprivation because of complex I inhibition. While

treatment with CCCP led to a strong reduction of ATP levels in uninfected as well as infected macrophages (Fig. 17D), treatment with rotenone did not further reduce ATP levels (Fig. 17E) or reduced membrane potential (Fig. 17F) in infected macrophages. These data suggest that the rotenone-induced effects in L.m.-infected macrophages described in section 3.1. are not side effects caused by energy deprivation.

Figure 19

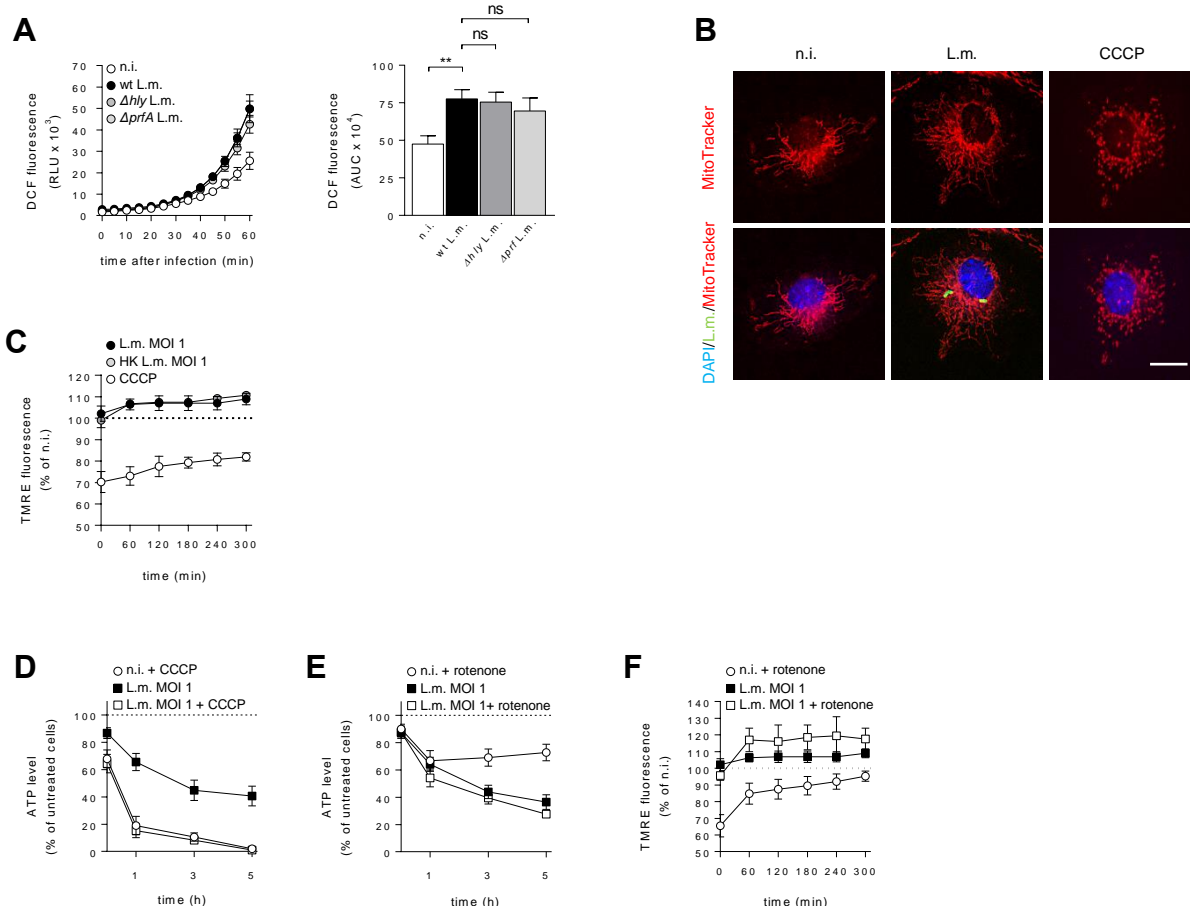


Figure 19: Infection-induced mtROS production is not caused by mitochondrial perturbation

(A) Macrophages were infected with wt L.m., Δhly L.m. or $\Delta prfA$ L.m. at a MOI of 1. The kinetics of ROS production and the area under the curve (AUC), as a measure for the total amount of ROS produced, are shown. Cytosolic ROS production was quantified by measuring DCF (n=2).

(B) Representative micrographs of Mitotracker Red-stained mitochondria in macrophages at 1 hour after infection or with 50 μ M CCCP as positive control are shown (n=2). Scale bar represents 4 μ m.

(C) Mitochondrial membrane potential was quantified by measuring TMRE fluorescence after infection with L.m. or HK L.m. at a MOI of 1. Treatment with 50 μ M CCCP was used as positive control. (n=5).

(D-E) Cellular ATP levels were quantified by measuring Luciferase luminescence after infection with L.m. at a MOI of 1 in the presence or absence of 100 μ M rotenone and with 50 μ M CCCP as positive control (n=6).

(F) Mitochondrial membrane potential was quantified by measuring TMRE fluorescence after infection with L.m. at a MOI of 1 in the presence or absence of 100 μ M rotenone (n=6).

3.2.2. TLR2/MyD88/TRAF6 signaling induces mtROS production

Since mtROS production was not a consequence of mitochondrial damage, I next investigated the pathway that triggers mtROS production in L.m.-infected macrophages. *Salmonella typhimurium* has been reported to induce mtROS production via the TLR4/MyD88/TRAF6 signaling pathway (West et al., 2011a). To investigate if L.m., as a gram-positive pathogen, induces mtROS production in an analogous manner via TLR2 signaling, I first analyzed TLR2-deficient macrophages. TLR2-deficient macrophages showed strongly reduced mtROS production (Fig. 20A) indicating that TLR2 is the main receptor triggering this response. TLR2 can act in synergism with other TLRs, and since mtROS production was not completely abolished in TLR2-deficient macrophages, I next used macrophages deficient for the TLR adaptor molecule MyD88. MyD88 is required for all TLRs except TLR3 and (partly) TLR4 (Ley et al., 2016), which allowed me to test if other TLRs contribute to induction of mtROS production. In MyD88-deficient macrophages, mtROS production was not induced by L.m. infection at all (Fig. 20B). Notably, the same was true in macrophages deficient for the signaling transducer TRAF6 (Fig. 20C), which functions as an accumulation point for signals coming from all TLRs. Pro-inflammatory cytokine secretion after L.m. infection was significantly reduced in TLR2-deficient (Fig. 20D) and even more reduced in MyD88- (Fig. 20E) and TRAF6-deficient macrophages (Fig. 20F).

Collectively, the data from this section show that mtROS production is not caused by mitochondrial perturbation. Instead, mtROS production and pro-inflammatory cytokine secretion are predominantly triggered via the TLR2/MyD88/TRAF6 signaling pathway in L.m.-infected macrophages.

Figure 20

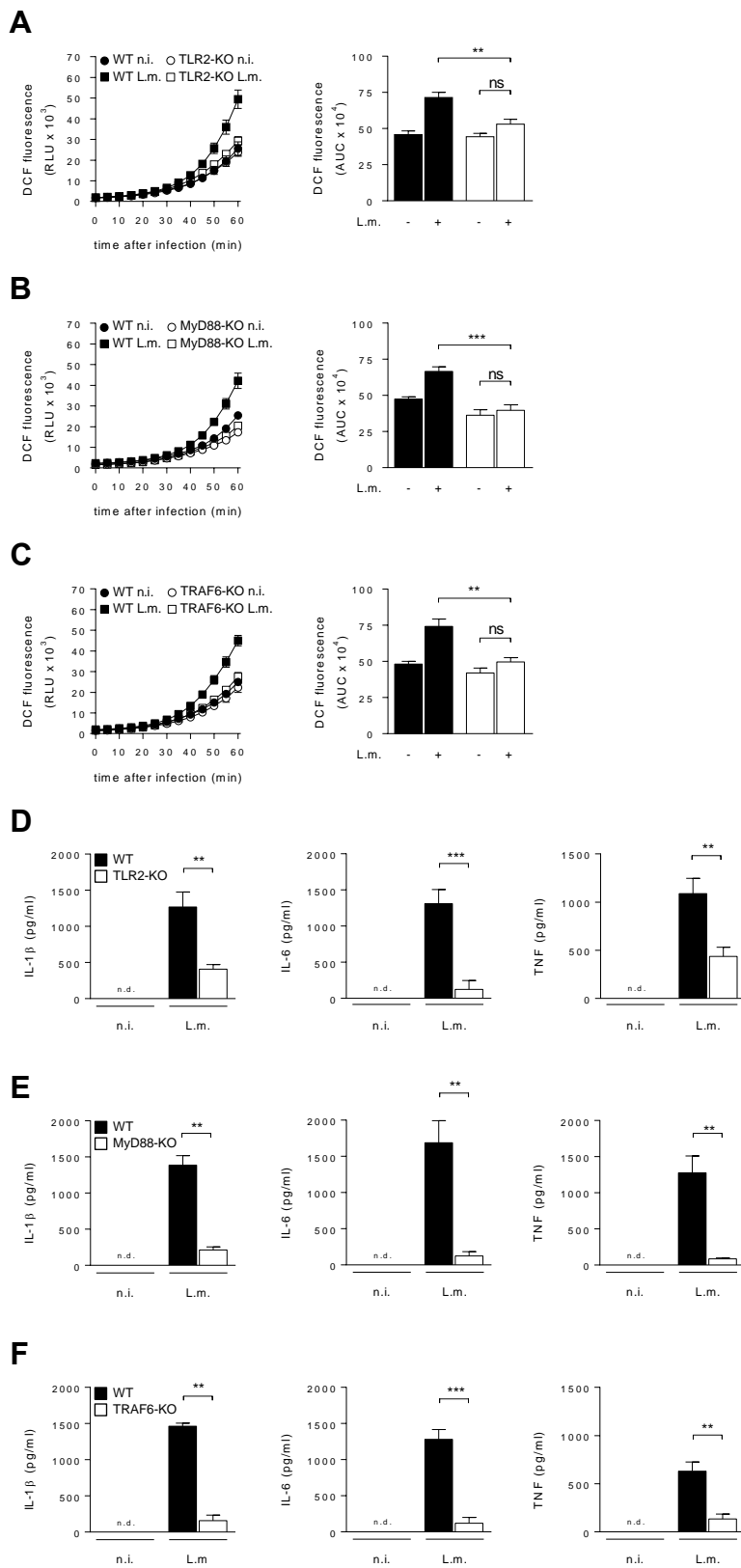


Figure 20: mtROS production in infected macrophages is induced by TLR2/MyD88/TRAF6 signaling (Legend on next page)

Figure 20 (continued): mtROS production in infected macrophages is induced by TLR2/MyD88/TRAF6 signaling

(A-C) Macrophages were infected with L.m. at a MOI of 1. The kinetics of ROS production and the area under the curve (AUC), as a measure for the total amount of ROS produced, are shown. Cytosolic ROS production by WT or TLR2-KO, MyD88-KO and TRAF6-KO macrophages was quantified by measuring DCF fluorescence (n=7, 7 and 6, respectively).

(D-F) Macrophages were infected with L.m. at a MOI of 1 for 5 hours. Secretion of IL-1 β , IL-6 and TNF by WT or TLR2-KO, MyD88-KO, TRAF6-KO macrophages was quantified by ELISA (n=5, 3 and 4, respectively).

3.4. Modulation of pro-inflammatory signaling pathways by mtROS

As secretion of pro-inflammatory cytokines depended on TLR/MyD88/TRAF6 signaling and mtROS production, I investigated in more detail which pro-inflammatory signaling pathways are modulated by mtROS in infected macrophages. The main pathways initiated by TLR/MyD88/TRAF6 signaling are the ERK1/2, JNK1/2 and p38 MAPK pathways and the pathways leading to activation of NF- κ B (Arthur et al., 2013; Newton et al., 2012).

3.4.1. mtROS are crucial for activation of the ERK1/2 pathway

All three investigated terminal kinases of the main MAPK pathways, namely ERK1/2, JNK1/2 and p38, were activated in L.m.-infected macrophages with strongest phosphorylation after 30 min (Fig. 21A). Phosphorylation of JNK1/2 was only slightly decreased and phosphorylation of p38 remained unchanged after global scavenging of ROS with NAC or by inhibiting mtROS production with rotenone (Fig. 21A). Importantly, both treatments strongly reduced phosphorylation of ERK1/2 and its upstream regulator kinase MEK1/2 (Fig. 21A) indicating that mtROS production is crucial for the activation of the MAPK ERK1/2 in infected macrophages.

Since mtROS production was crucial for both cytokine secretion and ERK1/2 activation, I used the MEK1/2-specific inhibitor PD98059 to investigate the role of ERK1/2 in pro-inflammatory cytokine secretion by L.m.-infected macrophages. Notably, treatment of infected macrophages with PD98059 resulted in a strongly reduced secretion of IL-1 β and IL-6, while TNF was significantly reduced (Fig. 21B). These data indicate that mtROS are crucial for activation of the ERK1/2 pathway that is necessary for pro-inflammatory cytokine secretion.

Figure 21

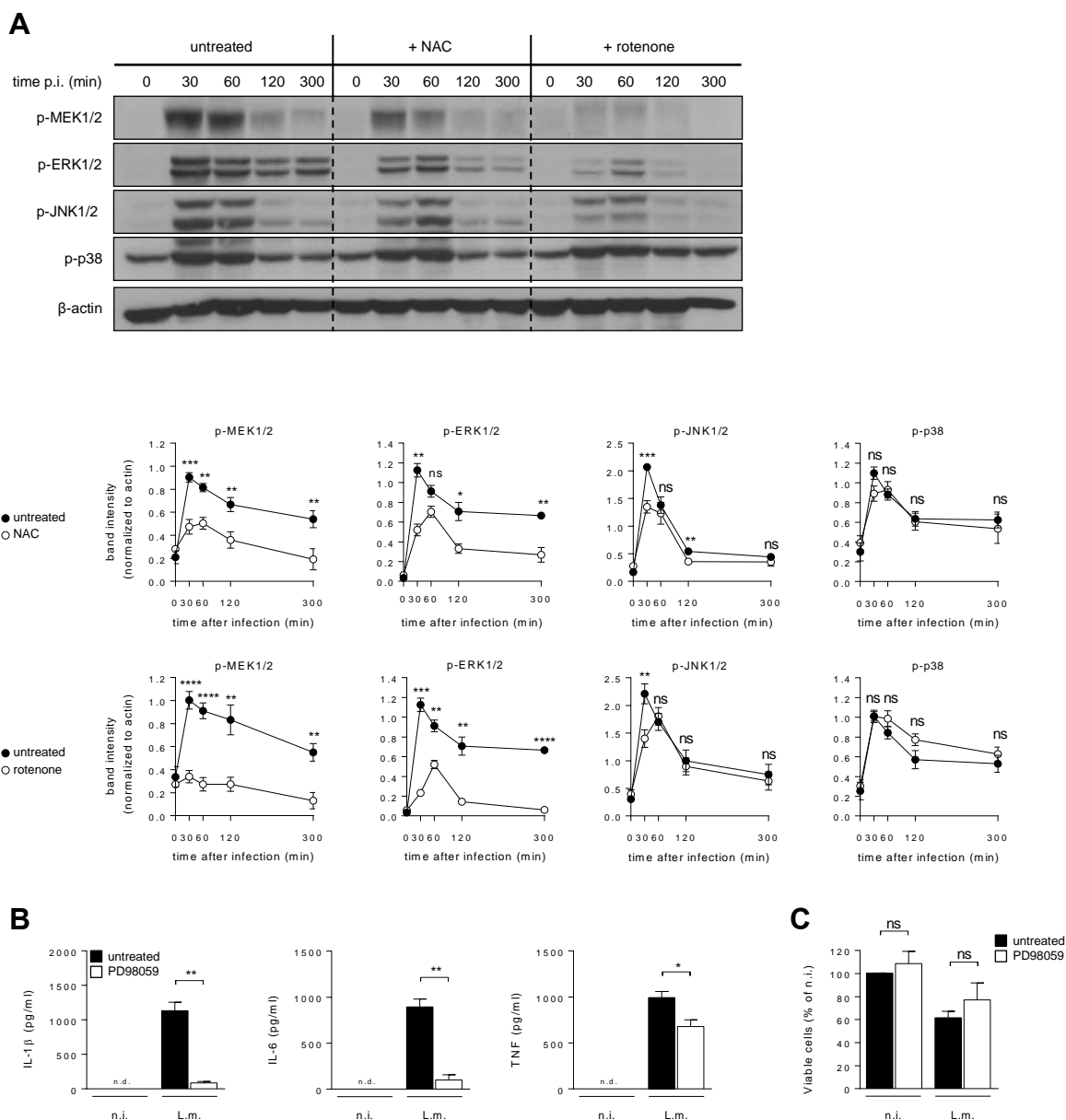


Figure 21: mtROS are crucial for activation of the ERK1/2 pathway

(A) At the indicated time points after infection with L.m. at a MOI of 1 in the presence or absence of 50 mM NAC or 100 μ M rotenone, phosphorylation status of MEK1/2 (n=6), ERK1/2 (n=3), JNK1/2 (n=7) and p38 (n=8) were analyzed by Western blot and quantified by densitometry of band intensities.

(B) Secretion of IL-1 β , IL-6 and TNF after 5 hours of infection with L.m. at a MOI of 1 in the presence or absence of 20 μ M PD98059 was quantified by ELISA (n=3)

(C) Viability of macrophages after infection at a MOI of 1 for 5 hours in the presence or absence of 20 μ M PD98059 (n=3).

3.4.2. mtROS are necessary for full activation of NF- κ B signaling

MAPK regulate cytokine secretion in conjunction with the NF- κ B pathway (Gantke et al., 2012). Degradation of I κ B α , a prerequisite for release of NF- κ B and phosphorylation of the NF- κ B subunit p65, which is necessary for optimal induction of NF- κ B target genes (Christian et al., 2016), were initiated in L.m.-infected macrophages (Fig. 22A). While I κ B α degradation was not reduced after global scavenging of ROS with NAC or rotenone-induced mtROS deficiency, both treatments led to a premature terminated phosphorylation of NF- κ B p65 (Fig. 22A). Moreover, translocation of NF- κ B into the nucleus was strongly reduced (Fig. 22B) and binding of NF- κ B to DNA was nearly abrogated in mtROS-deficient macrophages (Fig. 22C).

Collectively, the data from this section show that mtROS are crucial for activation of the ERK1/2 and NF- κ B pathway and both signaling pathways contribute to subsequent pro-inflammatory cytokine secretion by infected macrophages.

Figure 22

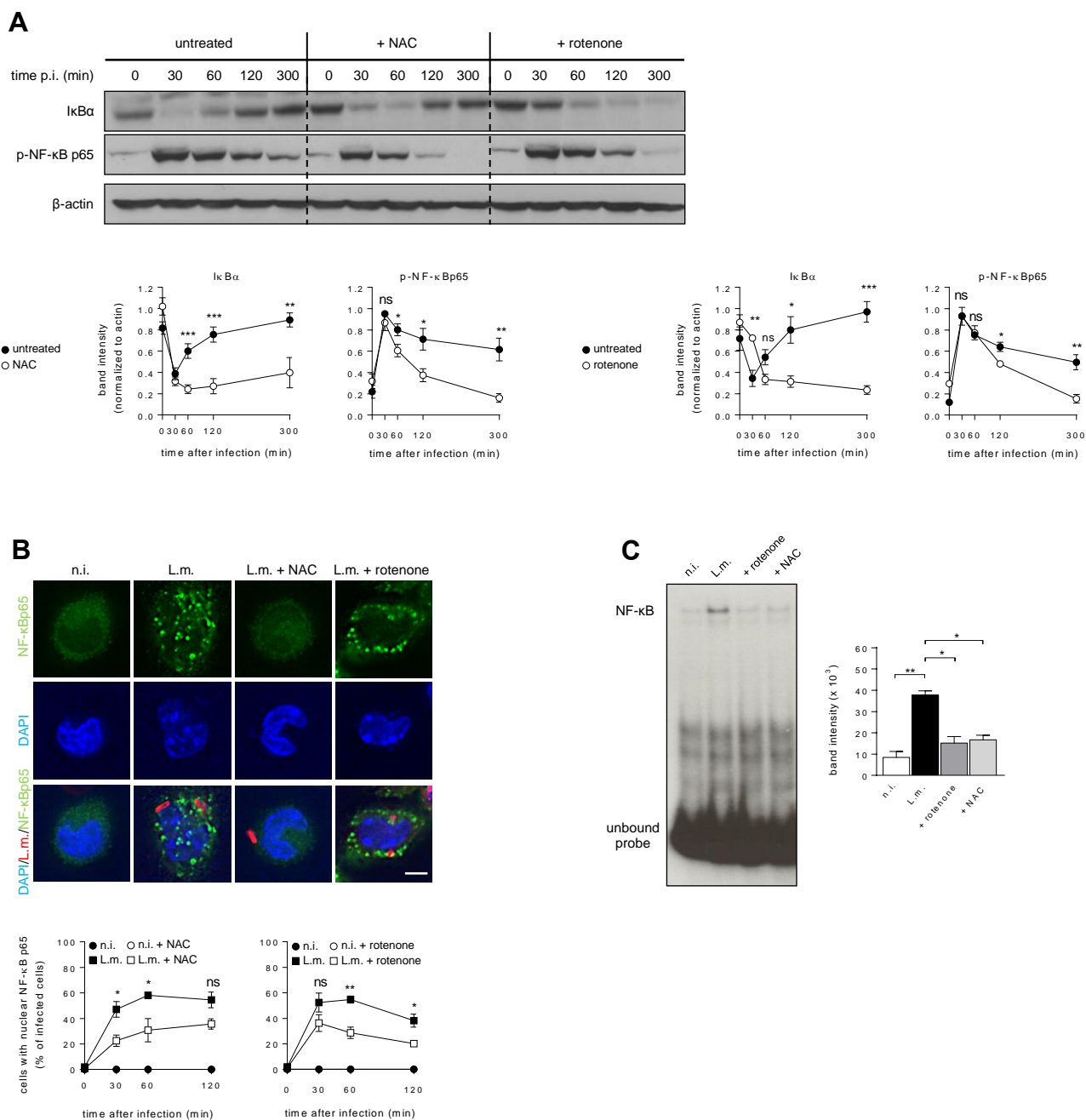


Figure 22: mtROS are necessary for full activation of NF-κB signaling

(A) At the indicated time points after infection with *L.m.* at a MOI of 1 in the presence or absence of 50 mM NAC or 100 μ M rotenone, phosphorylation status of NF-κB p65 (n=6), and degradation of IκBα (n=7) were analyzed by Western blot and quantified by densitometry of band intensities.

(B) At the indicated time points after infection with *L.m.* at a MOI of 1 in the presence or absence of 50 mM NAC or 100 μ M rotenone, macrophages showing translocation of NF-κB p65 into the nucleus were quantified by immunofluorescence microscopy (n=4). Scale bar represents 4 μ m.

(C) At 1 hour after infection with *L.m.* at a MOI of 1 in the presence or absence of 50 mM NAC or 100 μ M rotenone, DNA binding of NF-κB was analyzed by EMSA and quantified by densitometry of band intensities (n=3).

3.5. Mechanisms of mtROS-dependent pro-inflammatory signaling

Several studies addressed the question how ROS could influence pathways leading to cytokine secretion. Oxidative inhibition of phagosomal cathepsins (Allan et al., 2014; Deffert et al., 2012) or redox-sensitive phosphatases (Bulua et al., 2011a; Rao et al., 2002; Meinhard et al., 2001) have been suggested as possible targets for ROS.

3.5.1. mtROS do not regulate cytokine secretion by oxidative phosphatase inactivation

The phosphorylation status of IKK β , as well as that of several other kinases involved in pro-inflammatory signaling, is determined by the relative activities of upstream kinases and specific phosphatases such as PP2A and PP2C β (Hinz et al., 2014). Like many other phosphatases, PP2A are sensitive to oxidative inactivation (Rao et al., 2002; Meinhard et al., 2001), which favors phosphorylation of their substrates. Therefore, I investigated if oxidative inactivation of phosphatases by mtROS is required for pro-inflammatory signaling leading to cytokine secretion by L.m.-infected macrophages. To this end, I analyzed whether phosphatase inhibition could rescue impaired cytokine secretion by mtROS-deficient macrophages. Neither inhibition of protein tyrosine phosphatases with orthovanadate or PTP inhibitor I nor inhibition of serine/threonine phosphatases with okadaic acid, calyculin A, tautomycin or sanguinarine could rescue cytokine secretion by mtROS-deficient macrophages (Fig. 23). Thus, mtROS do not regulate pro-inflammatory signaling in L.m.-infected macrophages by inactivating redox-sensitive phosphatases.

Figure 23

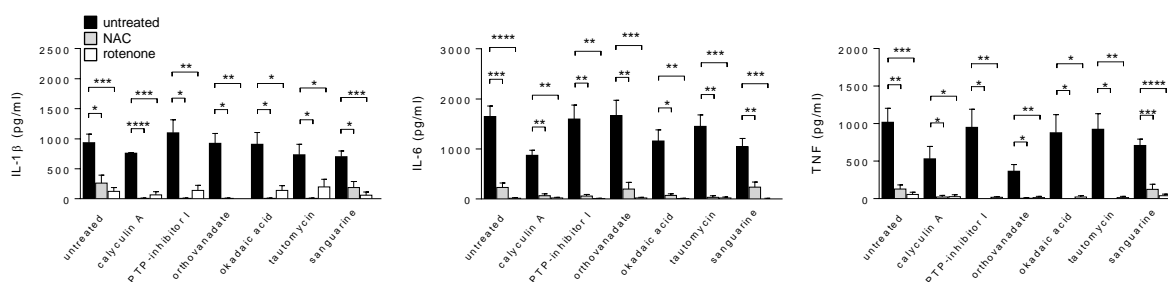


Figure 23: mtROS do not regulate cytokine secretion by oxidative phosphatase inactivation

Secretion of IL-1 β , IL-6 and TNF after 5 hours of infection with L.m. at a MOI of 1 in the presence or absence of 50 mM NAC or 100 μ M rotenone and with the inhibitors for protein tyrosine phosphatases (PTPs) orthovanadate (1 μ M) (all PTPs), PTP-inhibitor I (5 μ M) (PTP-1B and SHP-1) or for serine/threonine phosphatases (PPs) okadaic acid (1.5 nM) (PP1s and PP2As), calyculin A (100 μ M) (PP1s and PP2A-C), tautomycin (10 nM) (PP1s and PP2As) or sanguinarine (1 nM) (PP2Cs) was quantified by ELISA (n=3).

3.5.2. mtROS are crucial for IKK complex activation

Both the ERK1/2 and the NF- κ B pathway are initiated via the IKK complex (Gantke et al., 2012; Mercurio et al., 1997), whereas JNK1/2 and p38 pathways are activated independently of the IKK complex (Arthur et al., 2013; Israel, 2010; Sato et al., 2005; Shim et al., 2005). IKK complex activation leads to phosphorylation of IKK α /IKK β that is essential for subsequent pro-inflammatory signaling. Importantly, L.m. infection of macrophages resulted in phosphorylation of IKK β that was strongly reduced after treatment with NAC and rotenone (Fig. 24A) indicating that activation of the IKK complex requires mtROS-dependent signals.

3.5.3. mtROS induce covalent linkage of NEMO via disulfide bonds

An important regulator of IKK complex activation is its subunit NEMO. Function and structures of NEMO were investigated either with ligands that activate only one specific signaling pathway (Scholefield et al., 2016; Xu et al., 2009) or in infected non-immune cells (Brady et al., 2017). The structural and post-translational modifications as well as the role of NEMO during bacterial infection in immune cells in general and macrophages in particular remained completely elusive.

NEMO molecules have been shown to be covalently linked by ROS-dependent disulfide linkage in mouse embryonic fibroblasts (MEFS) (Herscovitch et al., 2008a) and, moreover, covalent disulfide linkage stabilized recombinant NEMO protein and increased its affinity to IKK β *in vitro* (Zhou et al., 2014b). Therefore, NEMO disulfide linkage is a promising potential target for mtROS-dependent regulation of pro-inflammatory signaling in infected macrophages.

To analyze the possible role of mtROS-dependent regulation of NEMO in infected macrophages, I used non-reducing SDS-PAGE under conditions that disrupt non-covalent interactions but preserve covalent links such as disulfide bonds (see section 2.2.14.2 and also (Herscovitch et al., 2008a). Uninfected macrophages contained only monomeric NEMO (~55 kDa), whereas L.m.-infection resulted in recruitment of NEMO into a complex of approximately 200 kDa (Fig. 24B). The other components of the IKK complex, IKK α and IKK β , were not included in the NEMO complex (Fig. 24B). Under standard reducing Western Blot conditions, which also disrupt covalent disulfide bonds, the NEMO complex was completely degraded to monomeric NEMO, but could be preserved by post-lysis protein crosslinking (Fig. 24C). Notably, even after crosslinking, uninfected macrophages contained only monomeric NEMO indicating that the NEMO complex is not present in naïve macrophages but forms after infection by covalent disulfide linkage. Importantly, covalent NEMO complex formation after L.m.-infection was strongly reduced in mtROS-deficient macrophages (Fig. 24D). These data show that, upon infection, NEMO is recruited into a complex, which is covalently linked via disulfide bonds and,

moreover, that mtROS are crucial for formation of this NEMO complex and subsequent IKK β activation.

Figure 24

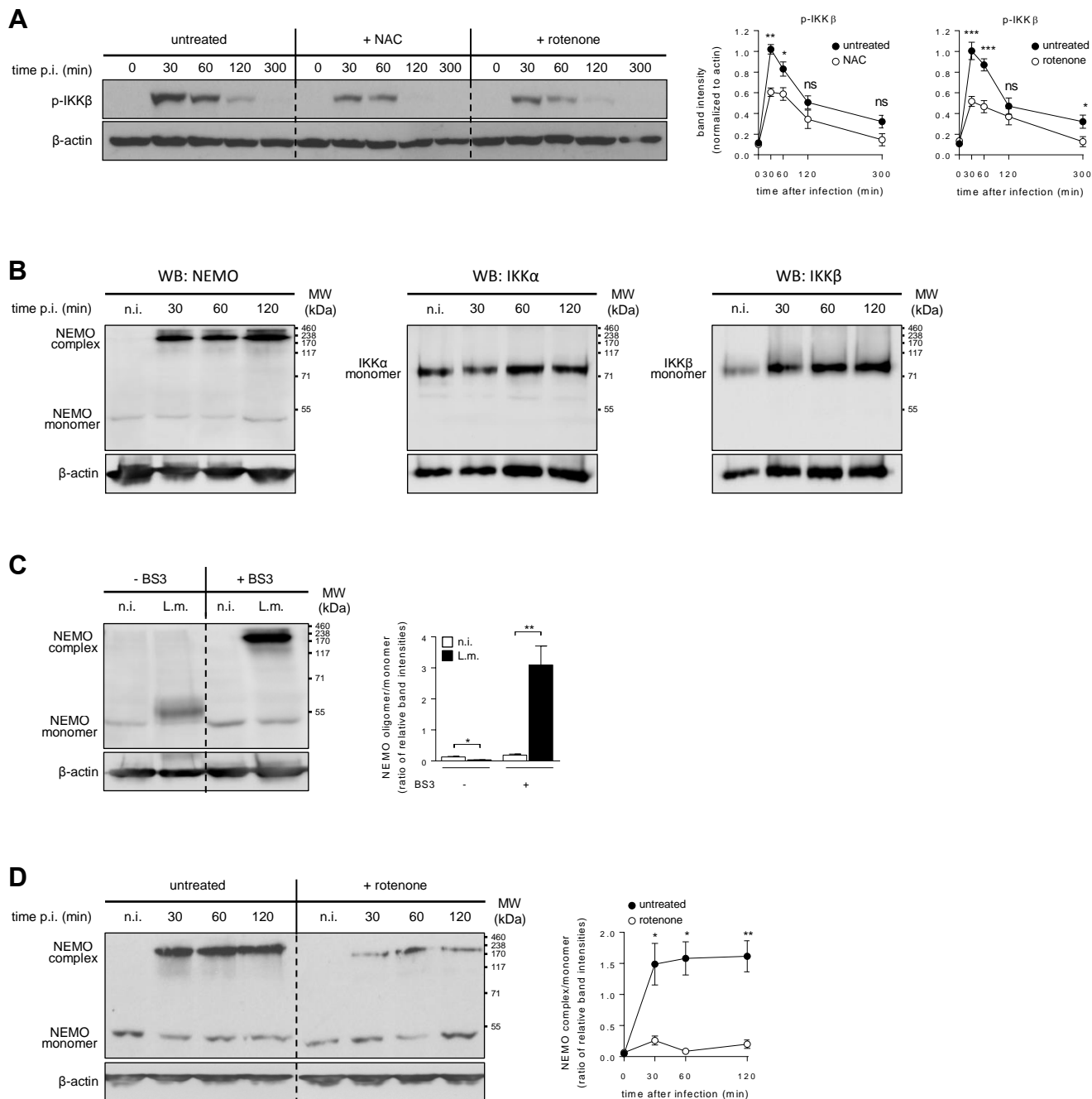


Figure 24: mtROS are crucial for covalent linkage of NEMO via disulfide bonds and subsequent IKK complex activation

(A) At the indicated time points after infection with L.m. at a MOI of 1 in the presence or absence of 50 mM NAC or 100 μ M rotenone, phosphorylation status of IKK β was analyzed by Western blot and quantified by densitometry of band intensities (n=6).

(B) At the indicated time points after infection with L.m. at a MOI of 1 presence of IKK α and IKK β in the covalently linked NEMO complex was analyzed by non-reducing SDS-PAGE and Western blot (n=3) (continued on next page).

Figure 24 (continued): mtROS are crucial for covalent linkage of NEMO via disulfide bonds and subsequent IKK complex activation

(C) Covalent linkage of NEMO via disulfide bonds was stabilized by amine-to-amine cross-linking with BS3 after 30 min infection with L.m. at a MOI 1 and analyzed by standard reducing SDS-PAGE and Western Blot and quantified by densitometry of band intensities (n=5).

(D) At the indicated time points after infection with L.m. at a MOI of 1 in the presence or absence of 100 μ M rotenone, covalent linkage of NEMO via disulfide bonds was analyzed by non-reducing SDS-PAGE and Western blot and quantified by densitometry of band intensities (n=3).

3.5.4. mtROS induce NEMO complex formation by covalent linkage via Cys⁵⁴ and Cys³⁴⁷

Herscovitch *et al.* identified the two redox-sensitive cysteines Cys⁵⁴ and Cys³⁴⁷ to be necessary for covalent dimerization of NEMO via disulfide bonds (Herscovitch *et al.*, 2008a). I hypothesized, that infection-induced mtROS induce NEMO complex formation by covalent linkage of Cys⁵⁴ and Cys³⁴⁷. To test this, I expressed a NEMO mutant in macrophages (Fig. 25A-B), in which Cys⁵⁴ and Cys³⁴⁷ are mutated to alanine (NEMO^{C54/347A}) and that therefore cannot form disulfide-linked dimers (Herscovitch *et al.*, 2008a). Importantly, the transfected NEMO^{C54/347A} construct was not able form covalently linked complexes in macrophages at all (Fig. 25C). Since two NEMO molecules with functional cysteine residues have to pair up to form disulfide bonds, expression of the NEMO^{C54/347A} mutant strongly impaired NEMO complex formation in infected macrophages (Fig. 25D). Together, these data show that mtROS produced in response to L.m. infection induce covalent linkage of NEMO via Cys^{54/347}.

Figure 25

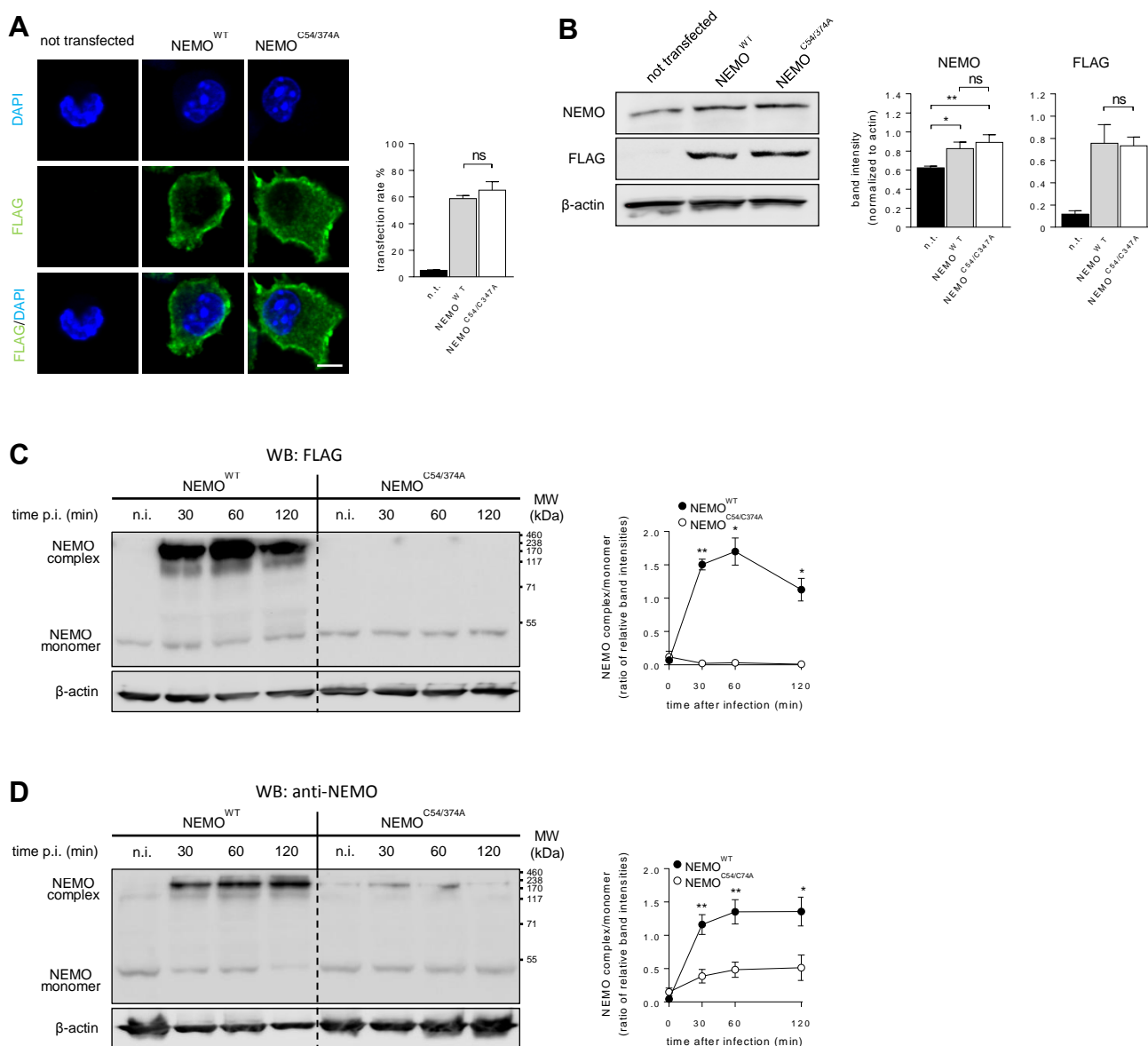


Figure 25: mtROS induce NEMO complex formation by covalent linkage via Cys⁵⁴ and Cys³⁴⁷

(A-D) Macrophages were transfected with mRNA encoding for wildtype NEMO (NEMO^{Wt}) or a NEMO mutant in which redox-sensitive Cys⁵⁴ and Cys³⁴⁷ are mutated to alanine (NEMO^{C54/347A}) for 6 h.

(A) Transfection rate was quantified by immunofluorescence microscopy (n=4).

(B) Expression levels of endogenous NEMO (n=5) and exogenous FLAG-tagged NEMO constructs (n=3) were analyzed by Western blot and quantified by densitometry of band intensities.

(C) At the indicated time points after infection with L.m. at a MOI of 1 covalent linkage of exogenous NEMO^{Wt} and NEMO^{C54/347A} constructs via disulfide bonds was analyzed by non-reducing SDS-PAGE and Western blot and quantified by densitometry of band intensities (n=3).

(D) At the indicated time points after infection with L.m. at a MOI of 1 covalent linkage of NEMO via disulfide bonds was analyzed by non-reducing SDS-PAGE and Western blot and quantified by densitometry of band intensities (n=5).

3.5.5. mtROS-mediated covalent linkage of NEMO via Cys⁵⁴ and Cys³⁴⁷ is crucial for pro-inflammatory signaling

I next wanted to investigate, if mtROS-dependent covalent linkage of NEMO via Cys⁵⁴ and Cys³⁴⁷ is the mechanistic step, which licenses pro-inflammatory signaling in infected macrophages. Strikingly, similar to mtROS-deficiency, expression of the NEMO^{C54/374A} mutant specifically reduced IKK β and ERK1/2 phosphorylation (Fig. 26A), DNA binding of NF- κ B (Fig. 26B) and pro-inflammatory cytokine secretion in L.m.-infected macrophages (Fig. 26C). These data show that mtROS regulate IKK complex activation as well as subsequent pro-inflammatory signaling and cytokine secretion by inducing covalent disulfide linkage of NEMO via Cys^{54/347}.

Figure 26

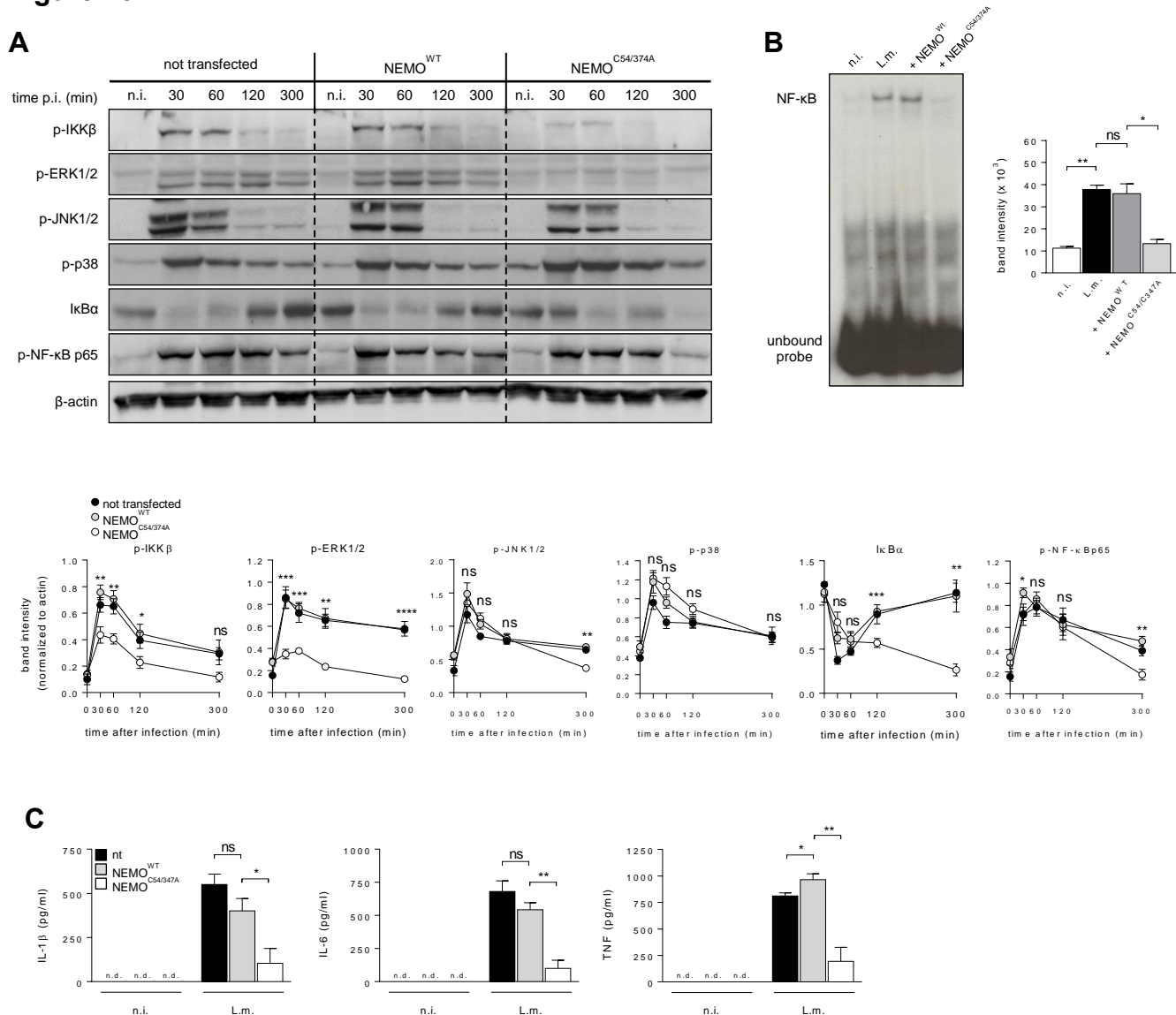


Figure 26: mtROS-mediated covalent linkage of NEMO via Cys⁵⁴ and Cys³⁴⁷ is crucial for pro-inflammatory signaling (legend on next page)

(A-C) Macrophages were transfected with mRNA encoding for wildtype NEMO (NEMO^{Wt}) or a NEMO mutant in which redox-sensitive Cys⁵⁴ and Cys³⁴⁷ are mutated to alanine (NEMO^{C54/347A}) for 6 h.

(A) At the indicated time points after infection with L.m. at a MOI of 1 phosphorylation of IKK β , ERK1/2, JNK1/2, p38 and NF- κ B p65 and degradation of I κ B α was analyzed by Western blot and quantified by densitometry of band intensities (n=3).

(B) At 1 hour after infection with L.m. at a MOI of 1 DNA binding of NF- κ B was analyzed by EMSA and quantified by densitometry of band intensities (n=3).

(C) Secretion of IL-1 β , IL-6 and TNF after 5 hours of infection with L.m. at a MOI of 1 was quantified by ELISA (n=3).

3.5.6. mtROS do not regulate processes up- or downstream of NEMO

If regulation of pro-inflammatory signaling leading to cytokine secretion by mtROS was exclusively by licensing activation of the IKK complex via disulfide linkage of NEMO, up- and downstream processes should not be affected by mtROS deficiency. The signaling cascade initiating IKK complex activation involves a complex consisting of MyD88, IRAK4, IRAK1/2 and TRAF6. IRAK1 is degraded shortly after activation of the IKK complex (Muroi et al., 2012; Yamin et al., 1997). IRAK1 degradation was induced in L.m.-infected macrophages and was not impaired by treatment with NAC or rotenone (Fig. 27A) suggesting that processes upstream of IKK complex activation do not depend on mtROS. Activation of IKK β was strongly dependent on mtROS-mediated NEMO complex formation (Fig. 24B). Therefore, expression of a constitutively active IKK β mutant (caIKK β) (Mercurio et al., 1997) should allow cytokine secretion even in the absence of mtROS production because it bypasses the redox-sensitive step of NEMO complex formation. Interestingly, expression of caIKK β (Fig. 27B+C) alone was not sufficient to induce MAPK- or NF- κ B-pathways (Fig. 27D) or cytokine secretion (Fig. 27E). An additional stimulus such as L.m. infection or LPS treatment was necessary to activate pro-inflammatory signaling. Notably, expression of caIKK β rescued pro-inflammatory cytokine secretion in macrophages deficient for ROS in general or mtROS in particular (Fig. 27E) indicating that mtROS are not required for processes downstream of IKK complex activation.

Collectively, the data from this section indicate that mtROS produced in response to L.m. infection license activation of the IKK complex and subsequent signaling via the ERK1/2 and NF- κ B pathways leading to cytokine secretion by inducing intermolecular disulfide linkage of NEMO via the redox-sensitive cysteines Cys^{54/347}

Figure 27

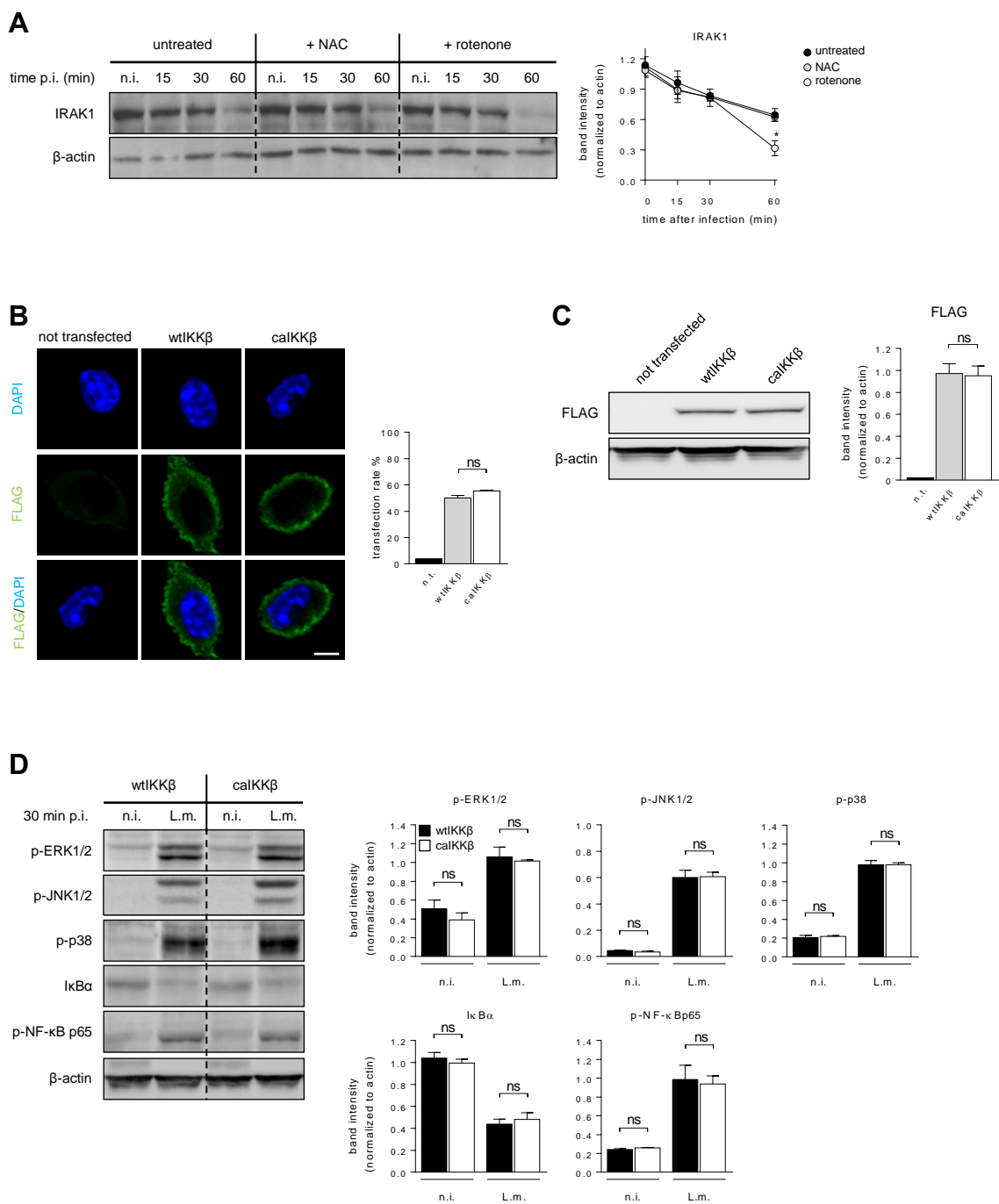


Figure 27: mtROS do not regulate processes up- or downstream of NEMO (Figure continued on next page)

Figure 27 (continued)

E

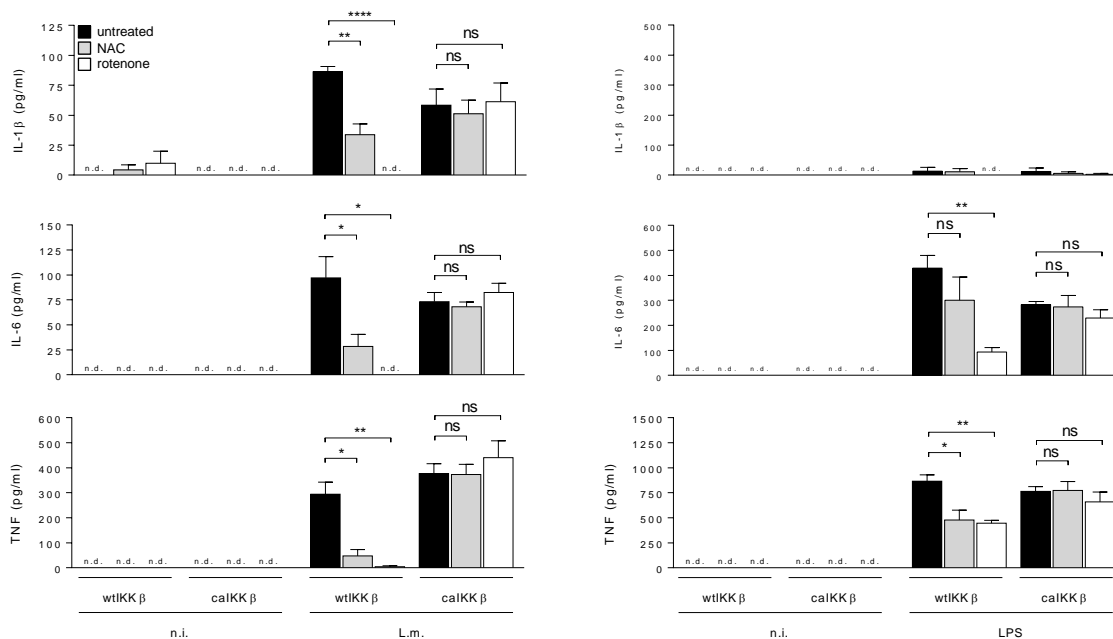


Figure 27 (continued): mtROS do not regulate processes up- or downstream of NEMO

(B-E) Macrophages were transfected with mRNA encoding for wildtype IKK β (wtIKK β) or a constitutively active IKK β mutant (caIKK β) for 6 h.

(A) At the indicated time points after infection with L.m. at a MOI of 1 in the presence or absence of 50 mM NAC or 100 μ M rotenone, degradation of IRAK1 was analyzed by Western blot and quantified by densitometry of band intensities (n=3).

(B) Transfection rate was quantified by immunofluorescence microscopy (n=2).

(C) Expression levels of FLAG-tagged IKK β were analyzed by Western blot and quantified by densitometry of band intensities (n=4).

(D) Phosphorylation status of ERK1/2, JNK1/2, p-p38 and NF- κ B p65 and degradation of I κ B α after infection with L.m. at a MOI of 1 for 30 min was analyzed by Western blot and quantified by densitometry of band intensities (n=3).

(E) Secretion of IL-1 β , IL-6 and TNF after 5 hours of infection with L.m. at a MOI of 1 or treatment with 5 μ g/ml LPS and in the presence or absence of 50 mM NAC or 100 μ M rotenone was quantified by ELISA (n=3).

3.5.7. Mechanism for mtROS-mediated pro-inflammatory signaling in infected macrophages

Based on the data described in this thesis I propose the following model for regulation of pro-inflammatory cytokine secretion by mtROS in L.m.-infected macrophages (Fig. 28): **(1)** Recognition of L.m. by TLR2 (in conjunction with other MyD88-dependent TLRs) induces activation of IRAK1/2 and TRAF6. **(2)** TRAF6 induces mtROS production. mtROS are produced as $\cdot\text{O}_2^-$ into the IMS by complex III of the ETC and converted into H_2O_2 by SOD1 allowing them

to access the cytosol by diffusion. **(3)** In the cytosol, mtROS mediate intermolecular covalent linkage of NEMO via disulfide bonds formed by the redox-sensitive cysteines Cys⁵⁴ and Cys^{347A}, which **(4)** allows full assembly and activation of the IKK complex. **(5)** Finally, the fully assembled IKK complex activates the ERK1/2 and NF- κ B pathways resulting in pro-inflammatory cytokine secretion. I thus identify mtROS-dependent disulfide linkage of NEMO as an essential regulatory step of the pro-inflammatory response of macrophages to bacterial infection.

Figure 28

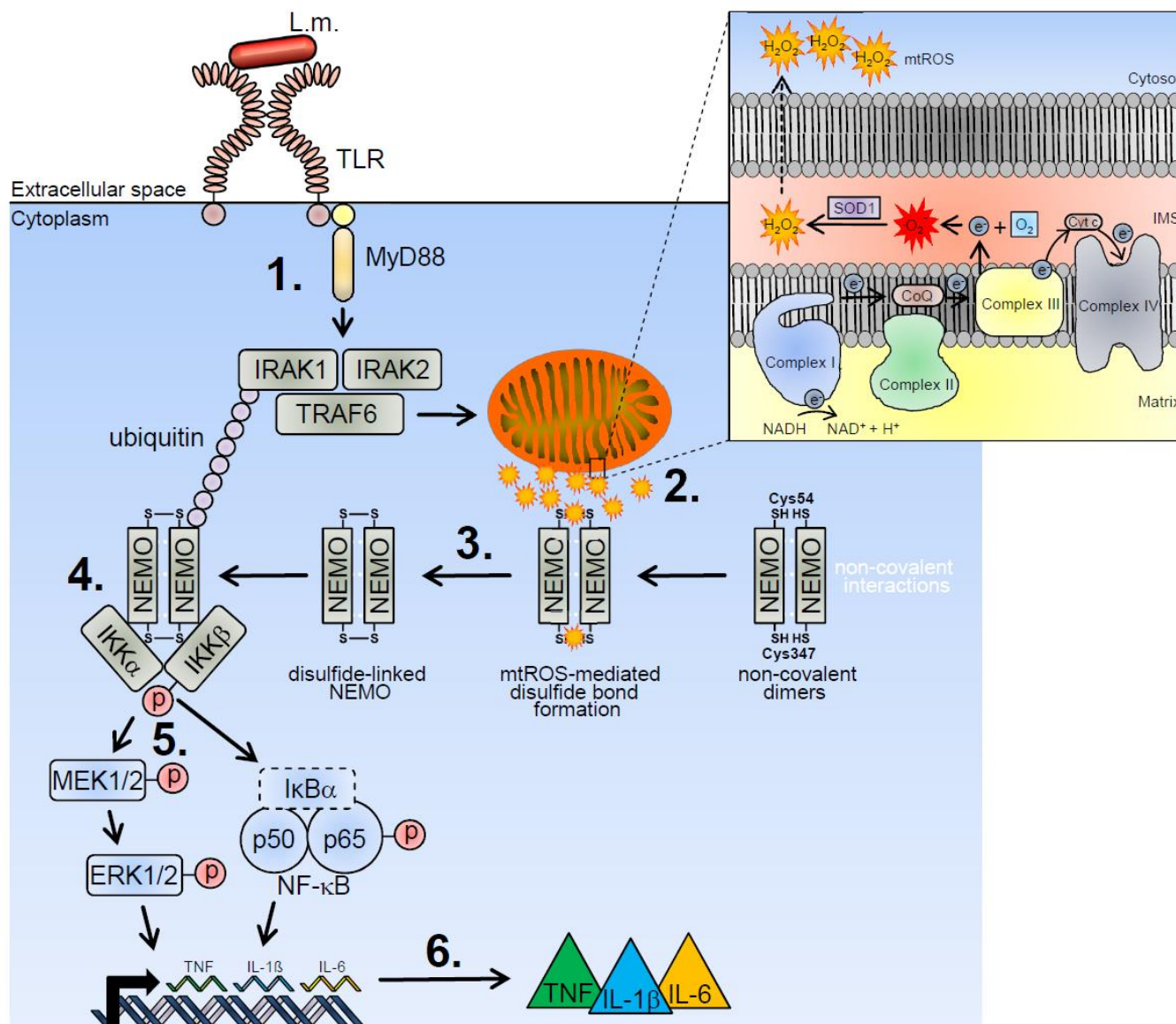


Figure 28: Model for regulation of pro-inflammatory cytokine secretion by mtROS in L.m.-infected macrophages

Detailed description can be found in the text.

4. Discussion

ROS have been reported to act in a number of different signaling pathways. However, the sources of ROS as well as the signaling pathways that are regulated by them largely depend on the specific cell type and stimulus (Holmström et al., 2014; Nathan et al., 2013b). Although ROS are clearly involved in cellular signaling processes on organ, tissue and cellular levels (Singel et al., 2016), surprisingly little is known about the molecular processes or proteins through which ROS influence pro-inflammatory signaling in general and during bacterial infection of macrophages in particular.

In this thesis, I used L.m. infection of peritoneal macrophages to model the anti-bacterial response of tissue macrophages to a complex pathogenic stimulus in order to investigate the cellular sources of ROS required for cytokine secretion and the molecular targets of ROS-dependent regulation of the pro-inflammatory response.

4.1. Mechanisms of ROS production in infected macrophages

Sources, locations, subspecies, quantities and specific roles of ROS vary greatly in dependency of the stimulus and the organ, tissue or cell type investigated. Therefore, consideration and definition of all these factors in each study that involves ROS as main research topic is essential to gain new mechanistic insights into ROS-dependent signaling. I used a respective panel of ROS detection probes, various knockout and knockin mouse lines and chemical inhibitors to define the source, subcellular locations and subspecies of ROS that play a role in pro-inflammatory signaling during bacterial infection of macrophages.

4.1.1 ROS production by Nox enzymes

Since the NADPH oxidase Nox2 is the predominant source of ROS in phagocytes, including macrophages, (Singel et al., 2016; Segal et al., 1981), Nox2-derived ROS often take center stage in the anti-microbial response of macrophages (Gluschko and Herb et al., 2018; Herb et al., 2018; Schramm et al., 2014; Pizzolla et al., 2012; Cornish et al., 2008; Gelderman et al., 2007). Upon stimulation, phagocytes produce robust quantities of Nox2-derived ROS into the extracellular space (Gluschko and Herb et al., 2018; Mocsai et al., 2002; Segal et al., 1981). Accordingly, macrophages showed a robust extracellular ROS production after bacterial infection and these extracellular ROS were exclusively produced by Nox2.

Recently, activation of Nox4 as a cytosolic ROS source after *Toxoplasma gondii* infection was described in BMDM (Kim et al., 2017). However, cytosolic ROS production by L.m.-infected macrophages was completely independent not only of Nox2 but also of all other isoforms of the

Nox/Duox family, namely Nox1, Nox4, Duox1 and Duox2. Even deficiency for the catalytic subunit p22^{phox}, which is essential for Nox1-4 did not alter infection-induced cytosolic ROS production. Of course, *Toxoplasma gondii*, as a eukaryotic parasite might trigger other ROS sources than bacterial infection. Moreover, BMDM have been described as not fully matured macrophages, expressing, for example, completely different surface receptors than mature tissue macrophages such as peritoneal or splenic macrophages (Wang et al., 2013; Murray et al., 2011). In addition, we could recently show that Nox2-derived extracellular ROS production in L.m.-infected BMDM was strongly reduced in comparison to peritoneal macrophages due to lower protein levels of Nox2 (Gluschko and Herb et al., 2018). Therefore, it is not surprising that ROS sources and quantities vary between cell types and stimuli. My data clearly define Nox2 as the exclusive extracellular ROS source, whereas cytosolic ROS production was completely independent of Nox/Duox family members after bacterial infection of tissue macrophages.

4.1.2 ROS production by mitochondria

Surprisingly, I identified mitochondria as the source of cytosolic ROS produced by macrophages after bacterial infection. Several studies showed that stimuli associated with Gram-negative pathogens induce mtROS production into the mitochondrial matrix (Garaude et al., 2016; West et al., 2011a). My data show that L.m. infection did not induce measurable production of ROS into the mitochondrial matrix and that matrix-derived ROS did not contribute to cytosolic ROS levels, since neither scavenging of $\cdot\text{O}_2^-$ nor that of H_2O_2 in the mitochondrial matrix did alter cytosolic ROS levels. Instead, blockade of electron flow from complex I to complex III with rotenone almost completely abrogated cytosolic ROS production. Complex III can produce ROS not only into the mitochondrial matrix but also into the IMS (Lanciano et al., 2013; West et al., 2011b; Murphy, 2009; Fridovich, 1997). Accordingly, inhibition of electron flow from complex III to complex IV with antimycin A (Bleier et al., 2013; Park et al., 2007) strongly increased cytosolic ROS levels not only in infected but also in uninfected macrophages indicating that complex III of the mitochondrial ETC produces ROS directly into the IMS. While $\cdot\text{O}_2^-$ needs VDAC to cross the outer mitochondrial membrane (Shoshan-Barmatz et al., 2010), H_2O_2 can reach the cytosol by diffusion from the IMS. Scavenging of cytosolic $\cdot\text{O}_2^-$ did not reduce cytosolic ROS levels, but scavenging of cytosolic H_2O_2 strongly reduced cytosolic ROS production in infected macrophages, identifying H_2O_2 as the cytosolic ROS subspecies produced by mitochondria.

Notably, inhibition of complex II did not alter cytosolic ROS levels. This is particularly interesting since BMDM challenged with the Gram-negative bacterium *Escherichia coli* transiently switch

the relative contributions to mitochondrial respiration from complex I to complex II by destabilization of complex I (Garaude et al., 2016). This rearrangement of the ETC depends on recognition of RNA from live bacteria by TLR3 and TLR7 and on phagosomal ROS production by Nox2 (Garaude et al., 2016). My data argue against a similar role for complex II in cytosolic ROS production during Gram-positive infection because 1) inhibition of complex II with malonate did not alter cytosolic ROS levels and 2) cytosolic ROS production was completely independent of Nox2, whereas electron transfer from complex I to complex III was essential for cytosolic ROS production. Thus, my data reveal a clear distinction to Gram-negative pathogens in the location of cytosolic ROS production by mitochondria indicating different mitochondrial targets for the signals induced by Gram-positive and Gram-negative pathogens.

Taken together, I identified two subcellular distinct ROS sources that contribute to ROS production in infected macrophages. On the one hand Nox2, as the exclusive extracellular ROS source, and on the other hand, complex III of the mitochondrial ETC that produces mtROS directly into the IMS from where they reach the cytosol as H₂O₂.

4.2 Induction of mtROS production

Several studies addressed the question which stimuli and signaling pathways induce ROS production in macrophages and induction of Nox2-derived ROS production is well-characterized for a broad spectrum of Gram-positive and Gram-negative pathogens and associated PAMPs (Remer et al., 2005; Werling et al., 2004; Vazquez-Torres et al., 2001; Adachi et al., 1998). We recently identified the β_2 integrin Mac-1 as an important receptor for L.m.-induced Nox2-derived phagosomal ROS production, which was crucial for listerial clearance *in vivo* (Gluschko and Herb et al., 2018; Herb et al., 2018). So far, studies that investigated induction of mtROS only used infection models with Gram-negative bacteria (Bulua et al., 2011a; West et al., 2011a) or LPS as a PAMP associated with Gram-negative bacteria (Kelly et al., 2015; Chandel et al., 2000). If and how Gram-positive pathogens such as L.m. stimulate mtROS in immune cells remained unknown.

4.2.1 Stress-induced mtROS production

Perturbation of mitochondrial function can result in increased mitochondrial ROS production (Zhang et al., 2016; Motori et al., 2013; Detmer et al., 2007). Stavru *et al.* reported that L.m. uses its pore-forming toxin LLO to induce fragmentation of the mitochondrial network in HeLa cells (Stavru et al., 2011). Therefore, I investigated if mtROS production in L.m.-infected macrophages was caused by LLO-dependent mitochondrial perturbation. L.m. deficient for LLO (Δhly) or for the transcriptional master regulator of L.m. virulence factors, *prfA* ($\Delta prfA$), induced

mtROS production to a similar level as wild type L.m. excluding a role for L.m. virulence factors in induction of mtROS. Furthermore, the mitochondrial network was not fragmented and the mitochondrial membrane potential, an indicator of mitochondrial health, was not reduced in L.m.-infected macrophages. Thus, L.m. infection induces mtROS production in macrophages not by damaging the mitochondrial network.

4.2.2 Receptor-induced mtROS production

mtROS production into the mitochondrial matrix was shown to be induced by infection with *Salmonella typhimurium* (West et al., 2011a). The signaling cascade leading to mtROS production into the mitochondrial matrix involves the TLR4/MyD88/TRAF6 signaling pathway and the protein ECSIT (Carneiro et al., 2018; West et al., 2011a; Vogel et al., 2007). Therefore, I investigated if L.m. infection induces mtROS production in an analogous manner via TLR2 signaling. Production of mtROS after L.m. infection was nearly abrogated in TLR2-, MyD88- and TRAF6-deficient macrophages indicating that mtROS production by L.m.-infected macrophages is predominantly triggered via the TLR2/MyD88/TRAF6 signaling pathway.

These data indicate that mtROS production in L.m.-infected macrophages is actively induced by TLR2/MyD88/TRAF6 signaling and not caused by perturbation of mitochondria.

4.3. Role of ROS for pro-inflammatory cytokine secretion

The role of ROS in the pro-inflammatory response of macrophages to infection with pathogenic bacteria in general or to L.m. in particular is incompletely understood (Brune et al., 2013; Forman et al., 2002). Global scavenging of ROS with NAC in infected macrophages resulted in strong reduction of the three pro-inflammatory cytokines IL-6, TNF and IL-1 β , suggesting an important role for ROS in general for pro-inflammatory signaling during bacterial infection. Since NAC scavenges both, extracellular and intracellular ROS, I investigated, which of the infection-induced subcellular ROS sources, namely Nox2 (extracellular ROS) or mitochondria (cytosolic mtROS), are necessary for pro-inflammatory signaling in macrophages.

4.3.1 Role of Nox/Duox enzymes for pro-inflammatory cytokine secretion

Deficiency for Nox2 leads to a hyper-inflammatory phenotype in mice (Grimm et al., 2013; Brown et al., 2003) accompanied by elevated cytokine levels (Allan et al., 2014; Deffert et al., 2012). Furthermore, redox-sensitive activation of the transcription factor NF- κ B in a Nox2-dependent manner during LPS-induced lung inflammation was reported (Han et al., 2013). These studies suggest a regulatory role for Nox2-derived ROS in the pro-inflammatory response. However, while IL-1 β secretion was even enhanced in Nox2- and p22^{phox}-deficient macrophages after L.m. infection, secretion of IL-6 and TNF was unaltered indicating that Nox2-

derived extracellular ROS are dispensable for cytokine secretion in infected macrophages. By contrast, further elimination of intracellular ROS by treatment of Nox2-deficient macrophages with NAC strongly reduced cytokine levels to a similar degree as in WT macrophages suggesting a crucial role for intracellular ROS during pro-inflammatory cytokine secretion. Since Nox1-4 and Duox1-2 did not contribute to cytosolic ROS production, macrophages deficient for these Nox isoforms also did not show any reduction in cytokine levels indicating that Nox/Duox enzymes do not contribute to cytosolic ROS production necessary for pro-inflammatory signaling in infected macrophages.

4.3.2 Role of mtROS for pro-inflammatory cytokine secretion

mtROS production into mitochondrial matrix was reported to be necessary for pro-inflammatory cytokine secretion after LPS stimulation (Kelly et al., 2015; Bulua et al., 2011b), but not after infection with the *Salmonella typhimurium* (West et al., 2011a). L.m.-infection did not induce mtROS production into the mitochondrial matrix. Furthermore, scavenging of $\cdot\text{O}_2^-$ and H_2O_2 in the mitochondrial matrix did not reduce pro-inflammatory cytokine secretion indicating that matrix-derived ROS do not contribute to cytosolic ROS levels and do not play a role in pro-inflammatory signaling in L.m.-infected macrophages. This is in accordance with the data from West *et al.* (bacterial infection) but differs from the study of Bulua *et al.* (stimulation with LPS). Recognition and phagocytosis of pathogenic bacteria such as L.m. and *Salmonella typhimurium* provide much more complex and sustained signals induced by several receptors than activation of a single type of receptor with a distinct stimulus such as LPS as they simultaneously activate multiple signaling pathways. Therefore, it is reasonable, that bacterial infection of macrophages elicits multiple and more complex pro-inflammatory signaling pathways compared to stimulation with a distinct substance, such as LPS, and that the pathways differ in regulation.

While L.m.-infection did not induce mtROS production into the mitochondrial matrix, it substantially induced mtROS production into the cytosol, which was nearly abolished after rotenone treatment of macrophages. Moreover, secretion of pro-inflammatory cytokines was strongly reduced in infected macrophages after rotenone treatment identifying infection-induced cytosolic mtROS production as crucial factor for pro-inflammatory cytokine secretion. Both H_2O_2 and $\cdot\text{O}_2^-$ can influence signaling pathways in cells (Holmström et al., 2014; Lambeth et al., 2014; Nathan et al., 2013a; Chen et al., 2009). Scavenging of cytosolic $\cdot\text{O}_2^-$ did not reduce cytosolic ROS levels or pro-inflammatory cytokine secretion, excluding $\cdot\text{O}_2^-$ as relevant signaling molecule for the pro-inflammatory response in L.m.-infected macrophages. Notably, scavenging of cytosolic H_2O_2 led not only to a strong reduction of cytosolic ROS levels but also to strong

reduction of IL-1 β and IL-6 secretion and to a significant reduction of TNF secretion indicating that H₂O₂ is the signaling intermediate necessary for the pro-inflammatory response. SOD1, which is localized in the IMS and the cytosol, quickly dismutates $\cdot\text{O}_2^-$ to H₂O₂. Accordingly, inhibition of SOD1 led to strongly reduced pro-inflammatory cytokine secretion in infected macrophages further strengthening the conclusion that H₂O₂ generated by complex III of the ETC is the ROS subspecies necessary for pro-inflammatory cytokine secretion.

Taken together, I could show that Nox2-derived extracellular ROS are dispensable for cytokine secretion, but cytosolic ROS are crucial for this process. None of the Nox/Duox family members contribute to cytosolic ROS production or pro-inflammatory cytokine secretion after bacterial infection of macrophages. Surprisingly, cytosolic ROS are, in fact, produced by mitochondria (mtROS), but do not originate from the mitochondrial matrix. Instead, my data show L.m.-infection induces TLR2/MyD88/TRAF6-dependent $\cdot\text{O}_2^-$ production into the IMS by complex III of the ETC. Here, $\cdot\text{O}_2^-$ is converted by SOD1 into H₂O₂ that diffuses into the cytosol where it regulates pro-inflammatory signaling.

4.4 mtROS-dependent pro-inflammatory signaling pathways

ROS act in a number of different signaling pathways (Holmström et al., 2014; Lambeth et al., 2014). However, whether mtROS contribute to the pro-inflammatory response of macrophages remains an open question as several studies had used LPS as a Gram-negative associated PAMP to address this topic, but came to different and partly contrasting conclusions (Kelly et al., 2015; Bulua et al., 2011a; Chandel et al., 2000). mtROS produced into the mitochondrial matrix either were 1) required for TNF secretion upon hypoxia but not upon LPS-stimulation (Chandel et al., 2000), 2) led to increased IL-1 β , unaltered TNF and decreased IL-10 secretion after LPS treatment (Kelly et al., 2015) or 3) partly reduced LPS-induced secretion of TNF, IL-6, IL-8 and IL-10 (Bulua et al., 2011a). If and how mtROS contribute to pro-inflammatory signaling in macrophages during infection with a Gram-positive pathogen remained completely elusive.

The main pathways leading to production of cytokines in macrophages are the MAPK pathways and the pathways leading to activation of NF- κ B (Arthur et al., 2013; Newton et al., 2012). Therefore, I investigated if these pathways are modulated by infection-induced mtROS production.

4.4.1 MAPK-pathways

Infection of macrophages with L.m. resulted in activation of all three MAPK pathways and their terminal kinases ERK1/2, JNK1/2 and p38. Importantly, preventing mtROS generation either by

scavenging of ROS with NAC or by inhibiting mtROS production with rotenone strongly reduced phosphorylation of ERK1/2 and its upstream regulator MEK1/2 indicating that mtROS are required for signaling via the ERK1/2 pathway. By contrast, phosphorylation of JNK1/2 was only slightly decreased and phosphorylation of p38 remained unchanged. Therefore, I hypothesized that the ERK1/2 pathway is the major pathway leading to secretion of cytokines by infected macrophages. Indeed, inhibition of the upstream kinase of ERK1/2, MEK1/2, was sufficient to completely block secretion of IL-1 β and IL-6 and to significantly reduce TNF secretion. These data indicate that mtROS are required for pro-inflammatory signaling leading to cytokine secretion by infected macrophages mainly because they regulate signaling via the ERK1/2 pathway.

4.4.2 The NF- κ B pathway

MAPK regulate cytokine secretion in conjunction with the NF- κ B pathway (Arthur et al., 2013; Newton et al., 2012; Chandrakesan et al., 2010). Degradation of I κ B α a prerequisite for release of the p65 subunit of NF- κ B, was not reduced in the absence of mtROS generation. However, phosphorylation of NF- κ B p65, that is necessary for optimal induction of NF- κ B target genes (Christian et al., 2016), translocation of NF- κ B p65 from the cytosol into the nucleus as well as DNA binding of NF- κ B were strongly reduced in the absence of mtROS generation indicating that mtROS also modulate signaling leading to activation of the NF- κ B pathway.

Thus, my data show that mtROS license pro-inflammatory signaling via activation the ERK1/2 and NF- κ B pathways in infected macrophages.

4.5 The molecular target of mtROS-dependent pro-inflammatory signaling

The molecular mechanisms by which mtROS regulate the pro-inflammatory response of macrophages during infection so far had remained completely unknown. Inactivation of redox-sensitive phosphatases by mtROS has been suggested as a potential mechanism after LPS stimulation (Bulua et al., 2011b). Notably, in infected macrophages, inhibition of protein tyrosine phosphatases or serine/threonine phosphatases by a respective panel of inhibitors did not restore cytokine secretion during mtROS deficiency excluding this regulatory step as target for mtROS during bacterial infection.

4.5.1 Activation of the IKK complex

The ERK1/2 and the NF- κ B pathways both depend on activation of the IKK complex (Ajibade et al., 2012; Gantke et al., 2012) and both pathways were not induced in mtROS-deficient macrophages. Therefore I analyzed, if mtROS deficiency during L.m. infection regulates IKK

complex activation. Notably, IKK β phosphorylation, as the final step of IKK complex activation, was strongly reduced in mtROS-deficient macrophages. Rearrangement of the regulatory subunit NEMO is essential for assembly and phosphorylation of the IKK α/β subunits (Maubach et al., 2017; Scholefield et al., 2016). Moreover covalent disulfide bonds between NEMO monomers formed by the redox-sensitive cysteines Cys⁵⁴ and Cys³⁴⁷ have been shown to stabilize the NEMO dimer and increase its affinity to IKK β (Zhou et al., 2014b; Cote et al., 2013b; Herscovitch et al., 2008a). Therefore, I hypothesized, that redox-sensitive regulation of NEMO by mtROS is the underlying mechanistic step that licenses IKK activation and subsequent pro-inflammatory signaling in infected macrophages.

4.5.2 Modulation of NEMO

All studies that investigated NEMO structure and function so far used substances that only activate a single type of cellular receptor (e.g. LPS, IL-1 β , TNF) (Scholefield et al., 2016; Xu et al., 2009; Herscovitch et al., 2008a; Windheim et al., 2008; Marienfeld et al., 2006), described the response of infected non-immune cells (Brady et al., 2017; de Jong et al., 2016; Wang et al., 2012), or performed *in vitro* studies with recombinant NEMO protein (Zhou et al., 2014b; Cote et al., 2013b). Nearly nothing is known about the structure and post-translational modifications of NEMO in infected immune cells in general or in macrophages in particular. Therefore, this study investigated for the first time NEMO structure and modifications in infected immune cells.

Uninfected macrophages contained only NEMO monomers that were not linked by covalent disulfide bonds. Notably, upon infection, NEMO was recruited into a covalently linked complex of approximately 200 kDa. The other subunits of the IKK complex than NEMO, IKK α and IKK β , were not included in the covalently linked complex. Importantly, complex formation was nearly abrogated in mtROS-deficient macrophages. The redox-sensitive residues Cys⁵⁴ and Cys³⁴⁷ have been shown to mediate disulfide linkage of NEMO monomers into a covalently linked dimer of about 100 kDa in TNF-stimulated non-immune cells (Zhou et al., 2014b; Cote et al., 2013b; Herscovitch et al., 2008b). Indeed, solely preventing mtROS-mediated disulfide linkage of NEMO by expression of a NEMO construct in which the cysteines Cys^{54/347} are mutated to alanine (NEMO^{C54/374A}) (Herscovitch et al., 2008a) was enough to abolish NEMO complex formation, IKK β and ERK1/2 phosphorylation, DNA binding of NF- κ B as well as pro-inflammatory cytokine secretion in infected macrophages.

Since the two cysteine residues Cys^{54/347} mediate formation of disulfide bonds between NEMO molecules (Zhou et al., 2014b; Cote et al., 2013b; Herscovitch et al., 2008a), and the other components of the IKK complex, IKK α and IKK β , were not included, the observed complex

represents most probably a dimerized NEMO dimer (four NEMO molecules x ~50 kDa = ~200 kDa) reported before by Tegethoff *et al.* (Tegethoff *et al.*, 2003). The precise composition of the NEMO complex as well as the specific consequences of disulfide linkage for NEMO function and interactions with its numerous binding partners will be investigated in future studies.

4.5.3 Up- and downstream processes of NEMO

Expression of a constitutively active mutant of IKK β (Mercurio *et al.*, 1997) that supersedes NEMO regulation of IKK complex activation completely rescued pro-inflammatory signaling in macrophages deficient for ROS in general or mtROS in particular. These data demonstrate that ROS deficiency does not affect processes downstream of IKK complex activation. Processes directly upstream of IKK complex activation such as IRAK1 degradation were also not impaired by ROS deficiency.

Thus, my data specifically introduce the mtROS-mediated disulfide linkage of NEMO as an essential regulatory step required for activation of the IKK complex and, thereby, for permitting ERK1/2 and NF- κ B signaling leading to pro-inflammatory cytokine secretion in infected macrophages.

4.6 Conclusion

Collectively, this thesis introduces a so far unknown molecular mechanism by which ROS in general and mtROS in particular regulate pro-inflammatory cytokine secretion in infected macrophages and identifies covalent disulfide linkage of NEMO via Cys^{54/347} by mtROS as a novel regulatory step critically required for activation of the IKK complex and subsequent signaling via the ERK1/2 and NF- κ B pathways.

5. References

- Adachi, O. et al.** Targeted disruption of the MyD88 gene results in loss of IL-1- and IL-18-mediated function. Immunity. **1998** 9, 143-150.
- Ago, T. et al.** Phosphorylation of p47phox directs phox homology domain from SH3 domain toward phosphoinositides, leading to phagocyte NADPH oxidase activation. Proceedings of the National Academy of Sciences of the United States of America. **2003** 100, 4474-4479.
- Agou, F. et al.** Inhibition of NF-kappa B activation by peptides targeting NF-kappa B essential modulator (nemo) oligomerization. J Biol Chem. **2004** 279, 54248-54257.
- Aguirre, J., and Lambeth, J.D.** Nox enzymes from fungus to fly to fish and what they tell us about Nox function in mammals. Free radical biology & medicine. **2010** 49, 1342-1353.
- Ajibade, A.A. et al.** TAK1 negatively regulates NF-kappaB and p38 MAP kinase activation in Gr-1+CD11b+ neutrophils. Immunity. **2012** 36, 43-54.
- Aktan, F.** iNOS-mediated nitric oxide production and its regulation. Life sciences. **2004** 75, 639-653.
- Al-Mehdi, A.B. et al.** Perinuclear mitochondrial clustering creates an oxidant-rich nuclear domain required for hypoxia-induced transcription. Science signaling. **2012** 5, ra47.
- Allan, E.R. et al.** NADPH oxidase modifies patterns of MHC class II-restricted epitopic repertoires through redox control of antigen processing. Journal of immunology. **2014** 192, 4989-5001.
- Alvarez-Dominguez, C. et al.** The contribution of both oxygen and nitrogen intermediates to the intracellular killing mechanisms of C1q-opsonized *Listeria monocytogenes* by the macrophage-like IC-21 cell line. Immunology. **2000** 101, 83-89.
- Arango Duque, G., and Descoteaux, A.** Macrophage cytokines: involvement in immunity and infectious diseases. Frontiers in immunology. **2014** 5, 491.
- Arsenijevic, D. et al.** Disruption of the uncoupling protein-2 gene in mice reveals a role in immunity and reactive oxygen species production. Nature genetics. **2000** 26, 435-439.
- Arthur, J.S., and Ley, S.C.** Mitogen-activated protein kinases in innate immunity. Nat Rev Immunol. **2013** 13, 679-692.
- Ashida, H. et al.** A bacterial E3 ubiquitin ligase IpaH9.8 targets NEMO/IKKgamma to dampen the host NF-kappaB-mediated inflammatory response. Nature cell biology. **2010** 12, 66-73; sup pp 61-69.
- Babior, B.M.** The activity of leukocyte NADPH oxidase: regulation by p47PHOX cysteine and serine residues. Antioxidants & redox signaling. **2002** 4, 35-38.
- Banfi, B. et al.** NOX3, a superoxide-generating NADPH oxidase of the inner ear. J Biol Chem. **2004** 279, 46065-46072.
- Banfi, B. et al.** A Ca(2+)-activated NADPH oxidase in testis, spleen, and lymph nodes. J Biol Chem. **2001** 276, 37594-37601.
- Banoth, B., and Cassel, S.L.** Mitochondria in innate immune signaling. Translational research : the journal of laboratory and clinical medicine. **2018**.
- Barford, D.** The role of cysteine residues as redox-sensitive regulatory switches. Current opinion in structural biology. **2004** 14, 679-686.
- Beauregard, K.E. et al.** pH-dependent perforation of macrophage phagosomes by listeriolysin O from *Listeria monocytogenes*. The Journal of experimental medicine. **1997** 186, 1159-1163.
- Bedard, K., and Krause, K.H.** The NOX family of ROS-generating NADPH oxidases: physiology and pathophysiology. Physiological reviews. **2007** 87, 245-313.

- Beinke, S. et al.** Lipopolysaccharide activation of the TPL-2/MEK/extracellular signal-regulated kinase mitogen-activated protein kinase cascade is regulated by I κ B kinase-induced proteolysis of NF- κ B1 p105. Mol Cell Biol. **2004** *24*, 9658-9667.
- Bleier, L., and Droese, S.** Superoxide generation by complex III: from mechanistic rationales to functional consequences. Biochimica et biophysica acta. **2013** *1827*, 1320-1331.
- Brady, G. et al.** Molluscum Contagiosum Virus Protein MC005 Inhibits NF- κ B Activation by Targeting NEMO-Regulated I κ B Kinase Activation. Journal of virology. **2017** *91*.
- Brand, M.D.** The sites and topology of mitochondrial superoxide production. Experimental gerontology. **2010** *45*, 466-472.
- Brown, E.J. et al.** Control of p70 s6 kinase by kinase activity of FRAP in vivo. Nature. **1995** *377*, 441-446.
- Brown, J.R. et al.** Diminished production of anti-inflammatory mediators during neutrophil apoptosis and macrophage phagocytosis in chronic granulomatous disease (CGD). J Leukoc Biol. **2003** *73*, 591-599.
- Brune, B. et al.** Redox control of inflammation in macrophages. Antioxidants & redox signaling. **2013** *19*, 595-637.
- Bulua, A.C. et al.** Mitochondrial reactive oxygen species promote production of proinflammatory cytokines and are elevated in TNFR1-associated periodic syndrome (TRAPS). The Journal of experimental medicine. **2011a** *208*, 519-533.
- Bulua, A.C. et al.** Mitochondrial reactive oxygen species promote production of proinflammatory cytokines and are elevated in TNFR1-associated periodic syndrome (TRAPS). J Exp Med. **2011b** *208*, 519-533.
- Carneiro, F.R.G. et al.** An Essential Role for ECSIT in Mitochondrial Complex I Assembly and Mitophagy in Macrophages. Cell reports. **2018** *22*, 2654-2666.
- Carnesecchi, S. et al.** A key role for NOX4 in epithelial cell death during development of lung fibrosis. Antioxidants & redox signaling. **2011** *15*, 607-619.
- Carter, R.S. et al.** In vivo identification of inducible phosphoacceptors in the IKK γ /NEMO subunit of human I κ B kinase. J Biol Chem. **2003** *278*, 19642-19648.
- Cavaillon, J.M.** Cytokines and macrophages. Biomedicine & pharmacotherapy = Biomedecine & pharmacotherapie. **1994** *48*, 445-453.
- Chandel, N.S.** Mitochondria as signaling organelles. Bmc Biol. **2014** *12*, 34.
- Chandel, N.S. et al.** Role of oxidants in NF- κ B activation and TNF- α gene transcription induced by hypoxia and endotoxin. Journal of immunology. **2000** *165*, 1013-1021.
- Chandrakesan, P. et al.** Novel changes in NF- κ B activity during progression and regression phases of hyperplasia: role of MEK, ERK, and p38. J Biol Chem. **2010** *285*, 33485-33498.
- Chariot, A. et al.** Association of the adaptor TANK with the I κ B kinase (IKK) regulator NEMO connects IKK complexes with IKK epsilon and TBK1 kinases. J Biol Chem. **2002** *277*, 37029-37036.
- Chavez, V. et al.** Ce-Duox1/BLI-3 generates reactive oxygen species as a protective innate immune mechanism in *Caenorhabditis elegans*. Infection and immunity. **2009** *77*, 4983-4989.
- Cheeseman, K.H., and Slater, T.F.** An introduction to free radical biochemistry. British medical bulletin. **1993** *49*, 481-493.
- Chen, G. et al.** TNF-induced recruitment and activation of the IKK complex require Cdc37 and Hsp90. Molecular cell. **2002** *9*, 401-410.
- Chen, Y. et al.** Superoxide is the major reactive oxygen species regulating autophagy. Cell death and differentiation. **2009** *16*, 1040-1052.
- Cheng, G. et al.** Homologs of gp91phox: cloning and tissue expression of Nox3, Nox4, and Nox5. Gene. **2001** *269*, 131-140.

- Chiarugi, P. et al.** Two vicinal cysteines confer a peculiar redox regulation to low molecular weight protein tyrosine phosphatase in response to platelet-derived growth factor receptor stimulation. J Biol Chem. **2001** 276, 33478-33487.
- Christian, F. et al.** The Regulation of NF-kappaB Subunits by Phosphorylation. Cells. **2016** 5.
- Clark, K. et al.** The TRAF-associated protein TANK facilitates cross-talk within the IkappaB kinase family during Toll-like receptor signaling. Proceedings of the National Academy of Sciences of the United States of America. **2011** 108, 17093-17098.
- Cooke, E.L. et al.** Functional analysis of the interleukin-1-receptor-associated kinase (IRAK-1) in interleukin-1 beta-stimulated nuclear factor kappa B (NF-kappa B) pathway activation: IRAK-1 associates with the NF-kappa B essential modulator (NEMO) upon receptor stimulation. Biochem J. **2001** 359, 403-410.
- Cornish, E.J. et al.** Reduced nicotinamide adenine dinucleotide phosphate oxidase-independent resistance to *Aspergillus fumigatus* in alveolar macrophages. Journal of immunology. **2008** 180, 6854-6867.
- Cortassa, S. et al.** Redox-optimized ROS balance and the relationship between mitochondrial respiration and ROS. Biochimica et biophysica acta. **2014** 1837, 287-295.
- Cote, S.M. et al.** Mutation of nonessential cysteines shows that the NF-kappaB essential modulator forms a constitutive noncovalent dimer that binds IkappaB kinase-beta with high affinity. Biochemistry. **2013a** 52, 9141-9154.
- Craig, M., and Slauch, J.M.** Phagocytic superoxide specifically damages an extracytoplasmic target to inhibit or kill *Salmonella*. PloS one. **2009** 4, e4975.
- Cross, C.E. et al.** Oxygen radicals and human disease. Annals of internal medicine. **1987** 107, 526-545.
- Dan Dunn, J. et al.** Reactive oxygen species and mitochondria: A nexus of cellular homeostasis. Redox Biol. **2015** 6, 472-485.
- Davies, L.C. et al.** Tissue-resident macrophages. Nat Immunol. **2013** 14, 986-995.
- de Jong, M.F. et al.** *Shigella flexneri* suppresses NF-kappaB activation by inhibiting linear ubiquitin chain ligation. Nature microbiology. **2016** 1, 16084.
- Deffert, C. et al.** Hyperinflammation of chronic granulomatous disease is abolished by NOX2 reconstitution in macrophages and dendritic cells. The Journal of pathology. **2012** 228, 341-350.
- del Cerro-Vadillo, E. et al.** Cutting edge: a novel nonoxidative phagosomal mechanism exerted by cathepsin-D controls *Listeria monocytogenes* intracellular growth. Journal of immunology. **2006** 176, 1321-1325.
- Deng, L. et al.** Activation of the IkappaB kinase complex by TRAF6 requires a dimeric ubiquitin-conjugating enzyme complex and a unique polyubiquitin chain. Cell. **2000** 103, 351-361.
- Denora, N., and Natile, G.** An Updated View of Translocator Protein (TSPO). International journal of molecular sciences. **2017** 18.
- Detmer, S.A., and Chan, D.C.** Functions and dysfunctions of mitochondrial dynamics. Nature reviews Molecular cell biology. **2007** 8, 870-879.
- Diaz, F. et al.** Cells lacking Rieske iron-sulfur protein have a reactive oxygen species-associated decrease in respiratory complexes I and IV. Mol Cell Biol. **2012** 32, 415-429.
- Dikalova, A.E. et al.** Upregulation of Nox1 in vascular smooth muscle leads to impaired endothelium-dependent relaxation via eNOS uncoupling. American journal of physiology Heart and circulatory physiology. **2010** 299, H673-679.
- Dillin, A. et al.** Rates of behavior and aging specified by mitochondrial function during development. Science (New York, NY). **2002** 298, 2398-2401.
- Djaldetti, M. et al.** Phagocytosis--the mighty weapon of the silent warriors. Microscopy research and technique. **2002** 57, 421-431.

- Donko, A. et al.** Urothelial cells produce hydrogen peroxide through the activation of Duox1. Free radical biology & medicine. **2010** *49*, 2040-2048.
- Ehlers, M.R.** CR3: a general purpose adhesion-recognition receptor essential for innate immunity. Microbes and infection. **2000** *2*, 289-294.
- Epelman, S. et al.** Origin and functions of tissue macrophages. Immunity. **2014** *41*, 21-35.
- Fang, F.C.** Antimicrobial actions of reactive oxygen species. mBio. **2011** *2*.
- Farber, J.M., and Peterkin, P.I.** Listeria monocytogenes, a food-borne pathogen. Microbiological reviews. **1991** *55*, 476-511.
- Fiers, W. et al.** More than one way to die: apoptosis, necrosis and reactive oxygen damage. Oncogene. **1999** *18*, 7719-7730.
- Finkel, T.** Signal transduction by reactive oxygen species. The Journal of cell biology. **2011** *194*, 7-15.
- Forman, H.J., and Torres, M.** Reactive oxygen species and cell signaling: respiratory burst in macrophage signaling. American journal of respiratory and critical care medicine. **2002** *166*, S4-8.
- Freitag, N.E. et al.** Listeria monocytogenes - from saprophyte to intracellular pathogen. Nature reviews Microbiology. **2009** *7*, 623-628.
- Fridovich, I.** Superoxide anion radical (O₂⁻), superoxide dismutases, and related matters. J Biol Chem. **1997** *272*, 18515-18517.
- Gantke, T. et al.** IkappaB kinase regulation of the TPL-2/ERK MAPK pathway. Immunological reviews. **2012** *246*, 168-182.
- Garaude, J. et al.** Mitochondrial respiratory-chain adaptations in macrophages contribute to antibacterial host defense. Nature immunology. **2016**.
- Gavazzi, G. et al.** Decreased blood pressure in NOX1-deficient mice. FEBS letters. **2006** *580*, 497-504.
- Gelderman, K.A. et al.** Macrophages suppress T cell responses and arthritis development in mice by producing reactive oxygen species. The Journal of clinical investigation. **2007** *117*, 3020-3028.
- Gluschko, A. and Herb, M., et al.** The beta2 Integrin Mac-1 Induces Protective LC3-Associated Phagocytosis of Listeria monocytogenes. Cell host & microbe. **2018** *23*, 324-337 e325.
- Goldberg, M.B.** Actin-based motility of intracellular microbial pathogens. Microbiology and molecular biology reviews : MMBR. **2001** *65*, 595-626, table of contents.
- Grimm, M.J. et al.** Monocyte- and macrophage-targeted NADPH oxidase mediates antifungal host defense and regulation of acute inflammation in mice. Journal of immunology. **2013** *190*, 4175-4184.
- Ha, E.M. et al.** An antioxidant system required for host protection against gut infection in Drosophila. Developmental cell. **2005** *8*, 125-132.
- Haas, A.** The phagosome: compartment with a license to kill. Traffic (Copenhagen, Denmark). **2007** *8*, 311-330.
- Hagmann, C.A. et al.** RIG-I detects triphosphorylated RNA of Listeria monocytogenes during infection in non-immune cells. PloS one. **2013** *8*, e62872.
- Hambleton, J. et al.** Activation of c-Jun N-terminal kinase in bacterial lipopolysaccharide-stimulated macrophages. Proceedings of the National Academy of Sciences of the United States of America. **1996** *93*, 2774-2778.
- Hamon, M.A. et al.** Listeriolysin O: the Swiss army knife of Listeria. Trends in microbiology. **2012** *20*, 360-368.
- Han, W. et al.** NADPH oxidase limits lipopolysaccharide-induced lung inflammation and injury in mice through reduction-oxidation regulation of NF-kappaB activity. Journal of immunology. **2013** *190*, 4786-4794.
- Harhaj, E.W., and Sun, S.C.** IKKgamma serves as a docking subunit of the IkappaB kinase (IKK) and mediates interaction of IKK with the human T-cell leukemia virus Tax protein. J Biol Chem. **1999** *274*, 22911-22914.

- Harrington-Fowler, L. et al.** Fate of *Listeria monocytogenes* in resident and activated macrophages. Infection and immunity. **1981** 33, 11-16.
- Haslund-Vinding, J. et al.** NADPH oxidases in oxidant production by microglia: activating receptors, pharmacology and association with disease. British journal of pharmacology. **2017** 174, 1733-1749.
- Hempel, S.L. et al.** Dihydrofluorescein diacetate is superior for detecting intracellular oxidants: comparison with 2',7'-dichlorodihydrofluorescein diacetate, 5(and 6)-carboxy-2',7'-dichlorodihydrofluorescein diacetate, and dihydrorhodamine 123. Free radical biology & medicine. **1999** 27, 146-159.
- Herb, M. et al.** LC3-associated phagocytosis initiated by integrin ITGAM-ITGB2/Mac-1 enhances immunity to *Listeria monocytogenes*. Autophagy. **2018** 14, 1462-1464.
- Herscovitch, M. et al.** Intermolecular disulfide bond formation in the NEMO dimer requires Cys54 and Cys347. Biochemical and biophysical research communications. **2008a** 367, 103-108.
- Hinz, M., and Scheidereit, C.** The I κ B kinase complex in NF- κ B regulation and beyond. EMBO reports. **2014** 15, 46-61.
- Hoeven, R. et al.** Ce-Duox1/BLI-3 generated reactive oxygen species trigger protective SKN-1 activity via p38 MAPK signaling during infection in *C. elegans*. PLoS pathogens. **2011** 7, e1002453.
- Holmström, K.M., and Finkel, T.** Cellular mechanisms and physiological consequences of redox-dependent signalling. Nature reviews Molecular cell biology. **2014** 15, 411-421.
- Huang, T.T. et al.** Sequential modification of NEMO/IKK γ by SUMO-1 and ubiquitin mediates NF- κ B activation by genotoxic stress. Cell. **2003** 115, 565-576.
- Imai, Y. et al.** Identification of oxidative stress and Toll-like receptor 4 signaling as a key pathway of acute lung injury. Cell. **2008** 133, 235-249.
- Ishitani, T. et al.** Role of the TAB2-related protein TAB3 in IL-1 and TNF signaling. The EMBO journal. **2003** 22, 6277-6288.
- Israel, A.** The IKK complex, a central regulator of NF- κ B activation. Cold Spring Harbor perspectives in biology. **2010** 2, a000158.
- Ito, H. et al.** Decreased superoxide dismutase activity and increased superoxide anion production in cardiac hypertrophy of spontaneously hypertensive rats. Clinical and experimental hypertension (New York, NY : 1993). **1995** 17, 803-816.
- Iwasaki, A., and Medzhitov, R.** Regulation of adaptive immunity by the innate immune system. Science (New York, NY). **2010** 327, 291-295.
- Johnson, K.R. et al.** Congenital hypothyroidism, dwarfism, and hearing impairment caused by a missense mutation in the mouse dual oxidase 2 gene, Duox2. Molecular endocrinology (Baltimore, Md). **2007** 21, 1593-1602.
- Jones, A.I. et al.** Extracellular Redox Regulation of Intracellular Reactive Oxygen Generation, Mitochondrial Function and Lipid Turnover in Cultured Human Adipocytes. PLoS one. **2016** 11, e0164011.
- Kaludercic, N. et al.** Reactive oxygen species and redox compartmentalization. Frontiers in physiology. **2014** 5, 285.
- Kamata, H. et al.** Reactive oxygen species promote TNF α -induced death and sustained JNK activation by inhibiting MAP kinase phosphatases. Cell. **2005** 120, 649-661.
- Kanarek, N., and Ben-Neriah, Y.** Regulation of NF- κ B by ubiquitination and degradation of the I κ Bs. Immunological reviews. **2012** 246, 77-94.
- Kanayama, A. et al.** TAB2 and TAB3 activate the NF- κ B pathway through binding to polyubiquitin chains. Molecular cell. **2004** 15, 535-548.

- Kawahara, T. et al.** Point mutations in the proline-rich region of p22phox are dominant inhibitors of Nox1- and Nox2-dependent reactive oxygen generation. J Biol Chem. **2005** 280, 31859-31869.
- Kawai, T., and Akira, S.** Toll-like receptors and their crosstalk with other innate receptors in infection and immunity. Immunity. **2011** 34, 637-650.
- Kelley, E.E. et al.** Hydrogen peroxide is the major oxidant product of xanthine oxidase. Free radical biology & medicine. **2010** 48, 493-498.
- Kelly, B. et al.** Metformin Inhibits the Production of Reactive Oxygen Species from NADH:Ubiquinone Oxidoreductase to Limit Induction of Interleukin-1 β (IL-1 β) and Boosts Interleukin-10 (IL-10) in Lipopolysaccharide (LPS)-activated Macrophages. The Journal of biological chemistry. **2015** 290, 20348-20359.
- Kim, J.J. et al.** TNF-alpha-induced ROS production triggering apoptosis is directly linked to Romo1 and Bcl-X(L). Cell death and differentiation. **2010** 17, 1420-1434.
- Kim, Y.M. et al.** ROS-induced ROS release orchestrated by Nox4, Nox2, and mitochondria in VEGF signaling and angiogenesis. American journal of physiology Cell physiology. **2017** 312, C749-C764.
- Kirkman, H.N., and Gaetani, G.F.** Mammalian catalase: a venerable enzyme with new mysteries. Trends in biochemical sciences. **2007** 32, 44-50.
- Lambeth, J.D. et al.** Regulation of Nox and Duox enzymatic activity and expression. Free radical biology & medicine. **2007** 43, 319-331.
- Lambeth, J.D., and Neish, A.S.** Nox enzymes and new thinking on reactive oxygen: a double-edged sword revisited. Annual review of pathology. **2014** 9, 119-145.
- Lanciano, P. et al.** Molecular mechanisms of superoxide production by complex III: a bacterial versus human mitochondrial comparative case study. Biochimica et biophysica acta. **2013** 1827, 1332-1339.
- Laplantine, E. et al.** NEMO specifically recognizes K63-linked poly-ubiquitin chains through a new bipartite ubiquitin-binding domain. The EMBO journal. **2009** 28, 2885-2895.
- Lartigue, L., and Faustin, B.** Mitochondria: metabolic regulators of innate immune responses to pathogens and cell stress. The international journal of biochemistry & cell biology. **2013** 45, 2052-2056.
- Lee, A.J. et al.** MyD88-BLT2-dependent cascade contributes to LPS-induced interleukin-6 production in mouse macrophage. Experimental & molecular medicine. **2015** 47, e156.
- Lee, M.H. et al.** NF-kappaB induction of the SUMO protease SENP2: A negative feedback loop to attenuate cell survival response to genotoxic stress. Molecular cell. **2011** 43, 180-191.
- Lee, S.R. et al.** Reversible inactivation of protein-tyrosine phosphatase 1B in A431 cells stimulated with epidermal growth factor. J Biol Chem. **1998** 273, 15366-15372.
- Leto, T.L. et al.** Targeting and regulation of reactive oxygen species generation by Nox family NADPH oxidases. Antioxidants & redox signaling. **2009** 11, 2607-2619.
- Levine, A. et al.** H₂O₂ from the oxidative burst orchestrates the plant hypersensitive disease resistance response. Cell. **1994** 79, 583-593.
- Ley, K. et al.** How Mouse Macrophages Sense What Is Going On. Frontiers in immunology. **2016** 7, 204.
- Li, X. et al.** Targeting mitochondrial reactive oxygen species as novel therapy for inflammatory diseases and cancers. Journal of hematology & oncology. **2013** 6, 19.
- Li, Z.W. et al.** The IKKbeta subunit of IkappaB kinase (IKK) is essential for nuclear factor kappaB activation and prevention of apoptosis. The Journal of experimental medicine. **1999** 189, 1839-1845.
- Liemburg-Apers, D.C. et al.** Interactions between mitochondrial reactive oxygen species and cellular glucose metabolism. Arch Toxicol. **2015** 89, 1209-1226.

- Lin, K.M. et al.** IRAK-1 bypasses priming and directly links TLRs to rapid NLRP3 inflammasome activation. Proceedings of the National Academy of Sciences of the United States of America. **2014** *111*, 775-780.
- Lischke, T. et al.** CD38 controls the innate immune response against *Listeria monocytogenes*. Infection and immunity. **2013** *81*, 4091-4099.
- Liu, C. et al.** TAK1 promotes BMP4/Smad1 signaling via inhibition of erk MAPK: a new link in the FGF/BMP regulatory network. Differentiation; research in biological diversity. **2012** *83*, 210-219.
- Lundqvist, H., and Dahlgren, C.** Isoluminol-enhanced chemiluminescence: a sensitive method to study the release of superoxide anion from human neutrophils. Free radical biology & medicine. **1996** *20*, 785-792.
- Mabb, A.M. et al.** PIASy mediates NEMO sumoylation and NF-kappaB activation in response to genotoxic stress. Nature cell biology. **2006** *8*, 986-993.
- Marienfeld, R.B. et al.** Dimerization of the I kappa B kinase-binding domain of NEMO is required for tumor necrosis factor alpha-induced NF-kappa B activity. Mol Cell Biol. **2006** *26*, 9209-9219.
- Marinho, H.S. et al.** The cellular steady-state of H₂O₂: latency concepts and gradients. Methods in enzymology. **2013** *527*, 3-19.
- Maubach, G. et al.** NEMO Links Nuclear Factor-kappaB to Human Diseases. Trends in molecular medicine. **2017** *23*, 1138-1155.
- McLauchlin, J.** Human listeriosis in Britain, 1967-85, a summary of 722 cases. 1. Listeriosis during pregnancy and in the newborn. Epidemiology and infection. **1990** *104*, 181-189.
- McLauchlin, J. et al.** *Listeria monocytogenes* and listeriosis: a review of hazard characterisation for use in microbiological risk assessment of foods. International journal of food microbiology. **2004** *92*, 15-33.
- Meinhard, M., and Grill, E.** Hydrogen peroxide is a regulator of ABI1, a protein phosphatase 2C from *Arabidopsis*. FEBS letters. **2001** *508*, 443-446.
- Melov, S. et al.** Mitochondrial disease in superoxide dismutase 2 mutant mice. Proceedings of the National Academy of Sciences of the United States of America. **1999** *96*, 846-851.
- Meng, T.C. et al.** Reversible oxidation and inactivation of protein tyrosine phosphatases in vivo. Molecular cell. **2002** *9*, 387-399.
- Mercurio, F. et al.** IKK-1 and IKK-2: cytokine-activated IkappaB kinases essential for NF-kappaB activation. Science (New York, NY). **1997** *278*, 860-866.
- Meyer-Morse, N. et al.** Listeriolysin O is necessary and sufficient to induce autophagy during *Listeria monocytogenes* infection. PloS one. **2010** *5*, e8610.
- Minton, K.** Calcium: 'Working out' mitochondrial calcium. Nature reviews Molecular cell biology. **2013** *14*, 750.
- Mitchell, G. et al.** Strategies Used by Bacteria to Grow in Macrophages. Microbiology spectrum. **2016** *4*.
- Mocsai, A. et al.** Syk is required for integrin signaling in neutrophils. Immunity. **2002** *16*, 547-558.
- Mosser, D.M., and Edwards, J.P.** Exploring the full spectrum of macrophage activation. Nat Rev Immunol. **2008** *8*, 958-969.
- Motori, E. et al.** Inflammation-induced alteration of astrocyte mitochondrial dynamics requires autophagy for mitochondrial network maintenance. Cell metabolism. **2013** *18*, 844-859.
- Motta, V. et al.** NOD-like receptors: versatile cytosolic sentinels. Physiological reviews. **2015** *95*, 149-178.
- Mukhopadhyay, P. et al.** Simultaneous detection of apoptosis and mitochondrial superoxide production in live cells by flow cytometry and confocal microscopy. Nature protocols. **2007** *2*, 2295-2301.
- Muroi, M., and Tanamoto, K.** IRAK-1-mediated negative regulation of Toll-like receptor signaling through proteasome-dependent downregulation of TRAF6. Biochimica et biophysica acta. **2012** *1823*, 255-263.

- Murphy, M.P.** How mitochondria produce reactive oxygen species. Biochem J. **2009** *417*, 1-13.
- Murray, P.J., and Wynn, T.A.** Protective and pathogenic functions of macrophage subsets. Nat Rev Immunol. **2011** *11*, 723-737.
- Nakamura, Y. et al.** Ebselen, a glutathione peroxidase mimetic seleno-organic compound, as a multifunctional antioxidant. Implication for inflammation-associated carcinogenesis. J Biol Chem. **2002** *277*, 2687-2694.
- Nakano, Y. et al.** Mutation of the Cyba gene encoding p22phox causes vestibular and immune defects in mice. The Journal of clinical investigation. **2008** *118*, 1176-1185.
- Nathan, C., and Cunningham-Bussell, A.** Beyond oxidative stress: an immunologist's guide to reactive oxygen species. Nat Rev Immunol. **2013a** *13*, 349-361.
- Nathan, C., and Cunningham-Bussell, A.** Beyond oxidative stress: an immunologist's guide to reactive oxygen species. Nat Rev Immunol. **2013b** *13*, 349-361.
- Newton, K., and Dixit, V.M.** Signaling in innate immunity and inflammation. Cold Spring Harbor perspectives in biology. **2012** *4*.
- Niethammer, P. et al.** A tissue-scale gradient of hydrogen peroxide mediates rapid wound detection in zebrafish. Nature. **2009** *459*, 996-999.
- Nohl, H. et al.** Cell respiration and formation of reactive oxygen species: facts and artefacts. Biochemical Society transactions. **2003** *31*, 1308-1311.
- Nomura, M. et al.** Fatty acid oxidation in macrophage polarization. Nat Immunol. **2016** *17*, 216-217.
- O'Neill, L.A. et al.** The history of Toll-like receptors - redefining innate immunity. Nat Rev Immunol. **2013** *13*, 453-460.
- Orr, A.L. et al.** Inhibitors of ROS production by the ubiquinone-binding site of mitochondrial complex I identified by chemical screening. Free radical biology & medicine. **2013** *65*, 1047-1059.
- Palkowitsch, L. et al.** Phosphorylation of serine 68 in the IkappaB kinase (IKK)-binding domain of NEMO interferes with the structure of the IKK complex and tumor necrosis factor-alpha-induced NF-kappaB activity. J Biol Chem. **2008** *283*, 76-86.
- Pamer, E.G.** Immune responses to *Listeria monocytogenes*. Nat Rev Immunol. **2004** *4*, 812-823.
- Park, W.H. et al.** An ROS generator, antimycin A, inhibits the growth of HeLa cells via apoptosis. Journal of cellular biochemistry. **2007** *102*, 98-109.
- Pendyala, S. et al.** Role of Nox4 and Nox2 in hyperoxia-induced reactive oxygen species generation and migration of human lung endothelial cells. Antioxidants & redox signaling. **2009** *11*, 747-764.
- Peters, C. et al.** Tailoring host immune responses to *Listeria* by manipulation of virulence genes -- the interface between innate and acquired immunity. FEMS immunology and medical microbiology. **2003** *35*, 243-253.
- Pillich, H. et al.** Activation of the unfolded protein response by *Listeria monocytogenes*. Cellular microbiology. **2012** *14*, 949-964.
- Pizzolla, A. et al.** Reactive oxygen species produced by the NADPH oxidase 2 complex in monocytes protect mice from bacterial infections. Journal of immunology. **2012** *188*, 5003-5011.
- Poljsak, B. et al.** Achieving the balance between ROS and antioxidants: when to use the synthetic antioxidants. Oxidative medicine and cellular longevity. **2013** *2013*, 956792.
- Polley, S. et al.** A structural basis for IkappaB kinase 2 activation via oligomerization-dependent trans auto-phosphorylation. PLoS biology. **2013** *11*, e1001581.
- Pollock, J.D. et al.** Mouse model of X-linked chronic granulomatous disease, an inherited defect in phagocyte superoxide production. Nature genetics. **1995** *9*, 202-209.

- Prajapati, S., and Gaynor, R.B.** Regulation of I κ B kinase (IKK) γ /NEMO function by IKK β -mediated phosphorylation. *J Biol Chem*. **2002** 277, 24331-24339.
- Radoshevich, L., and Cossart, P.** Listeria monocytogenes: towards a complete picture of its physiology and pathogenesis. *Nature reviews Microbiology*. **2018** 16, 32-46.
- Rahighi, S. et al.** Specific recognition of linear ubiquitin chains by NEMO is important for NF- κ B activation. *Cell*. **2009** 136, 1098-1109.
- Rangasamy, T. et al.** Disruption of Nrf2 enhances susceptibility to severe airway inflammation and asthma in mice. *The Journal of experimental medicine*. **2005** 202, 47-59.
- Rao, R.K., and Clayton, L.W.** Regulation of protein phosphatase 2A by hydrogen peroxide and glutathionylation. *Biochemical and biophysical research communications*. **2002** 293, 610-616.
- Raturi, A., and Simmen, T.** Where the endoplasmic reticulum and the mitochondrion tie the knot: the mitochondria-associated membrane (MAM). *Biochimica et biophysica acta*. **2013** 1833, 213-224.
- Ray, K. et al.** Life on the inside: the intracellular lifestyle of cytosolic bacteria. *Nature reviews Microbiology*. **2009** 7, 333-340.
- Reczek, C.R., and Chandel, N.S.** ROS-dependent signal transduction *Curr Opin Cell Biol*. **2014** Oct 8;33C:8-13. doi: 10.1016/j.ceb.2014.09.010.
- Regan, T. et al.** Tracing innate immune defences along the path of Listeria monocytogenes infection. *Immunology and cell biology*. **2014** 92, 563-569.
- Remer, K.A. et al.** Evidence for involvement of peptidoglycan in the triggering of an oxidative burst by Listeria monocytogenes in phagocytes. *Clinical and experimental immunology*. **2005** 140, 73-80.
- Rhee, S.G.** Cell signaling. H₂O₂, a necessary evil for cell signaling. *Science (New York, NY)*. **2006** 312, 1882-1883.
- Rieber, N. et al.** Current concepts of hyperinflammation in chronic granulomatous disease. *Clinical & developmental immunology*. **2012** 2012, 252460.
- Robinson, K.M. et al.** Selective fluorescent imaging of superoxide in vivo using ethidium-based probes. *Proceedings of the National Academy of Sciences of the United States of America*. **2006** 103, 15038-15043.
- Roca, F.J., and Ramakrishnan, L.** TNF dually mediates resistance and susceptibility to mycobacteria via mitochondrial reactive oxygen species. *Cell*. **2013** 153, 521-534.
- Rothwarf, D.M. et al.** IKK- γ is an essential regulatory subunit of the I κ B kinase complex. *Nature*. **1998** 395, 297-300.
- Sato, S. et al.** Essential function for the kinase TAK1 in innate and adaptive immune responses. *Nat Immunol*. **2005** 6, 1087-1095.
- Sazanov, L.A.** The mechanism of coupling between electron transfer and proton translocation in respiratory complex I. *Journal of bioenergetics and biomembranes*. **2014** 46, 247-253.
- Schafer, M. et al.** Nrf2 establishes a glutathione-mediated gradient of UVB cytoprotection in the epidermis. *Genes & development*. **2010** 24, 1045-1058.
- Scholefield, J. et al.** Super-resolution microscopy reveals a preformed NEMO lattice structure that is collapsed in incontinentia pigmenti. *Nature communications*. **2016** 7, 12629.
- Schramm, M. et al.** Riboflavin (vitamin B₂) deficiency impairs NADPH oxidase 2 (Nox2) priming and defense against Listeria monocytogenes. *European journal of immunology*. **2014** 44, 728-741.
- Schriner, S.E. et al.** Extension of murine life span by overexpression of catalase targeted to mitochondria. *Science (New York, NY)*. **2005** 308, 1909-1911.
- Schrofelbauer, B. et al.** NEMO ensures signaling specificity of the pleiotropic IKK β by directing its kinase activity toward I κ B α . *Molecular cell*. **2012** 47, 111-121.

- Schumacher, B. et al.** Age to survive: DNA damage and aging. Trends in genetics : TIG. **2008** 24, 77-85.
- Segal, A.W. et al.** The respiratory burst of phagocytic cells is associated with a rise in vacuolar pH. Nature. **1981** 290, 406-409.
- Seth, R.B. et al.** Identification and characterization of MAVS, a mitochondrial antiviral signaling protein that activates NF-kappaB and IRF 3. Cell. **2005** 122, 669-682.
- Seveau, S.** Multifaceted activity of listeriolysin O, the cholesterol-dependent cytolysin of *Listeria monocytogenes*. Sub-cellular biochemistry. **2014** 80, 161-195.
- Sheppard, F.R. et al.** Structural organization of the neutrophil NADPH oxidase: phosphorylation and translocation during priming and activation. J Leukoc Biol. **2005** 78, 1025-1042.
- Shifera, A.S.** The zinc finger domain of IKKgamma (NEMO) protein in health and disease. Journal of cellular and molecular medicine. **2010** 14, 2404-2414.
- Shim, J.H. et al.** TAK1, but not TAB1 or TAB2, plays an essential role in multiple signaling pathways in vivo. Genes & development. **2005** 19, 2668-2681.
- Short, J.D. et al.** Protein Thiol Redox Signaling in Monocytes and Macrophages. Antioxidants & redox signaling. **2016** 25, 816-835.
- Shoshan-Barmatz, V. et al.** VDAC, a multi-functional mitochondrial protein regulating cell life and death. Molecular aspects of medicine. **2010** 31, 227-285.
- Singel, K.L., and Segal, B.H.** NOX2-dependent regulation of inflammation. Clinical science (London, England : 1979). **2016** 130, 479-490.
- Skaug, B. et al.** The role of ubiquitin in NF-kappaB regulatory pathways. Annual review of biochemistry. **2009** 78, 769-796.
- Soundararajan, V. et al.** The many faces of the YopM effector from plague causative bacterium *Yersinia pestis* and its implications for host immune modulation. Innate immunity. **2011** 17, 548-557.
- Stavru, F. et al.** *Listeria monocytogenes* transiently alters mitochondrial dynamics during infection. Proceedings of the National Academy of Sciences of the United States of America. **2011** 108, 3612-3617.
- Tai, T.C. et al.** Hypoxic stress-induced changes in adrenergic function: role of HIF1 alpha. Journal of neurochemistry. **2009** 109, 513-524.
- Tang, E.D. et al.** A role for NF-kappaB essential modifier/IkappaB kinase-gamma (NEMO/IKKgamma) ubiquitination in the activation of the IkappaB kinase complex by tumor necrosis factor-alpha. J Biol Chem. **2003** 278, 37297-37305.
- Tarantino, N. et al.** TNF and IL-1 exhibit distinct ubiquitin requirements for inducing NEMO-IKK supramolecular structures. The Journal of cell biology. **2014** 204, 231-245.
- Taylor, P.R. et al.** The mannose receptor: linking homeostasis and immunity through sugar recognition. Trends in immunology. **2005** 26, 104-110.
- Tegethoff, S. et al.** Tetrameric oligomerization of IkappaB kinase gamma (IKKgamma) is obligatory for IKK complex activity and NF-kappaB activation. Mol Cell Biol. **2003** 23, 2029-2041.
- Tenekeci, U. et al.** K63-Ubiquitylation and TRAF6 Pathways Regulate Mammalian P-Body Formation and mRNA Decapping. Molecular cell. **2016** 62, 943-957.
- Thimmulappa, R.K. et al.** Nrf2-dependent protection from LPS induced inflammatory response and mortality by CDDO-Imidazolide. Biochemical and biophysical research communications. **2006** 351, 883-889.
- Tokunaga, F., and Iwai, K.** LUBAC, a novel ubiquitin ligase for linear ubiquitination, is crucial for inflammation and immune responses. Microbes and infection. **2012** 14, 563-572.
- Tonks, N.K.** Redox redux: revisiting PTPs and the control of cell signaling. Cell. **2005** 121, 667-670.

- Traenckner, E.B. et al.** Phosphorylation of human I kappa B-alpha on serines 32 and 36 controls I kappa B-alpha proteolysis and NF-kappa B activation in response to diverse stimuli. The EMBO journal. **1995** *14*, 2876-2883.
- Ushio-Fukai, M.** Compartmentalization of redox signaling through NADPH oxidase-derived ROS. Antioxidants & redox signaling. **2009** *11*, 1289-1299.
- Utermohlen, O. et al.** Severe impairment in early host defense against *Listeria monocytogenes* in mice deficient in acid sphingomyelinase. Journal of immunology. **2003** *170*, 2621-2628.
- Vazquez-Torres, A., and Fang, F.C.** Oxygen-dependent anti-Salmonella activity of macrophages. Trends in microbiology. **2001** *9*, 29-33.
- Vogel, R.O. et al.** Cytosolic signaling protein Ecsit also localizes to mitochondria where it interacts with chaperone NDUFAF1 and functions in complex I assembly. Genes & development. **2007** *21*, 615-624.
- Wang, C. et al.** Characterization of murine macrophages from bone marrow, spleen and peritoneum. BMC immunology. **2013** *14*, 6.
- Wang, Y. et al.** Inhibition of type I interferon production via suppressing IKK-gamma expression: a new strategy for counteracting host antiviral defense by influenza A viruses? Journal of proteome research. **2012** *11*, 217-223.
- Waterfield, M. et al.** I kappa B kinase is an essential component of the Tpl2 signaling pathway. Mol Cell Biol. **2004** *24*, 6040-6048.
- Weiss, G., and Schaible, U.E.** Macrophage defense mechanisms against intracellular bacteria. Immunological reviews. **2015** *264*, 182-203.
- Werling, D. et al.** Differential production of cytokines, reactive oxygen and nitrogen by bovine macrophages and dendritic cells stimulated with Toll-like receptor agonists. Immunology. **2004** *111*, 41-52.
- West, A.P. et al.** TLR signalling augments macrophage bactericidal activity through mitochondrial ROS. Nature. **2011a** *472*, 476-480.
- West, A.P. et al.** Recognition and signaling by toll-like receptors. Annual review of cell and developmental biology. **2006** *22*, 409-437.
- West, A.P. et al.** Mitochondria in innate immune responses. Nat Rev Immunol. **2011b** *11*, 389-402.
- Windheim, M. et al.** Two different classes of E2 ubiquitin-conjugating enzymes are required for the mono-ubiquitination of proteins and elongation by polyubiquitin chains with a specific topology. Biochem J. **2008** *409*, 723-729.
- Winterbourn, C.C., and Hampton, M.B.** Thiol chemistry and specificity in redox signaling. Free radical biology & medicine. **2008** *45*, 549-561.
- Winterbourn, C.C., and Kettle, A.J.** Redox reactions and microbial killing in the neutrophil phagosome. Antioxidants & redox signaling. **2013** *18*, 642-660.
- Wooten, R.M. et al.** Toll-like receptor 2 is required for innate, but not acquired, host defense to *Borrelia burgdorferi*. Journal of immunology. **2002** *168*, 348-355.
- Wu, C.J. et al.** Sensing of Lys 63-linked polyubiquitination by NEMO is a key event in NF-kappaB activation [corrected]. Nature cell biology. **2006a** *8*, 398-406.
- Wu, Z.H. et al.** Molecular linkage between the kinase ATM and NF-kappaB signaling in response to genotoxic stimuli. Science (New York, NY). **2006b** *311*, 1141-1146.
- Xu, M. et al.** A ubiquitin replacement strategy in human cells reveals distinct mechanisms of IKK activation by TNFalpha and IL-1beta. Molecular cell. **2009** *36*, 302-314.
- Yamin, T.T., and Miller, D.K.** The interleukin-1 receptor-associated kinase is degraded by proteasomes following its phosphorylation. J Biol Chem. **1997** *272*, 21540-21547.

- Yang, Y. et al.** Mitochondria and Mitochondrial ROS in Cancer: Novel Targets for Anticancer Therapy. Journal of cellular physiology. **2016** 231, 2570-2581.
- Yazdanpanah, B. et al.** Riboflavin kinase couples TNF receptor 1 to NADPH oxidase. Nature. **2009** 460, 1159-1163.
- Yuan, X. et al.** Activation of TLR4 signaling promotes gastric cancer progression by inducing mitochondrial ROS production. Cell death & disease. **2013** 4, e794.
- Zhang, J. et al.** ROS and ROS-Mediated Cellular Signaling. Oxidative medicine and cellular longevity. **2016** 2016, 4350965.
- Zhang, W. et al.** Competition between TRAF2 and TRAF6 regulates NF-kappaB activation in human B lymphocytes. Chinese medical sciences journal = Chung-kuo i hsueh k'o hsueh tsa chih. **2010** 25, 1-12.
- Zhou, L. et al.** Disulfide-mediated stabilization of the IkappaB kinase binding domain of NF-kappaB essential modulator (NEMO). Biochemistry. **2014a** 53, 7929-7944.
- Zhou, R. et al.** A role for mitochondria in NLRP3 inflammasome activation. Nature. **2011** 469, 221-225.
- Zorov, D.B. et al.** Mitochondrial reactive oxygen species (ROS) and ROS-induced ROS release. Physiological reviews. **2014** 94, 909-950.

6. Summary

A major function of macrophages during infection is the initiation of the pro-inflammatory response leading to secretion of cytokines that help to orchestrate the immune response. Reactive oxygen species (ROS) produced by NADPH oxidases, such as Nox2, and by mitochondria are key components of host cell defense against invading microbial pathogens. However, nearly nothing is known about the role of ROS in general or mitochondrial ROS (mtROS) in particular during pro-inflammatory signaling in infected macrophages. Moreover, the underlying molecular mechanisms by which mtROS may regulate pro-inflammatory signaling and cytokine secretion upon bacterial infection have remained completely elusive.

In this thesis, I delineate ROS as crucial regulators of pro-inflammatory signaling and cytokine secretion in *Listeria monocytogenes* (L.m.)-infected macrophages. Surprisingly, my data show that the ROS, which license pro-inflammatory signaling, are produced, in fact, by mitochondria (mtROS). Infection of macrophages triggers O_2^- production into the mitochondrial intermembrane space (IMS) by complex III of the ETC initiated via the TLR2/MyD88/TRAF6 signaling pathway. In the IMS O_2^- is converted by superoxide dismutase (SOD1) into H_2O_2 that diffuses into the cytosol where it regulates secretion of pro-inflammatory cytokines.

Mechanistically, I identify the regulatory IKK complex subunit NEMO as the molecular target for mtROS. Specifically, the redox-dependent intermolecular covalent linkage of NEMO via disulfide bonds formed by Cys⁵⁴ and Cys³⁴⁷ is the underlying molecular mechanism by which mtROS license full activation of the IKK complex and subsequent signaling via the ERK1/2 and NF- κ B pathways that eventually lead to secretion of pro-inflammatory cytokines.

Taken together, this thesis introduces mtROS-dependent disulfide linkage of NEMO as a so far unknown novel regulatory step critically required for the pro-inflammatory response of infected macrophages.

7. Zusammenfassung

Eine wichtige Aufgabe von Makrophagen während einer Infektion ist die Koordination der Immunantwort. Dafür notwendig ist die Initiierung einer pro-inflammatorischen Signalkaskade, die zur Sekretion von Zytokinen führt. Reaktive Sauerstoffspezies (ROS), welche in Makrophagen vor allem durch die Phagozyten-Oxidase Nox2 und durch Mitochondrien produziert werden, sind zentrale Komponenten der Abwehr gegen Pathogene. Es ist jedoch noch gänzlich unbekannt, ob und wie ROS pro-inflammatorische Signalwege in infizierten Makrophagen steuern.

In dieser Doktorarbeit identifiziere ich, anhand von mit *Listeria monocytogenes* infizierten Makrophagen, ROS als notwendige Regulatoren des zur Sekretion von Zytokinen führenden pro-inflammatorischen Signalwegs. Überraschenderweise zeigen meine Daten, dass die für die Regulation der pro-inflammatorischen Signalkaskade verantwortlichen ROS nicht durch Nox2, sondern von Mitochondrien (mtROS) produziert werden. Stimuliert über TLR2 und andere MyD88- und TRAF6 abhängige Rezeptoren produziert Komplex III der mitochondrialen Atmungskette vermehrt Superoxid in den Intermembranraum. Dort wird es mittels der Superoxid-Dismutase 1 (SOD1) zu Wasserstoffperoxid umgewandelt, welches, nach seiner Diffusion ins Zytosol, die zur Sekretion von Zytokinen führende pro-inflammatorische Signalkaskade reguliert.

Auf mechanistischer Ebene habe ich die regulatorische Untereinheit des IKK-Komplex, NEMO/IKK γ , als Zielmolekül der mtROS identifiziert. Durch mtROS werden NEMO Moleküle über Disulfidbrücken zwischen den beiden redox-sensitiven Cysteinresten Cys⁵⁴ und Cys³⁴⁷ kovalent miteinander verknüpft. Diese Verknüpfung ist für die vollständige Aktivierung des IKK-Komplex und die nachfolgende Aktivierung der MAP-Kinase ERK1/2 und des Transkriptionsfaktors NF- κ B, welche notwendig für die Sekretion von pro-inflammatorischen Zytokinen sind, von großer Bedeutung.

Zusammenfassend deckt diese Doktorarbeit, mit der mtROS-abhängigen kovalenten Verknüpfung von NEMO über Disulfidbrücken, einen bisher unbekanntem kritischen regulatorischen Schritt des zur Sekretion von pro-inflammatorischen Zytokinen durch infizierte Makrophagen führenden Signalweges auf.

8. Danksagung

Ich danke,

Prof. Dr. Martin Krönke, für die Möglichkeit die Doktorarbeit in seinem Institut anzufertigen, für die Vergabe eines fordernden Themas, für die Übernahme des Zweitgutachtens meiner Arbeit, sowie für viele hilfreichen Diskussionen und nicht abbreißende Unterstützung.

Prof. Dr. Björn Schumacher, für die Übernahme des Erstgutachtens meiner Arbeit.

Prof. Dr. Olaf Utermöhlen, für die Aufnahme in seine Arbeitsgruppe während der ersten Jahre, für viele gute Hilfestellungen und für den Ansporn zum Selberdenken.

In ganz besonderer Weise meinem Betreuer Dr. Michael Schramm. Meinen tiefsten freundschaftlichen Dank für die unzähligen Hilfestellungen, die hervorragende Einarbeitung, die heftigen, aber nützlichen Diskussionen, die unendliche Geduld mit meinem Hitzkopf, die vielen Motivationsreden und den nicht abbreißenden Glauben an den Erfolg dieses Projekts. Ohne dich hätte ich dieses Ziel nicht erreicht.

Dr. Alexander Gluschko, in einer Weise, wie man nur einem guten Freund und nicht einem Kollegen danken kann. Ohne dich als Freund und Partner hätte ich diese Arbeit nicht bis zum Ende durchgestanden. Aus tiefster Seele Dank für die andauernden Motivationsschübe, Tröstungen, sowie die tolle Zusammenarbeit und Freundschaft der vergangenen und hoffentlich zukünftigen Jahre.

Alina Farid, Arlette Paillard, Ulrike Karow, Katja Krönke-Wiegmann, Daniela Grumme, Tina Tossetti, Sandra Schramm, Alzbeta Machova, sowie allen anderen ehemaligen und aktuellen Arbeitskollegen, nicht nur für eine unglaublich familiäre Arbeitsatmosphäre und unzählige Motivationsreden, sondern ebenso für die vielen neu gewonnenen Freundschaften.

Alina Farid und Michael Schramm für die Korrekturlesung meiner Arbeit.

In unveränderter Weise meinem Vater Wilfried und meiner Mutter Johanna für ihre permanente liebevolle Unterstützung in jeder Hinsicht. Ohne euch hätte ich auch dieses Ziel niemals erreicht. Ein weiteres Mal tausendfachen Dank.

Meiner Schwester Susan und meiner Cousine Sabine, zu denen ich in Bezug auf Intelligenz und emotionale Wärme stets mit Stolz und Bewunderung aufblicken kann und die mich mit Liebe sowie Unterstützung ebenso zu diesem Ziel getragen haben.

Meinem gesamten Freundeskreis, für viele tolle Jahre voller Spaß und vieler schöner Stunden.

Ich widme diese Arbeit in dankbarer und liebevoller Erinnerung meiner verstorbenen Tante Helga Derichweiler und meinen verstorbenen Großeltern Matthias und Gertrud Derichweiler.

9. List of publications

First authorships

Herb M, Gluschko A, Schramm M. LC3-associated phagocytosis initiated by integrin ITGAM-ITGB2/Mac-1 enhances immunity to *Listeria monocytogenes*. Autophagy. (2018) Jun 20. doi: 10.1080/15548627.2018.1475816

Gluschko A and **Herb M (shared first authorship)**, Wiegmann K, Krut O, Neiss WF, Utermöhlen O, Krönke M, Schramm M (2018). The β 2 Integrin Mac-1 Induces Protective LC3-Associated Phagocytosis of *Listeria monocytogenes*. Cell Host Microbe. (2018) Mar 14;23(3):324-337.e5. doi: 10.1016/j.chom.2018.01.018.

Co-authorships

Schramm M, Wiegmann K, Schramm S, Gluschko A, **Herb M**, Utermöhlen O, Krönke M (2014). Riboflavin (vitamin B2) deficiency impairs NADPH oxidase 2 (Nox2) priming and defense against *Listeria monocytogenes*. Eur J Immunol. (2014) Mar;44(3):728-41. doi: 10.1002/eji.201343940.

10. List of Figures

Figure 1:	<u>Major ROS subspecies in organisms</u>	page 1
Figure 2:	<u>Balance of cellular ROS</u>	page 2
Figure 3:	<u>The Nox family enzymes</u>	page 3
Figure 4:	<u>ROS production of the ETC</u>	page 4
Figure 5:	<u>Oxidation and reduction of cysteine residues by ROS</u>	page 5
Figure 6:	<u>Protein modifications induced by ROS</u>	page 6
Figure 7:	<u>ROS production in different subcellular compartments</u>	page 7
Figure 8:	<u>Receptor repertoire of macrophages</u>	page 9
Figure 9:	<u>The activation of NF-κB and the MAPKs p38, JNK1/2 and ERK1/2</u>	page 10
Figure 10:	<u>Activation and ROS production by Nox2</u>	page 13
Figure 11:	<u>Mitochondrial ROS production is necessary for direct antimicrobial host defense</u>	page 14
Figure 12:	<u>Macrophages produce extracellular and cytosolic ROS upon bacterial infection</u>	page 37
Figure 13:	<u>ROS are required for pro-inflammatory cytokine secretion during bacterial infection</u>	page 39
Figure 14:	<u>Nox2 is the exclusive source of extracellular ROS, whereas Nox/Duox enzymes do not contribute to cytosolic ROS production</u>	page 41
Figure 15:	<u>Cytosolic ROS production independent of Nox/Duox enzymes is necessary for pro-inflammatory cytokine secretion</u>	page 43
Figure 16:	<u>Cytosolic ROS do not originate from the mitochondrial matrix</u>	page 45
Figure 17:	<u>Cytosolic ROS are produced by complex III of the mitochondrial ETC</u>	page 47
Figure 18:	<u>Cytosolic H₂O₂ regulates pro-inflammatory signaling</u>	page 49
Figure 19:	<u>Infection-induced mtROS production is not caused by mitochondrial perturbation</u>	page 51
Figure 20:	<u>mtROS production in infected macrophages is induced by TLR2/MyD88/TRAF6 signaling</u>	page 53
Figure 21:	<u>mtROS are crucial for activation of the ERK1/2 pathway</u>	page 55
Figure 22:	<u>mtROS are necessary for full activation of NF-κB signaling</u>	page 57
Figure 23:	<u>mtROS do not regulate cytokine secretion by oxidative phosphatase inactivation</u>	page 58
Figure 24:	<u>mtROS are crucial for covalent linkage of NEMO via disulfide bonds and subsequent IKK complex activation</u>	page 60

- Figure 25:** mtROS induce NEMO complex formation by covalent linkage
via Cys⁵⁴ and Cys³⁴⁷ **page 62**
-
- Figure 26:** mtROS-mediated covalent linkage of NEMO
via Cys⁵⁴ and Cys³⁴⁷ is crucial for pro-inflammatory signaling **page 63**
-
- Figure 27:** mtROS do not regulate processes up- or downstream of NEMO **page 65**
-
- Figure 28:** Model for regulation of pro-inflammatory cytokine secretion
by mtROS in L.m.-infected macrophages **page 67**
-

11. List of Tables

Table 1:	<u>List of Chemicals and additives</u>	page 18
Table 2:	<u>List of Buffers, solutions and media</u>	page 19
Table 3:	<u>List of antibodies</u>	page 21
Table 4:	<u>Molecularbiological materials, constructs and primers</u>	page 21
Table 5:	<u>PCR programs</u>	page 22
Table 6:	<u>Consumable materials</u>	page 22
Table 7:	<u>Technical equipment and devices</u>	page 23
Table 8:	<u>Kits</u>	page 24
Table 9:	<u>Software</u>	page 24

12. Erklärung

Ich versichere, dass ich die von mir vorgelegte Dissertation selbständig angefertigt, die benutzten Quellen und Hilfsmittel vollständig angegeben und die Stellen der Arbeit - einschließlich Tabellen, Karten und Abbildungen -, die anderen Werken im Wortlaut oder dem Sinn nach entnommen sind, in jedem Einzelfall als Entlehnung kenntlich gemacht habe; dass diese Dissertation noch keiner anderen Fakultät oder Universität zur Prüfung vorgelegen hat; dass sie - abgesehen von unten angegebenen Teilpublikationen - noch nicht veröffentlicht worden ist sowie, dass ich eine solche Veröffentlichung vor Abschluss des Promotionsverfahrens nicht vornehmen werde. Die Bestimmungen der Promotionsordnung sind mir bekannt. Die von mir vorgelegte Arbeit ist von Herrn Prof. Dr. Björn Schumacher und Herrn Dr. Michael Schramm betreut worden.

Teilpublikationen:

Gluschko A and **Herb M (shared first authorship)**, Wiegmann K, Krut O, Neiss WF, Utermöhlen O, Krönke M, Schramm M (2018). *The β 2 Integrin Mac-1 Induces Protective LC3-Associated Phagocytosis of Listeria monocytogenes*. **Cell Host Microbe**. 2018 Mar 14;23(3):324-337.e5. doi: 10.1016/j.chom.2018.01.018.

Herb M, Gluschko A, Schramm M (2018). *LC3-associated phagocytosis initiated by integrin ITGAM-ITGB2/Mac-1 enhances immunity to Listeria monocytogenes*. **Autophagy**. 2018 Jun 20. doi: 10.1080/15548627.2018.1475816

Herb M, Gluschko A, Wiegmann K, Farid A, Wolf A, Utermöhlen O, Krut O, Krönke M, Schramm M. *Mitochondrial reactive oxygen species regulate pro-inflammatory signaling via disulfide linkage of NEMO*. In 2nd revision in **Science Signaling**.

Köln, den 08.11.2018

Marc Herb

12. Curriculum vitae

Marc Herb

Date of birth: 18.03.1984

Birthplace: Cologne

Family status: single

Citizenship: german

Educational career

- Since 02/2018 **GSfBS PhD student** at the Cluster of Excellence CECAD Research Center, Cologne, junior research group of Dr. Michael Schramm and research group of Prof. Dr. Martin Krönke
- 12/2012 – 01/2018 **GSfBS PhD student** at the Institute of Medical Microbiology, Immunology and Hygiene, University of Cologne. Junior research group of Dr. Michael Schramm and research group of Prof. Dr. Olaf Utermöhlen
- 09/2010 – 05/2011 **Diploma thesis** at the Institute of Cellular and Molecular Botany (IZMB), University of Bonn.
1st Supervisor: PD Dr. Rochus Franke
2nd Supervisor: Prof. Dr. Lukas Schreiber
Title: Characterization of the gene *At1g55940* (*CYP708A1*) in *Arabidopsis thaliana*
Final mark: 1.0
- 10/2005 – 05/2011 **Studies of biology** at the Rheinische Friedrich-Wilhelms-University of Bonn
Main subject: Plant physiology
Minor subject: Microbiology
Minor subject: Organic chemistry
Additional subject: Micropalaeontology
Additional subject: Cell biology
- 03/1994 - 05/2003 **High-school diploma**, Ernst-Mach-Gymnasium (formerly Gymnasium Bonnstrasse)

Professional career

- 05/2011 – 11/2012 **Business assistant** in the chemical company LyondellBasell